ENCAPSULATION OF ORGANIC PHASE CHANGE MATERIALS WITHIN METAL OXIDES FOR THERMAL ENERGY STORAGE SYSTEMS

SARA TAHAN LATIBARI

THESIS SUBMITTED IN FULFILMENT OF

THE REQUIREMENT FOR THE DEGREE OF

DOCTOR OF PHILOSOPHY

FACULTY OF ENGINEERING

UNIVERSITY OF MALAYA

KUALA LUMPUR

2016

UNIVERSITI MALAYA

ORIGINAL LITERARY WORK DECLARATION

Name of Candidate: SARA TAHAN LATIBARI

Registration/Matric No: KHA120084

Name of Degree: DOCTOR OF PHILOSOPHY

Title of Project Paper/Research Report/Dissertation/Thesis ("this Work"):

ENCAPSULATION OF ORGANIC PHASE CHANGE MATERIALS WITHIN METAL OXIDES FOR THERMAL ENERGY STORAGE SYSTEMS

Field of Study: **ADVANCE MATERIALS / NANOMATERIALS**

I do solemnly and sincerely declare that:

(1) I am the sole author/writer of this Work;
(2) This Work is original;
(3) Any use of any work in which copyright exists was done by way of fair dealing and for permitted purposes and any excerpt or extract from, or reference to or reproduction of any copyright work has been disclosed expressly and sufficiently and the title of the Work and its authorship have been acknowledged in this Work;
(4) I do not have any actual knowledge nor do I ought reasonably to know that the making of this work constitutes an infringement of any copyright work;
(5) I hereby assign all and every rights in the copyright to this Work to the University of Malaya ("UM"), who henceforth shall be owner of the copyright in this Work and that any reproduction or use in any form or by any means whatsoever is prohibited without the written consent of UM having been first had and obtained;
(6) I am fully aware that if in the course of making this Work I have infringed any copyright whether intentionally or otherwise, I may be subject to legal action or any other action as may be determined by UM.

Candidate's Signature Date:

Subscribed and solemnly declared before,

Witness's Signature Date:

Name:

Designation:

ABSTRACT

Solar energy is receiving a lot of attention nowadays since it is a clean, renewable, and sustainable energy. A major limitation of solar energy is that it is available for only about 2000 hours a year in many places. Thermal energy storage is a major contributor to bridge the gap between energy demand (consumption) and energy production (supply) by solar power. The utilization of high latent heat storage capability of phase change materials is one of the keys to an efficient way to store thermal energy. Several kinds of organic PCMs like fatty acids have been applied recently as they have a high latent heat and appropriate thermal properties. However, direct use of such PCMs in practical thermal applications is not easy due to their low thermal conductivity, flammability, instability, and leakage problems. To overcome these problems, PCMs have been encapsulated in various organic and inorganic shell materials. An inorganic shell material with high thermal conductivity and superior strength not only enhances the thermal transfer performance of the PCM system but also improves the durability and working reliability of them.

This study presents state of the art of nano/microencapsulated PCMs (NE/MEPCMs) for thermal energy storage applications and provides an insight into our efforts to develop novel nano/microencapsulated phase change materials with enhanced performance and safety. Specific attention was given to the encapsulation process of some inorganic materials for the first time and the improvement of thermal conductivity and thermal stability of the prepared materials. In addition, the thermal energy storage properties and performance are discussed for thermal energy applications.

In this research three types of nano/microcapsules were prepared with organic fatty acids as the core phase change material and SiO_2 (silica), TiO_2 (titania), and Al_2O_3 (aluminum oxide) as the inorganic shell materials through a sol-gel method. The structural, morphological and thermal features of the newly developed NE/MEPCMs

were evaluated by a series of modern instruments and characterization technologies, including DSC, TGA, FT-IR, TEM, SEM and XRD. The thermal reliability of prepared nano/microcapsules was investigated using a thermal cycler for a large number of heating and cooling processes.

In this research the influences of several types of parameters during the preparation method on the morphology, thermal performance and thermal conductivity of the prepared materials have been studied. The experimental results indicate that the fatty acids were successfully encapsulated in the shell materials in spherical shapes. Encapsulated fatty acids confirmed the outstanding phase-change performance with specific heat and thermal stability enhancement. The thermal conductivities of the encapsulated PCMs are significantly improved compared to pure PCMs. In conclusion, the outstanding latent heat, high thermal conductivity, thermal stability and reliability of the prepared nano/microcapsules make these materials appropriate phase change materials for thermal energy storage applications like slurry systems.

ABSTRAK

Tenaga solar menerima banyak perhatian sekarang kerana ia ialah tenaga yang bersih, dapat diperbaharui, dan mampan. Satu had utama tenaga solar adalah bahawa ia hanya berfungsi kira-kira 2000 jam setahun dan didapati di banyak tempat. Penyimpanan tenaga haba merupakan penyumbang utama untuk merapatkan jurang antara keperluan tenaga (penggunaan) dan pengeluaran tenaga (bekalan) yang dihasilkan oleh kuasa solar. Penggunaan keupayaan penyimpanan haba pendam tinggi dalam bahan-bahan perubahan fasa adalah salah satu cara yang berkesan untuk menyimpan tenaga haba. Beberapa jenis PCMS organik seperti asid lemak telah digunakan baru-baru ini kerana mereka mempunyai haba pendam yang tinggi dan sifat terma yang sesuai. Walau bagaimanapun, penggunaan PCMS secara langsung dalam aplikasi terma yang praktikal tidak mudah kerana masalah kekonduksian terma, kemudahbakaran, ketidakstabilan, dan kebocoran. Untuk mengatasi masalah ini, PCMS telah dicampurkan dalam pelbagai bahan shell organik dan bukan organik. Bahan shell bukan organik dengan kekonduksian terma yang tinggi dan kekuatan unggul bukan sahaja meningkatkan prestasi pemindahan terma sistem PCM tetapi juga meningkatkan ketahanan dan kebolehpercayaan kerja mereka.

Kajian ini membentangkan kesenian nano/microencapsulated PCMs untuk aplikasi penyimpanan tenaga haba dan memberi pandangan dalam usaha kita untuk membangunkan nano/microencapsulated bahan perubahan fasa (NE/MEPCMs) yang baru dengan prestasi dan keselamatan yang dipertingkatkan. Perhatian khusus diberikan kepada proses pengkapsulan sesetengah bahan bukan organik untuk kali pertama serta kepda peningkatan kekonduksian terma dan kestabilan terma bagi bahan-bahan yang disediakan. Di samping itu, ciri-ciri penyimpanan tenaga haba dan prestasi dibincangkan untuk aplikasi tenaga haba.

Dalam kajian ini tiga jenis nano/microcapsules disediakan dengan asid lemak organik sebagai bahan perubahan fasa teras dan SiO_2 (silika), TiO_2 (Titania), dan Al_2O_3 (aluminium oksida) sebagai bahan shell bukan organik melalui kaedah sol-gel. Ciri-ciri struktur, morfologi dan terma NE/MEPCMs yang baru dibangunkan dinilaikan oleh satu siri instrumen moden dan alat teknologi pencirian, termasuk DSC, TGA, FT-IR, TEM, SEM dan XRD. Kebolehpercayaan terma nano/microcapsules yang disediakan telah disiasat dengan menggunakan cycler terma untuk sejumlah besar proses pemanasan dan penyejukan.

Dalam kajian ini pengaruh beberapa jenis parameter dalam kaedah penyediaan terhadap morfologi, prestasi terma dan kekonduksian terma bahan-bahan spesimen kajian telah dikaji. Keputusan eksperimen menunjukkan bahawa asid lemak telah berjaya dikurungkan dalam bahan shell dalam bentuk sfera. Asid lemak yang terkurung mengesahkan prestasi fasa perubahan yang luar biasa dengan haba tentu dan peningkatan kestabilan terma. Kekonduksian terma PCMS yang terkandung adalah jauh lebih baik berbandingkan PCMS tulen. Kesimpulannya, haba pendam yang cemerlang, kekonduksian terma yang tinggi, kestabilan terma dan kebolehpercayaan nano/microcapsules yang dihasilkan menjadikan mereka sebagai bahan-bahan perubahan fasa yang sesuai untuk aplikasi penyimpanan tenaga haba seperti sistem sluri.

ACKNOWLEDGEMENT

I give all praise and thanks to Allah, the most merciful, who has given me the inspiration, patience, strength and health for completing this thesis. I have experienced His guidance day by day.

I would like to express my special appreciation to my supervisor Associate Prof. Dr. Hendrik Simon Cornelis Metselaar, who has been a tremendous advisor for me. I would like to thank him for encouraging my research and for allowing me to grow as a research scientist. His advices and supports have been invaluable. I also appreciate my other supervisor Dr Amalina Binti Muhamad Affifi for her kindness and helpful advices and support.

I would like to thank my best colleague and compassionate beloved husband Dr. Mohammad Mehrali, not only for his encourage and support but also for all the valuable discussions, suggestions and helps during my study. I also like to acknowledge Dr. Mehdi Mehrali for his useful advices.

I would like to convey thanks to the University of Malaya and the Ministry of Higher Education (MOHE) of Malaysia, Grant number UM.C/HIR/MOHE/ENG/21, for providing the financial support and laboratory facilities.

Lastly but not the least, I would like to dedicate my love and deepest appreciation to my family, specifically my parents for allowing me to realize my own potential. All the support, encouragement and advices they have provided for me over the years were the greatest gifts anyone has ever given me. I am greatly indebted to them and without them I may never have gotten to where I am today.

TABLE OF CONTENTS

LIST OF FIGURES

LIST OF TABLES

LIST OF SYMBOLS AND ABBREVIATIONS

Nomenclature

ΔH	Latent heat
ΔT	Temperature difference
ΔE	Energy difference
A	Cross sectional area
a_m	Fraction melted
C	Specific heat capacity
d	Distance
dm/dt	Rate of change in weight
E_r	Encapsulation ratio
E_e	Encapsulation efficiency
e	Thermal effusivity
g	Gram
hr	Hour
h	Planck`s constant
Js	Jules second
Kα	Radiation
k	Thermal conductivity
kV	Voltage
K	Kelvin
L	Length
m	Mass
mL	Milliliters
min	Minutes

mg	Milligrams
nm	Nano meter
n	Diffraction order
Q	Amount of stored heat
q	Magnitude of heat transmission
rpm	Round per minute
R	Capsule radius
R_{PCM}	Core PCM radius
R_{Shell}	Shell thickness
T	Temperature
v	Classical frequency
wt.%	Weight ratio

Greek symbols

μ	Micro
θ	Angle
φ	Thermal storage capability
α	Thermal diffusivity
ρ	Density
λ	Wave length

Subscripts

c	Crystallization
ef	Extrapolated end
ei	Extrapolated peak onset
f	End peak

i	Initial peak
m	Melting
P,s	Solid PCM
P,l	Liquid PCM
p	peak
t	Total

Acronyms

AA/AG	Agar-agar/arabic gum
CAES	Compressed air energy storage
DSC	Differential Scanning Calorimetry
DTG	Derivative Thermogravimetric
EPCM	Encapsulated PCM
FTIR	Fourier-Transform Infrared Spectroscopy
FESEM	Field Emission Scanning Electron Microscopy
LFA	Laser Flash Technique
LHTES	Latent heat thermal energy storage systems
MEPCMS	Microencapsulated phase change slurry
NEPCM	Nano encapsulated PCM
NE/MEPCM	Nano/microencapsulated PCM
O/W	Oil/water
PCM	Phase change material
PHPS	Pumped hydropower storage
PA	Palmitic acid
PSD	Particle size distribution
SEM	Scanning Electron Microscopy

SHTES	Sensible heat thermal energy storage
SMES	Superconducting magnetic energy storage
SG/AG	Sterilized gelatine/arabic gum
SA	Stearic acid
SDS	Sodium dodecyl sulfate
TEM	Transmission Electron Microscopy
TGA	Thermal Gravimetry
THW	Transient Hot-Wire Method
TES	Thermal energy storage
TEOS	Tetraethoxysilane
TTIP	Titanium tetraisopropoxide
XRD	X-Ray Diffractometry

CHAPTER 1

INTRODUCTION

1.1 Background

The economic and technological development worldwide leads to an increasing energy demand. Fossil fuels are combusted to generate electricity, fuel transportation and for heating and cooling purposes. Fossil fuels are a significant energy source, but conventional fossil energy sources are limited, and their use results in the emission of harmful gases, which are responsible for climate change and environmental pollution. Experts around the world have warned that greenhouse gases have to be reduced globally, up to 50% in the next 50-100 years (Sorensen, 2015) (Tatsidjodoung et al., 2013). These drawbacks generated an increased interest in renewable energy from natural sources, like wind, sunlight, hydropower as well as alternatives such as nuclear and geothermal energy. Renewable energy has been used over the last two decades to save cost and prevent adverse environmental pollution effects of fossil fuel. Solar energy is an essentially inexhaustible source potentially capable of meeting a significant portion of the world's future energy needs with a minimum of adverse environmental consequences (Frankl & Nowak, 2010). However, there are numerous problems that have to be resolved to successfully utilize solar energy. Solar radiation is intermittent by its nature. It varies as a factor of time, weather condition such as cloud cover; location and season. Therefore, solar energy is not widely used at present. According to U.S. Energy Information Administration 2012 annual energy outlook, the supplies for U.S. electricity generation were 70% fossil fuels, 20% nuclear, and only 10% renewable energy in 2010 (Khatib, 2012). Therefore, scientists investigated technically to solve these problems. They found that energy storage is one of the possible solutions for energy conservation and leveling of energy demand patterns, and improving the performance of energy systems and increasing the reliability. Energy storage not only

reduces the mismatch between supply and demand but plays an important role in conserving the energy. It leads to saving of premium fuels which are limited and contribute to a green environment. The excess heat from solar radiation during the daytime can be collected and stored for use during the night time. This is convenient in the areas of heat recovery systems and electricity generation (Farid et al., 2004). Solar energy can be stored in various forms such as hydrogen energy storage, electrochemical storage and thermal energy storage (TES). Among various energy storage techniques, thermal energy storage can be considered as one of the effective ones (Goswami et al., 2000). TES system can store part of the solar energy captured during times of high incidence of solar radiation to use during cloudy or night periods. Therefore; TES leads to a more efficient power distribution. Apart from the utility applications, TES also has its usages in active and passive solar heating, water heating and building heating and cooling.

1.2 Importance of the Study

TES can be classified as latent, sensible and thermochemical energy storage. Latent heat refers to the heat released or absorbed when a material changes its phase at constant temperature. Latent heat energy storage contains PCMs and possesses advantages like high energy storage density and small temperature difference between charging and discharging (Sari & Kaygusuz, 2002). This facilitates reducing the impression of the system and the cost. Storage of thermal energy using latent heat is potentially an attractive method to store solar thermal energy as it can provide near isothermal and high exergy storage conditions. These latent heat storage materials are known as phase change materials (PCMs). Due to this inherent property of PCMs, they are recognized as promising candidates for storage materials in solar applications and are been researched extensively throughout the world. Some of the desirable properties of PCMs include that the thermal heat storage is not obligatorily considered in the

design because the heat storage is over a narrow range of temperature and their isothermal nature make them the proper choice in passive storage and they store higher amount of energy per unit volume in a slight temperature difference as compared to sensible and thermochemical heat storage materials (Dincer & Dost, 1996).

There is a wide variety of PCMs available which melt and solidify at a broad range of temperatures and are utilized in various applications. The PCMs are categorized into three main groups: organic, inorganic, and eutectic materials. Organic PCMs include mainly paraffin waxes, fatty acids, and sugar alcohols (Pielichowska & Pielichowski, 2014). They have been used in several developmental studies and have been commercially functioned recently. Organic PCMs, specifically fatty acids, have a high heat of fusion and usually do not suffer segregation and high supercooling problems during melt-solidify cycling, which can be a severe issue for some inorganic ones like salt hydrates. Among the organic PCMs studied, fatty acids have desirable characteristics including a suitable melting temperature, negligible supercooling through a phase change, outstanding phase transition performance, and non-toxicity nature.

1.3 Research Problem Statement

The direct employment of the organic PCMs for heat storage has several limitations because of their low thermal conductivity, which leads to low charging and discharging rates, leakage through the solid-liquid phase transition and their flammability and instability (Salunkhe & Shembekar, 2012). Several studies have been conducted to overcome these disadvantages. In recent years, there has been considerable interest in employment of supporting materials, such as polymers or porous materials, for shape stabilizing the composite PCMs (Mehrali et al., 2013a; Mehrali et al., 2013b). However, due to large differences between solid inclusions and organic matrix, PCM composites usually show poor stability. To conquer these obstacles encapsulation of PCMs into inert materials is the most potential and beneficial method indeed.

The most profitable objective for PCM encapsulation would be to not only make PCMs easier and safer to use with higher stability but also decrease the reactivity of PCMs and enhance their thermal properties by increasing their heat transfer area (Konuklu et al., 2014; Qiu et al., 2012). Therefore, NE/MEPCMs (nano/microencapsulated PCMs) have numerous benefits, such as preventing the leakage of melted PCMs, control of the volume change during a phase transition, and protection from damaging environmental interactions. These characteristics make NE/MEPCMs much more practical for energy storage applications, such as heat transfer, solar energy storage, building materials, and thermally regulated fibres and textiles (Li et al., 2012).

The traditional encapsulated PCMs were fabricated using polymeric shell materials, such as melamine−formaldehyde resin, urea−formaldehyde resin, polyurethane, polystyrene, styrene−butadiene−styrene copolymer, or poly-(methyl methacrylate) (PMMA), through in situ polymerization or interfacial polymerization in an emulsion system (Tumirah et al., 2014; Zhang et al., 2011). There are several defects, such as flammability, toxicity, inadequate thermal and chemical stability, and low thermal conductivity, for these encapsulated PCMs because of the polymeric shells (Zhou & Zhao, 2011). Likewise encapsulated PCMs with more rigid shells must be produced to prevent the leakage of core material over numerous thermal cycles. Furthermore; since the functional group of fatty acids makes the nano/microencapsulation process more difficult to control than for paraffins, few research studies have been conducted on the nano/microencapsulation of fatty acids (Jamekhorshid et al., 2014).

1.4 Objective of Present Work

According to the previous literatures there is a lack of experimental work on encapsulation of fatty acids, solving the disadvantages of the encapsulated PCMs within

polymeric shell materials and also on investigation of the thermal cycles test on NE/MEPCMs. The overall objective of this study is to synthesize medium temperature (50°C–80°C) encapsulated phase change material with different types of inorganic shell material specifically metal oxides via sol-gel method. The present work is concerned with encapsulation efficiency, the improvement of core and coating materials, energy storage and release capacities, surface morphology and inner structure for prepared materials. A comprehensive knowledge of thermal reliability of the nano/micro-encapsulated PCM as functions of repeated heating and cooling cycles is essential for assurance the long-term performance and economic feasibility of a latent heat storage system. In this regard, this study aims at determining the change of energy storage/release capacities, melting temperature and specific heat capacities of all prepared materials after large number of melt/solidify cycles.

The emphasis of this research is to develop a systematic scientific understanding of the new NE/MEPCMs based on inorganic materials. This is fundamental and substantial for the establishment of knowledge for the development of practical applications in various industries.

The objectives encompass the following aspects of work:

- Preparation of nano/microencapsulated fatty acids as the phase change materials with different types of inorganic shell materials.
- Structural characteristic evaluation of nano/micro-encapsulated phase change material within different types of inorganic shell materials.
- Investigating and optimizing the encapsulation properties of the prepared NE/MEPCMs.

- Investigating the thermal behavior of NE/MEPCMs in terms of latent heat enthalpy, melting features, thermal conductivity, thermal stability and etc.

- Studying the relationship between physical properties such as diameter size or the shell structure of the NE/MEPCMs and thermal properties involved.

- Testing thermal reliability and chemical stability of the prepared NE/MEPCMs.

1.5 Thesis Structure

The entire work of this project is presented in this report in five chapters described briefly as follows. In CHAPTER 1 an introduction is provided which portrays the importance of solar energy and gives a general overview of the research work. CHAPTER 2 includes a literature review on the thermal energy storage, performance enhancement techniques, PCMs and encapsulation of PCMs for latent heat thermal energy storage systems (LHTES). In CHAPTER 3, preparation procedure of NE/MEPCMs and various characterization methods adopted for evaluation of prepared materials are described. CHAPTER 4 explicates the experimental results and discussions on the prepared encapsulated PCMs. CHAPTER 5 gives a summary and conclusion of the current study and recommendations for future work.

CHAPTER 2

LITERATURE REVIEW

2.1 Introduction

In recent years, renewable energy sources, such as solar energy, have emerged as suitable solutions to many environmental issues. These energy sources are intermittent by nature and require a storage system. One of the most significant storage systems is the TES system, of which there are two types, sensible heat thermal energy storage (SHTES) and latent heat thermal energy storage (LHTES). PCMs are among the latent heat storage system. PCMs are attractive materials for thermal energy storage due to their large latent heat and their characteristic of constant temperature in the course of absorbing or releasing energy. They are utilized in applications such as solar energy, smart textiles, heat transfer media, and intelligent buildings (Agyenim et al., 2010; Ling & Poon, 2013; Pielichowska & Pielichowski, 2014). There is a wide variety of PCMs available which melt and solidify at a broad range of temperatures and are utilized in many applications. PCMs should meet some essential characterizations such as, an appropriate phase change temperature, a superior melting enthalpy at the temperature under consideration, and a high density. PCMs must also be non-toxic, non-polluting and inexpensive (Esen et al., 1998; He et al., 2004). PCMs are generally classified into three major types: organics (e.g., paraffins, fatty acids and esters), inorganics (e.g., salt hydrates and metallic alloys), and eutectics (mixtures of inorganics and/or organics). Among all types of PCMs organic PCMs have desirable characteristics including a suitable melting temperature, negligible supercooling through a phase change, outstanding phase transition performance, and non-toxicity. However, the direct employment of these organic PCMs for heat storage has several limitations because of the flammability and instability, low thermal conductivity which leads to low charging and discharging rates and problems with leakage through the solid-liquid phase

transition(Kenisarin & Mahkamov, 2007; Sari & Kaygusuz, 2002). Several studies have been conducted to overcome these disadvantages. In recent years, there has been considerable interest in shape-stable composite PCMs (Kenisarin & Kenisarina, 2012; Zhang et al., 2012) and encapsulation of PCMs within a solid shell (Hawlader et al., 2003; Qiu et al., 2012). Encapsulation of PCMs is a practical solution for these kinds of problems. The most beneficial objective for PCM encapsulation would be to not only make PCMs easier and safer to use but also to decrease the reactivity of PCMs and enhance their thermal properties by increasing their heat transfer area (Salunkhe & Shembekar, 2012). Therefore, NE/MEPCMs have numerous benefits, such as preventing the leakage of melted PCMs, control of the volume change during a phase transition, protection from damaging environmental interactions, etc. These characteristics make NE/MEPCMs more practical for energy storage applications, such as heat transfer, solar energy storage, and etc (Sarier & Onder, 2007).

This study reviews the present state of the art of phase change materials for thermal energy storage applications and provides a deep insight into recent efforts to develop new PCMs showing enhanced performance and safety. Specific attention is given to the improvement of disadvantages of PCMs and PCMs encapsulation procedures. The broad range of PCM applications in the industries is presented and future research directions are outlined.

2.2 Energy Storage

The continuous increase in the level of greenhouse gas emissions and the climb in fuel prices are the main issues these days, therefore generating energy and transmitting it are the forces behind efforts to more effectively utilize various sources of renewable energy (wind and solar energy) (Nema et al., 2012). For instance, solar energy is abundant, cheap and easy to implement with the help of renewable technology, but it is hard to utilize the energy during the scarcity of sunlight. Solar

energy is available only during the day, and hence, its application requires efficient thermal energy storage so that the excess heat collected during sunshine hours may be stored for later use during the night. Here, energy storage system technology could be the only option to store this energy for instant or further implementation of such energy (Waqas & Kumar, 2012). Similar problems arise in heat recovery systems where the waste heat availability and utilization periods are different, requiring some thermal energy storage. Also, electrical energy consumption varies significantly during the day and night, especially in extremely cold and hot climate countries where the major part of the variation is due to domestic space heating and air conditioning. Such variation leads to an off peak period, usually after midnight until early morning (Jin et al., 2013). Short and long term storage of a few hours or months is sufficient in most applications. Energy storage not only reduces the mismatch between supply and demand but also improves the performance and reliability of energy systems and plays an important role in conserving energy and improving its utilization, since many energy sources are intermittent in nature. The fundamental idea of energy storage is to transfer the excess of power (energy) produced by the power plant during the weak load periods to the peak periods. Three different forms of energy that can be stored are mechanical, electrical and thermal energy (Anisur et al., 2013).

2.2.1 Mechanical Energy Storage

Mechanical energy storage systems include gravitational energy storage or pumped hydropower storage (PHPS), compressed air energy storage (CAES) and flywheels. The PHPS and CAES technologies can be used for large-scale utility energy storage while flywheels are more suitable for intermediate storage. Storage is carried out when inexpensive off-peak power is available, e.g., at night or weekends. The storage is discharged when extra power is needed because of insufficient supply from the base-load plant (Huggins, 2010).

2.2.2 Electrical Energy Storage

Energy storage through batteries and capacitors and supercapacitors, and superconducting magnetic energy storage are options for storing the electrical energy. A battery is charged, by connecting it to a source of direct electric current and when it is discharged, it converts stored chemical energy into electrical energy (Chen et al., 2009). Capacitors and supercapacitors (double-layer capacitors) both are electrical components that are used to store electric charge. Capacitors are typically used as short-term backup power, while supercapacitors can also be used to power large engines including vehicles. Superconducting magnetic energy storage (SMES) refers to a relatively new technology which stores electricity from the grid within a magnetic field that is created by the flow of current in a coil (Baker & Collinson, 1999).

2.2.3 Thermal Energy Storage

One very popular form of conversion and storage of variable renewable energy, such as solar energy, is the thermal energy. Thermal energy storage (TES) is a technology that provides the potential to attain energy savings, which in turn reduces the environmental impact related to energy use (Hasnain, 1998). TES systems store thermal energy by heating a storage medium when the solar energy is most available during the daytime, so that the stored energy can be used hours, days or many months later (Gil et al., 2010). Thermal energy storage has various heating applications and power generation in the areas of building heating/cooling systems, solar energy collectors, power and industrial waste heat recovery, auto battery thermal management system and so on (Baylin & Institute, 1979).

The thermal energy storage system can use different techniques to store energy. As it is mentioned in Figure 2-1, TES is divided into three major classifications on the basis of storage mechanism; sensible heat storage by sensible heating or cooling a liquid or solid storage medium such as water, sand, molten salts, rocks, etc., latent heat storage

utilizing the latent heat of the phase change material at its transition temperature, and chemical storage using endothermal and exothermal chemical reaction to store and release thermal energy (Abhat, 1983; Dincer & Rosen, 2002).

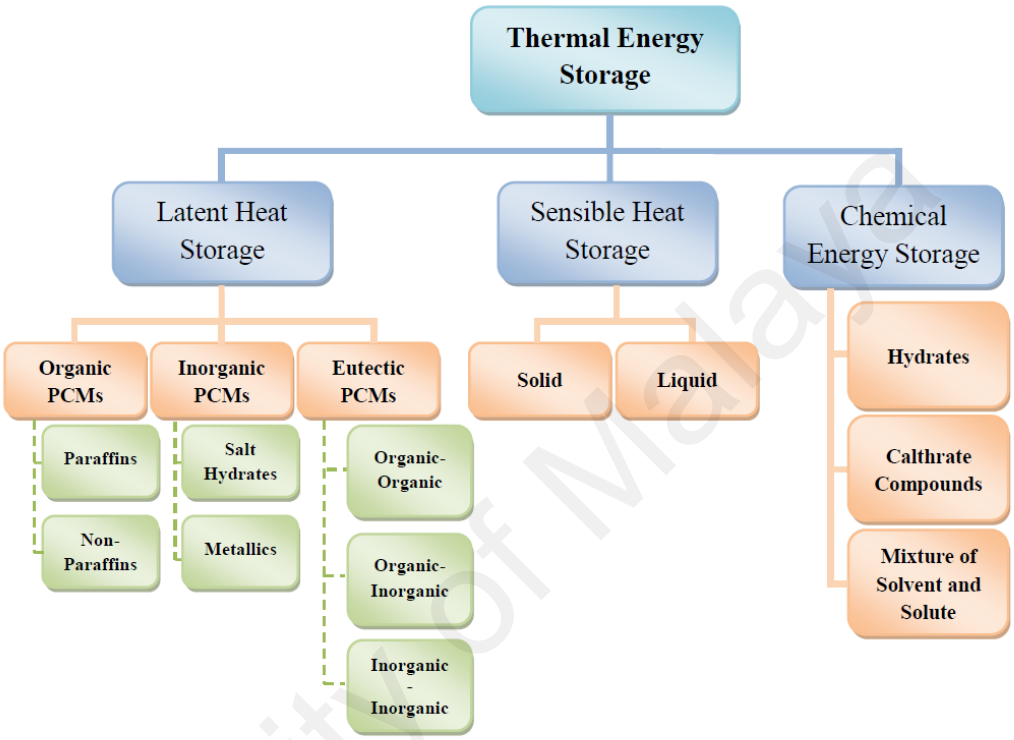

Figure 2-1: Thermal energy storage classifications

2.2.3.1 Chemical Energy Storage

The storage of thermal energy when chemicals either form bonds or break bonds during a chemical reaction is essentially the theory behind chemical energy storage. In thermochemical heat storage systems, heat is stored or released by using reversible endothermic chemical reactions (Khartchenko & Kharchenko, 2013). When a chemical reaction takes places, there is a difference between the enthalpy of the substances present at the end of the reaction and the enthalpy of the substances at the start of the

reaction. This enthalpy difference is known as the heat of reaction. If the reaction is endothermic, it will absorb heat when reaction takes place; if the reaction is exothermic, it will release heat. Therefore, a chemical reaction with a high heat of reaction can be used for thermal energy storage. However, although thermo-chemical heat storage can store large quantities of thermal energy, the use of chemical storage is highly limited. Drawbacks include complexity, uncertainties in the thermodynamic properties of the reaction components and the reaction kinetics under a wide range of operating conditions, high cost, toxicity, and flammability (Aho et al., 2012; Ibrahim et al., 2008).

2.2.3.2 Sensible Heat Storage

The most common way of thermal energy storage is as sensible heat storage. Sensible heat is the amount of heat released or absorbed by a liquid medium (water, oil-based liquids, certain inorganic molten salts etc.) or a solid medium (like rocks, metals, pebbles, and refractory etc.) during a change of temperature. Gases are not good candidates for sensible heat storage due to their low volumetric heat capacity (Demirbas, 2006). The choice of the substances used largely depends upon the temperature level of the application. The amount of heat stored is a function of the mass, specific heat of the medium, and the temperature change which is given by (Zalba et al., 2003):

$$Q = \int_{T_i}^{T_f} mC_p\,dT = mC_p\,(T_f - T_i) \tag{2-1}$$

Where Q is the amount of stored heat, m is the mass of heat storage material, C_p is specific heat of storage material, T_f is final temperature, and T_i is initial temperature (Kuznik et al., 2011).

The sensible heat storage systems require a large volume of material and also a larger temperature difference occurs between storing and retrieval energy process for storing

relatively small quantities of thermal energy which makes the systems thermo dynamically inefficient. These kinds of drawbacks limit the utilization of the sensible heat storage materials. Compared to sensible heat storage, latent heat storage can store larger quantities of thermal energy with smaller temperature difference. Therefore, to decrease the volume of material required, latent heat of phase change could be utilized (Lane, 1983; Sharma et al., 2009).

2.2.3.3 Latent Heat Storage

Of all the thermal heat storage techniques, latent heat storage shows the most promising method due to its capability of storing a large amount of energy with small temperature deviation from storage to retrieval (Hawes et al., 1993). Latent heat storage uses phase change materials (PCM) to store or release thermal energy by changing its phase at a constant temperature. Latent heat materials can store about three to four times more heat per volume than is stored as sensible heat in solids or liquids in a temperature interval of 20℃ (Mehling & Cabeza, 2008). Therefore, as latent heat storage has a higher storage density and it can greatly minimize the volume of the materials and thus reduce the size of the storage system, it seems to be a better method to store heat than sensible and chemical storages. Figure 2-2 shows the difference between sensible and latent heat storage.

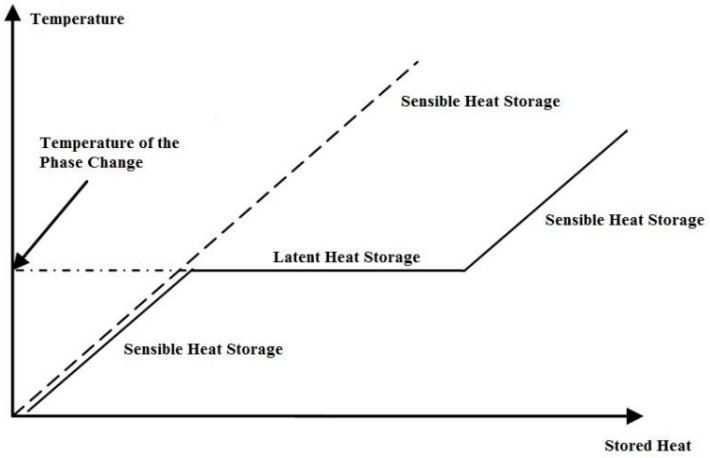

Figure 2-2: Comparison between the heat storage as a sensible heat and the latent heat

Latent heat materials not only store latent energy but also store the sensible heat energy gained from its increase in temperature before and after the phase change. If the melting is completed, further transfer of heat results again in sensible heat storage. The amount of energy that is stored over the phase change temperature range is thus the sum of the latent heat and the sensible heat over this temperature range according to the (Zalba et al., 2003):

$$Q_t = \int_{T_i}^{T_m} mC_p \,.\, dT + ma_m \Delta H_m + \int_{T_m}^{T_f} mC_p \,.\, dT \qquad (2\text{-}2)$$

Where a_m is the fraction melted and ΔH_m is the heat of melting per unit mass (J/kg). The storage of the heat of melting cannot be detected from the temperature, because the melting proceeds at a constant temperature. The latent heat stored during the phase change process, is then calculated from the enthalpy difference (ΔH) between the solid and the liquid phase. Therefore, the heat storage capacity of the material depends on its specific heat and latent heat values. Thus, it is preferable for the storage material to have high specific heat capacity and latent heat values (Jegadheeswaran & Pohekar, 2009).

2.3 Phase Change Materials

Using phase change materials (PCMs) as the latent heat material is an effective way of storing thermal energy. Phase change materials act as thermal storage and they release and absorb relatively large amounts of heat during phase change at constant temperature. PCMs have been widely used in textile, building, solar systems, heat pumps, and spacecraft thermal control applications (Christensen, 1983; Ghahremanzadeh et al., 2010; Stritih & Butala, 2010). The PCMs operate by absorbing heat (charging) and increasing in temperature until phase change temperature. During the phase change stage, it is able to continue to store additional energy by transitioning phases at almost constant temperature and once the temperature begins to cool, the same process repeats with release of heat during the solidification (discharging) process (Kenisarin & Mahkamov, 2007). The latent heat, or heat of fusion, is the energy required for the entire melting of the material. It signifies the variation in thermal energy levels concerning the material's liquid and solid states. PCMs are materials that are known to have a high heat of fusion. This can all be seen in Figure 2-3.

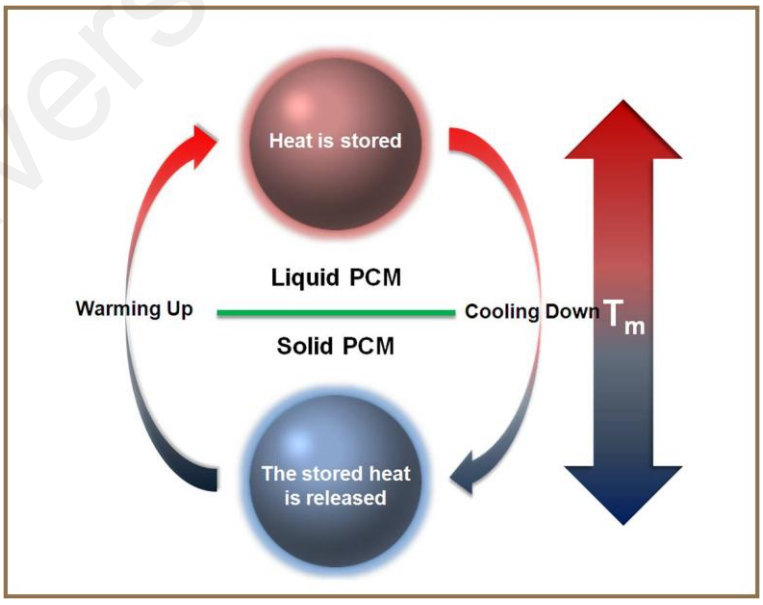

Figure 2-3: The melting and solidifying process of the PCMs

For employment of the PCMs as latent heat storage materials they should meet the following criteria (Humphries et al., 1977).

- High latent heat of fusion and specific heat on a volumetric basis.

The latent heat per volume must be as high as possible to store a large amount of thermal energy in a minimum physical size of the heat store. The high specific heat provides additional significant sensible heat storage.

- High thermal conductivity of both solid and liquid states.

The high thermal conductivity could accelerate the charging and discharging of the energy storage and cause faster heat transfer overall so that the PCM can reach thermal equilibrium (Zhang et al., 2010).

- Suitable phase-transition temperature.

For a specific TES system the transition temperature of the PCM should be in the required operating temperature range of the application.

- High nucleation rate.

To avoid supercooling of the liquid phase during the solidification the nucleation rate must be high. Supercooling which is also known as sub-cooling represents the cooling of the liquid phase to a temperature below its solidification point without it becoming a solid. During the supercooling there is no latent heat release due to the fact that the material remains in the liquid state and no phase transition happens. This phenomenon will decrease the transfer efficiency of this material (Abhat, 1983).

- High rate of crystal growth.

Usually a high rate of crystal growth is required to achieve solidification at a satisfactory rate which assists the system to meet demands of heat recovery from the storage system.

- High density.

The higher density would reduces the mass of the required PCM and maximize the heat storage per unit.

- Small volume change on phase transformation and low vapor pressure at operating temperature.
- Desired chemical properties such as: chemical stability, no thermal decomposition after a large number of freeze/melt cycles, compatibility with other used materials, non-corrosiveness, no toxicity and non flammability.
- Availability and cost effectiveness.

2.4 Classifications of PCMs

Phase change materials can be classified according to some aspects. PCMs could be categorized depending on the temperature ranges over which their phase change happens including: the low temperature PCMs (with the phase change temperature below 15℃, which can be utilized in food industry or air conditioning), mid temperature PCMs (with the phase change temperature in the range of 15–90℃, which can be used in the solar, medical, textile, electronic and energy-saving applications in building design), and the high temperature PCMs (with the phase change above 90℃ for industrial and aerospace applications) (Agyenim et al., 2010). From the other aspect of view PCMs could be listed in their mode of phase change: gas–liquid, solid–gas, solid–liquid and solid–solid systems. In solid–solid transitions, heat is stored as the material is transformed from a low symmetry crystal structure to a high symmetry one. This type of

solid-solid phase change materials has advantages such as the small change in volume over the heating process, no leakage, a low level of corrosion, and a long life span. However the disadvantages are the lower latent heat and the higher phase change temperature compared to the other two types (Sharma & Sagara, 2005). On the other hand, a liquid to gas latent heat material, has a very large phase change enthalpy, but any phase change to gas is impractical for a closed system due to the large volume expansion of the material that requires either a large storage tank to minimize the increases in pressure or a fixed volume container strong enough to withstand the pressure increase without rupturing. Therefore, using a liquid gas transition is a poor choice for TES (Banaszek et al., 1999). By contrast, solid-liquid phase change is more favorable practically due to the fact that during a solid-liquid transformation about 10% of volumetric expansion occurs which is less than the expansion that occurs during vaporization, although, the latent heat of solid – liquid is high compared to the solid – solid transition (Farid et al., 2004). The solid-liquid PCMs could be categorized into three major categories: organic, inorganic, and eutectic PCMs (Farid et al., 2004) based on their components.

2.4.1 Organic PCMs

Organic PCMs typically have a lower latent heat capacity and melting temperature making them less beneficial as latent heat storage materials. However, they are the safest PCMs to use and they do not segregate, which is a common problem for PCMs over time. They can also be used with metals. Organic materials are further classified as paraffins and non-paraffins (fatty acids, esters, alcohols and glycols) (Mehling & Cabeza, 2007).

2.4.1.1 Paraffins

Paraffins contain alkanes with the general formula C_nH_{2n+2}. The n-alkane content in paraffin waxes usually exceeds 75% and may reach 100%. Pure paraffins contain

only alkanes in them, such as the paraffin octadecane $C_{18}H_{38}$. Paraffins possess high latent heat storage capacities and are suitable candidates for PCMs because of their very broad range of melting temperature. For example, the melting points of $C_{10}H_{22}$, $C_{30}H_{62}$, and $C_{40}H_{82}$ are 29.7^{o}C, 65.4^{o}C, and 81.5^{o}C, respectively. In these materials, the melting point increases with increasing average molecular weight (Finke et al., 1954; Parks et al., 1946).

Pure paraffin waxes are very expensive, therefore only commercial paraffin waxes may be used as PCMs in latent heat storage systems. Commercial paraffin waxes, which melt around 55℃, have been studied most. Farid et al. (1990) have employed three commercial waxes having melting temperatures of 44, 53 and 64℃ with latent heats of 167, 200 and 210kJ/kg, respectively, in the storage unit to improve its performance. Normal or straight chain and symmetrically branched chain paraffin waxes are the most stable. Paraffins are safe, non-reactive, nontoxic, less expensive and non-corrosive. They do not undergo phase segregation and do not significantly degrade with thermal cycling.

However, they have some inherent disadvantages like their low thermal conductivity and flammability, and supercooling which might limit their efficient use (Oró et al., 2012). They have also relatively lower thermal storage capacity compared to the other PCMs, which is the result of their lower density and lower latent heat of fusion. Thermo-physical properties of some paraffins are given in Table 2-1 (Babich et al., 1994; Nagano et al., 2003; Paris et al., 1993).

Table 2-1: Thermo-physical properties of some paraffins

Material	Formula	Melting point (℃)	Latent heat (kJ/kg)
Tetradecane	$C_{14}H_{30}$	5.5	228
Pentadecane	$C_{15}H_{32}$	10	205
Hexadecane	$C_{16}H_{34}$	16.7	237
Heptadecane	$C_{17}H_{36}$	21.7	213
Icosane	$C_{20}H_{42}$	36.7	246
Tricosane	$C_{23}H_{48}$	47.5	232
Hexacosane	$C_{26}H_{54}$	56.3	256
Nonacosane	$C_{29}H_{60}$	63.4	240
Dotriacontane	$C_{32}H_{66}$	69.5	170
Tetratriacontane	$C_{34}H_{70}$	75.9	269

2.4.1.2 Non-paraffins

The non-paraffin organics are the most numerous phase change materials including fatty acids (caprylic, capric, lauric, myristic, palmitic and stearic) and other non-paraffins such as esters, alcohols and glycols. Each of these materials will have its own properties unlike the paraffins which all possess very similar properties. Abhat and Buddhi have conducted extensive surveys of organic materials and identified a number of esters, fatty acids, alcohols and glycols promising for latent heat storage (Abhat, 1983; Buddhi & Sharma, 1999). Feldman et al. (1989) have analyzed the thermal properties of fatty acids and their binary mixtures. They concluded that the fatty acids have a fairly high heat of fusion comparable to the other organic PCMs like paraffins. The general chemical formula of fatty acids is $CH_3(CH_2)_{2n}COOH$. Because fatty acids consist of one component, they are stable upon cycling. They are known to have a sustained melting and solidifying behavior with no or minor supercooling which qualifies them as good phase change materials. However, fatty acids are flammable, have a low thermal conductivity and have varying level of toxicity (Sharma et al., 2009)

The melting range of the fatty acids was found to vary from 15℃ to 80℃, while their latent heat of transition was observed to vary from 140kJ/kg to 250kJ/kg. With an increasing number of carbon atoms in the fatty acids molecule, the melting and solidifying points, the heat of melting and the degree of crystallization gradually increase. Thermo-physical properties of some saturated fatty acids are given in Table 2-2 (Rozanna et al., 2005).

Table 2-2: Thermo-physical Properties of Fatty Acids

Material	Formula	Melting point (℃)	Latent heat (kJ/kg)
Caprylic acid	$CH_3(CH_2)_6.COOH$	16-17	148-149
Capric acid	$CH_3(CH_2)_8.COOH$	30-32	153-163
Lauric acid	$CH_3(CH_2)_{10}.COOH$	41-44	178-183
Myristic acid	$CH_3(CH_2)_{12}.COOH$	49-58	167-205
Palmatic acid	$CH_3(CH_2)_{14}.COOH$	61-64	186-212
Stearic acid	$CH_3(CH_2)_{16}.COOH$	65-70	196-253
Nonadecylic acid	$CH_3(CH_2)_{17}.COOH$	67	192
Tricosylic acid	$CH_3(CH_2)_{21}.COOH$	79	212

2.4.2 Inorganic PCMs

Inorganic materials cover a wide temperature range but usually have similar melting enthalpies per unit mass. The phase change enthalpies per unit volume of inorganic PCMs are higher than those of the organics due to their high density. They are also non-flammable. Their main disadvantages are sub-cooling, phase segregation, and incompatibility with metals since severe corrosion can be developed in some PCM-metal combinations. Inorganic compounds are further classified as salt hydrate and metallics (Ling & Poon, 2013).

2.4.2.1 Salt hydrates

Salt hydrates are inorganic salts consisting of salts and water which combine in a crystalline matrix of general formula $AB.nH_2O$. Hydrated salts are attractive materials for application in thermal energy storage due to their appropriate properties such as; high latent heat of fusion per unit volume, relatively high thermal conductivity (almost double of the paraffin's) and moderate costs compared to organic PCMs, with few exceptions. They are the best options for low temperature ranging from 0℃ to 99℃, based on their thermal properties. However, they are corrosive and not very compatible with most metallic materials. Additionally some of the salt hydrates have the major problem of incongruent melting which is caused by the fact that the released water of crystallization is not sufficient to dissolve all the solid phase present and subcooling before crystallization which is due to their poor nucleating properties. Thermo-physical properties of some salt hydrates are shown in Table 2-3 (Regin et al., 2008; Zhou et al., 2012).

Table 2-3: Thermo-physical Properties of salt hydrates

Material	Melting point (℃)	Latent heat (kJ/kg)
$K_2HO_4.6H_2O$	14	109
$FeBr_3.6H_2O$	27	105
$LiNO_3.3H_2O$	30	189
$Na_2SO_4.10H_2O$	32.4	241
$KF.2H_2O$	42	162
$Ca(NO_3).4H_2O$	47	153
$MgCl_2.4H_2O$	58	151
$Al(NO_3)_2.9H_2O$	72	155
$Ba(OH)_2.8H_2O$	78	265

2.4.2.2 Metallics

Metallic alloys include the low melting metals and metal mixtures which could be employed as PCMs since they provide large storage capacity on a volume basis, high thermal reliability and high thermal conductivity. The large phase change heat has been achieved for binary and ternary alloys from the relatively abundant elements like Al, Cu, Mg and Zn, Ga, etc (Chen et al., 1997). However, the use of metallics has not seriously been considered for thermal energy storage applications due to their lower latent heat of fusion compared to the other PCMs and the weight penalties. A list of some selected metallics is given in Table 2-4 (Birchenall & Riechman, 1980).

Table 2-4: Thermo-physical properties of metallics

Material	Melting point (℃)	Latent heat (kJ/kg)
Gallium	30	80.3
Cerrolow eutectic	58	90.9
Bi-Cd-In eutectic	61	25
Bi-In eutectic	72	25

2.4.3 Eutectic PCMs

A eutectic PCM is a minimum-melting composition of two or more PCMs to formulate mixtures with sufficient properties to achieve the desired melting temperature point, high latent heat storage capacity, low flammability, and controlled supercooling. There are three groups of eutectics: organic-organic, inorganic-inorganic, and organic-inorganic combinations of PCMs. Eutectics nearly always melt and freeze without segregation since they freeze to an intimate mixture of crystals, leaving little opportunity for the components to separate. On melting both components liquefy simultaneously, again without separation (Baetens et al., 2010). They have a sharper melting point and slightly higher thermal storage density per volume than organic

compounds. However, they are relatively new to thermal storage applications therefore there is limited research focused on the thermo-physical properties of eutectics such as chemical composition, latent heat, and thermal stability. In Table 2-5 the thermo-physical properties of some selected eutectics are given (Baran & Sari, 2003; Sharma et al., 2009).

Table 2-5: Thermo-physical properties of some selected eutectics

Material	Composition (wt.%)	Melting point (℃)	Latent heat (kJ/kg)
$CaCl_2.6H_2O+CaBr_2.6H_2O$	45+55	14.7	140
$C_{14}H_{28}O_2+C_{10}H_{20}O_2$	34+66	24	147.7
Triethylolethane+urea	62.5+37.5	29.8	218
$Mg(NO_3)_3.6H_2O+NH_4NO_3$	53+47	46	95
Napthalene+benzoic acid	67.1+32.9	67	123.4

2.5 Limitations of PCMs in Applications and their Obviation Methods

Advantages of PCMs in general are their availability in a large temperature range for different working requirements, their high thermal energy storage density and quasi-constant phase change temperature (Zhang et al., 2010). Organic PCMs have a number of important specifications including, the wide variety to choose from, low volumetric latent heat storage capacity, chemically and thermally stability, compatibility with various materials, high heat of fusion (ranging from 45kJ/kg to 210kJ/kg), low or no subcooling, small phase segregation, and non toxicity. Despite the obstacles of inorganic PCMs like the large volume change in the melting process, corrosion, poor thermal stability, and phase separation, the main advantages of them in comparison to organic PCMs are their greater phase change enthalpy, higher thermal conductivity,

easy availability and inflammability (Kuznik et al., 2011; Zalba et al., 2003). Eutectics are presented as a parallel category for comprehensibility; they are mixtures of organic and/or inorganic materials at specific composition providing a sharp phase change temperature (Cabeza et al., 2011). In spite of all the desirable properties of PCMs mentioned earlier, there are some major problems associated with the applications. The major obstacle to the wide application of PCMs is the leakage of the molten PCM after they absorb enough energy to complete the phase change to a liquid. This leakage of the PCM causes failure in its application value, therefore; preventing this leakage is one of the major requirements for widespread use of PCMs in the thermal energy storage applications (Dincer & Rosen, 2002). The leakage of PCMs may be an issue over the lifetime of many years. The other most important disadvantage of the PCMs is their low thermal conductivity which leads to slow charging and discharging rates and causes low heat transfer performance. Although inorganic PCMs exhibit higher thermal conductivity, it rarely surpasses 0.7W/m.K (Pasupathy et al., 2008; Zalba et al., 2003). As reported by (Bugaje, 1997) the phase change process (charging and discharging) time is the most important design parameter in latent heat storage systems. Several studies have been conducted to overcome these disadvantages. Typical solutions like adding materials with high thermal conductivity to the pure PCM (Ding & Yin, 2004; Wen & Ding, 2004), using extended surfaces by addition of fins (Ettouney et al., 2004; Solomon et al., 2013), shape stabilized PCMs and impregnation of PCMs to highly conductive matrices (Mesalhy et al., 2006; Siahpush et al., 2008) and encapsulation of PCMs (Qiu et al., 2012; Zheng et al., 2013).

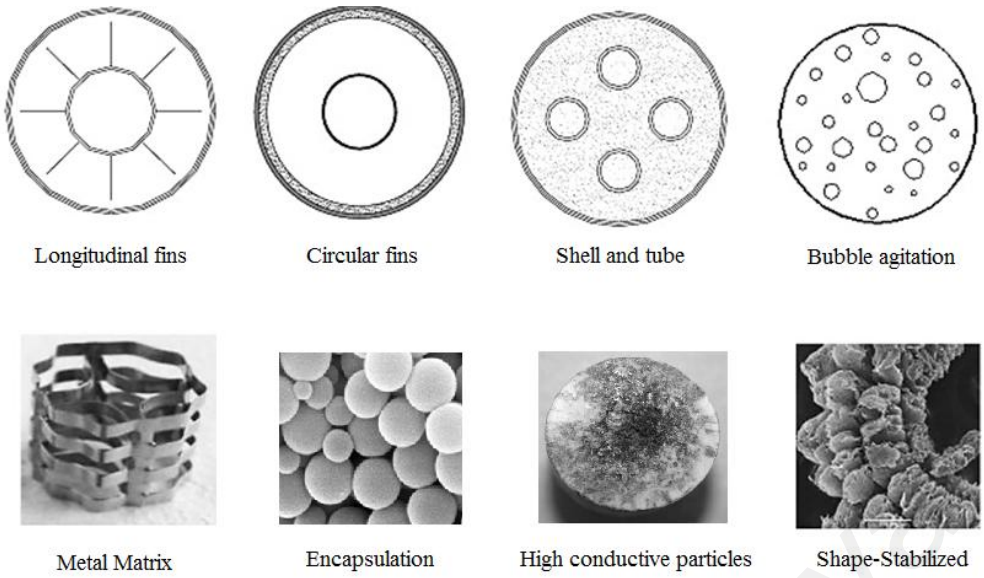

Figure 2-4: Heat transfer enhancement methods employed for PCMs (Salunkhe & Shembekar, 2012)

Other properties, such as flammability, volume change, and corrosion issues also limit the use of PCMs in building structures, and impose constraints on the storage containers as well as on the heat exchanger materials. These issues can however be overcome with adequate choice of storage container and heat exchanger material (Tyagi et al., 2012). Among these solutions encapsulation is an effective process in which small particles of PCMs are coated by some shell material (Salunkhe & Shembekar, 2012). Hawlader et al. (2003) concluded that the encapsulated paraffin wax shows an impressive potential for solar thermal-energy storage applications.

2.6 Phase Change Materials Encapsulation

Phase change material encapsulation is one of the most practical solutions for overcoming the problems due to the disadvantages of PCMs. Encapsulation is defined as the process of covering the PCM as the core material within another substance as the shell material (Hawlader et al., 2002). The functioning process of the encapsulated PCM (EPCM) can be explained as follows. In solid state, the supplied heat to the PCM increases its temperature until it reaches the melting point. As the shell resides the PCM

in a solid state, when the melting point is reached, the shell transfer the heat from the surrounding to the PCM. The PCM melts into a liquid state at a constant temperature while remaining inside the shell. Through this phase transition process significant volume of heat is stashed. The molten PCM transforms to solid when the surrounding has a temperature lower than its melting point through the same procedure as the melting process. The phase change accomplish through discharge of thermal energy throughout sensible cooling and the phase change procedure from the liquid to solid (Figure 2-5).

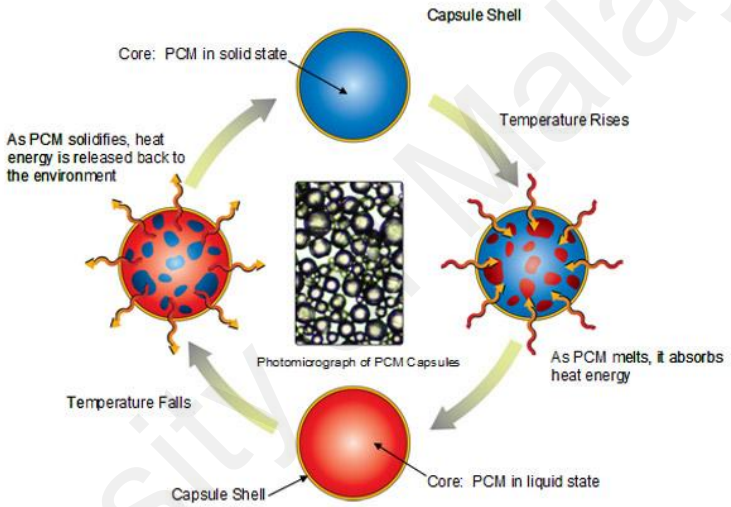

Figure 2-5: Encapsulated PCM melting/solidifying process

A major aim of encapsulation is retaining the liquid and/or solid phase of the PCM and holding it separated from the surrounding. This assures proper composition of the PCM that might have otherwise changed because of mixing of the PCM with the surrounding materials. Additional benefits of encapsulation include decrease in reaction PCM with all the surrounding, flexibility in frequent phase change processes, increase in the heat transfer area which causes increase in heat transfer coefficient of the system and improvement in thermal and mechanical stability of the PCM. It may also enhance the compatibility of hazardous PCMs that cannot be directly utilized or immersed in some applications like food storage, building cooling/ heating, etc. A significant issue

for the encapsulation of inorganic PCMs is their corrosion with metals and complete solubility in water. In comparison, organic PCMs are non-corrosive and display negligible or incomplete solubility in water (Li et al., 2007; Su et al., 2015).

However, most of the organic PCMs are flammable. The flammability can be reduced by encapsulating the PCM with an inorganic material. The shell should be strong enough to sustain the stresses that are generated due to volumetric changes during the phase change process of the PCM. Encapsulations are usually classified by their size as macro (larger than 1mm), micro (1 μm to 1 mm) and nano (smaller than 1 μm) encapsulated PCMs (Yamagishi et al., 1999).

Macroencapsulation, is comprising the PCMs which are encapsulated in a container in some form of package such as tubes, spheres, panels or other receptacles. These containers usually are larger than 1mm and made of metal or plastics. Macroencapsulation is very common in long thin heat pipes, PVC panels, heat exchangers or in building products because such containers or bags are available in a large variety (Chen et al., 2000). However, large macro encapsulation has not performed well in earlier studies due to the poor thermal conductivity of the PCM, and also because in the phase change process the edge remains solid, whereas, core part may still remain in the liquid form, thus this prevent the effective heat transfer (Cho & Choi, 2000).

Manufacturing of nano/microencapsulated PCM (NE/MEPCM) is more complex than macroencapsulated but nano/microencapsulation is more efficient and applicable in the thermal storage applications. Nano/microcapsules have higher heat transfer rates than macrocapsules attributed to a substantially higher surface area to volume ratio, ability to withstand the change in volume during phase change process and less chemical reactivity of PCM with the shell material. A higher heat transfer rate results in

rapid melting and solidification of the NE/MEPCMs (Khudhair & Farid, 2004). Nano/microencapsulating PCM has several considerable benefits such as providing a larger surface area for heat transfer to the surroundings because of the large surface-to-volume ratio of the capsules, and the leakage preventing of the molten core material. Furthermore, it is also possible to integrate microencapsulated PCM into other materials, such as building insulations, or food containers (Fang et al., 2009). However, in some fields, especially in latent functionally thermal fluids, microencapsulated PCMs are not appropriate for repeated cycling, because the large size particles of the PCM microcapsules increase the fluid's viscosity; thus it is obligatory to develop PCM nanocapsules with smaller particle sizes as compared with microcapsules (Fang et al., 2008). In recent years, several kinds of nanoencapsulated PCMs were synthesized by different methods. Nanocapsules of n-octacosane with PMMA (poly (methyl methacrylate)) shells were investigated by Sarı et al. (2009a) . The nanocapsules had energy storage and release capacity of 86.4-88.5 kJ/kg during their phase change. Kwon et al. (2010) also prepared nanocapsules of n-octacosane. Nanocapsules of n-hexadecane with the shell of poly (alkyl methacrylate) were fabricated by Black et al. (2010) while Alay et al. (2010) synthesized PMMA/n-hexadecane nanocapsules as a fiber additive in textile application.

Depending on the physico-chemical properties of the core, the wall composition, and the used microencapsulation techniques, nano/microcapsules may be shaped in different types as shown in Figure 2-6: simple sphere with a continuous wall surrounding the core; particle containing an irregular shape core; smaller droplets of core material embedded throughout the capsule; several distinct cores within the same capsule and multi-walled capsules (Gharsallaoui et al., 2007). Among all of them, simple sphere particle is the most common one being fabricated and utilized.

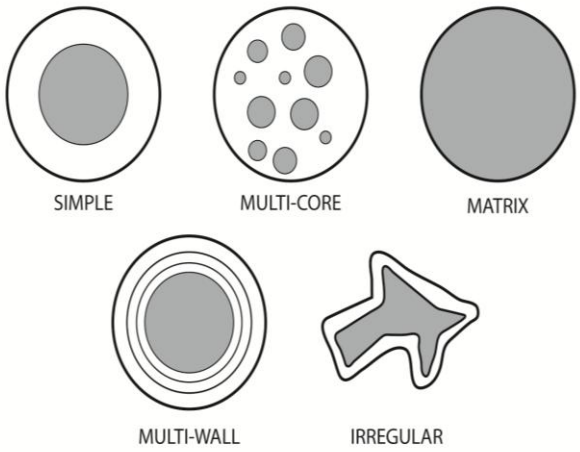

Figure 2-6: Morphology of different types of microcapsules

Core materials commonly act as the main functional component in a core/shell capsule structure and the shell materials provide insulation from the environment and also can enhance some properties of the nano/microcapsules like thermal conductivity. The shell material must be compatible with PCM and can be from a wide range of materials including organic polymers or inorganic materials. Among the phase change materials encapsulation of the inorganic PCMs is more difficult than the organic ones and also their stability during temperature cycling is not as good as organic PCMs.

2.6.1 Shell Materials

The shell material plays an important role in the mechanical and thermal characteristics of the encapsulated PCMs. An appropriate shell material should have sufficient structural and thermal stability to withstand the phase change process of PCM, should retain all the thermo-physical properties at the nano/micro level size, be leak proof, not react with the core PCM, have a high thermal conductivity to ease the heat transfer between the PCM and its surrounding. A high strength shell material with suitable thermal characteristics not only enhances the performance of a system but also

allows the PCM nano/microcapsules to withstand the large number of thermal cycles (Khodadadi & Hosseinizadeh, 2007; Mettawee & Assassa, 2007).

2.6.1.1 Polymers Used as Shell Materials

Common materials that have been selected as the shell materials for the traditional nano/microencapsulated PCMs are organic polymers or macromolecules (Zhao & Zhang, 2011). Zhang and Wang (2009) synthesized microencapsulated n-octadecane with polyurea shells. Polyurea was considered as an optimal shell material because it has good physical properties and chemical stabilities, and it also does not cause environmental and health problems like melamine–formaldehyde resin and urea–formaldehyde resin do. Fan et al. (2004) synthesized n-alkane microcapsules using 70 wt.%. n-octadecane with melamine formaldehyde shell by in situ polymerization. They studied the stirrer rate and the dosage of emulsifier in the process. Sun and Zhang (2002) investigated effect of different coating materials, namely, melamine–formaldehyde, urea–formaldehyde and gelatin on the mechanical strength of the microcapsule. It was observed that melamine–formaldehyde and urea–formaldehyde ruptured under the compression test, whereas, gelatin was found to be structurally stable. In another survey, Shin et al. (2005) prepared melamine–formaldehyde microcapsules containing eicosane. They concluded that the prepared materials had heat storage capacities of 0.91–4.44kJ/kg. Alkan et al. (2009) investigated preparation, characterization and thermal analysis of the microcapsules with docosane as the core material and PMMA as the coating material. The microcapsules had a smooth and compact surface with an average diameter of 0.16μm. After 1000, 3000 and 5000 thermal cycles, a substantially improved thermal reliability was observed in terms of change in temperature and enthalpy. Bayés-García et al. (2010) assessed thermal stability of microcapsules synthesized by different shell compositions, namely, sterilized gelatine/arabic gum (SG/AG) and agar-agar/arabic gum (AA/AG). Onder et

al. (2008) also used a gum arabic–gelatin mixture as the shell material with different types of paraffin waxes, namely n-hexadecane, n-octadecane and n-nonadecane as the core materials. The microcapsules with n-octadecane gave the highest enthalpy value of 166kJ/kg. Sánchez et al. (2008) investigated the influence of reaction temperature, stirring rate, and the mass ratio of paraffin wax to styrene on the thermal properties of microcapsules.

The organic polymeric wall materials play an important role in improving the structural flexibility, permeability, and controlled release with easier processing toward the nano/microencapsulated PCMs, it is no doubt that these NE/MEPCMs with polymeric shells also have some disadvantages including poor thermal and chemical stabilities, flammability and low thermal conductivity (Cai et al., 2009; Fang et al., 2010a).

2.6.1.2 Inorganic Materials as the Shell Materials

Regarding to the obstacles of the organic polymers as the shell material, it is necessary to find other types of materials which can overcome the limitations of the polymers. Compared to the organic polymer materials the thermal conductivity, the chemical and thermal stabilities, mechanical strength, and flame retardancy of inorganic materials are always significantly higher. So employing an appropriate inorganic material as shell for the NE/MEPCMs is a promising idea to improve their phase-change performance, whereas few studies report on the nano/microencapsulation technologies for PCMs with inorganic shell (Salunkhe & Shembekar, 2012). Use of inorganic shell materials has gained growing interest recently and just some attempts have been accomplished to encapsulate PCMs within the silica shell. Silica materials are nontoxic; in addition, they have a high surface area and tunable pore sizes. Their structures are stable and their surface properties well-defined. Silica spheres have a desirable thermal conductivity (Pan et al., 2009). In a survey Jin et al. (2010) developed

a one-step synthetic technique for the microencapsulated PCMs with the silica wall under a surfactant or dispersant free condition. Moreover, Li et al. (2013) and Fang et al. (2010a) reported the preparation and phase change properties of the PCM microcapsules based on paraffin core and silica wall through in-situ polycondensation.

The sol-gel process as one of the applicable methods enables the encapsulation of different compounds by metal oxides in very mild conditions like room temperature and atmospheric pressure. The sol-gel process usually is combined with emulsion technology to obtain the metal oxide encapsulated compounds (Livage et al., 1988).

2.6.2 Applications of Nano/Microencapsulated PCMs

Nano/microencapsulated phase change materials are very attractive in improving the thermal performance in some application such as textile fabrics, building, slurry applications and solar water heating (Griffiths & Eames, 2007) (Shin et al., 2005) (Tyagi et al., 2012; Zhang et al., 2010).

2.6.2.1 Textile Applications

Many studies have been done on NE/MEPCM textile materials. Sarier and Onder (2007) used four types of polyurea–formaldehyde microcapsules containing different waxes for the design of thermally enhanced fabrics. They demonstrated that a combination of microcapsule containing different types of PCMs were better than those including a mixture of them.

2.6.2.2 Building Applications

By encapsulating suitable PCMs within the surfaces of walls, ceilings and floors of buildings, energy storage in those surfaces can be increased which can accumulate solar energy in the daytime to be used for heating at nights or during cloudy periods. (Tyagi et al., 2012). Su et al. (2005) prepared a double shell MEPCM with a melting point of 24℃ and a heat of fusion of 225.5kJ/kg for building application. They

concluded that the double shell microcapsules were better than single shell ones in terms of avoiding penetration, and the average diameter of 5μm were better than 1μm. Hawlader et al. (2003) investigated the microencapsulation of paraffin wax in polymeric films. Results from differential scanning calorimeter tests showed that the paraffin microcapsules had high heat storage and release capacities and were suitable for building energy storage applications.

2.6.2.3 Nano/Microencapsulated PCM Slurries

The concept of a carrier fluid for encapsulated particles of phase change materials was first introduced by Mehalick and Tweedie (1975). When the NE/MEPCM is dispersed into the carrier fluid like water, a kind of suspension named as nano/microencapsulated phase change slurry (NE/MEPCMS) is formed. Due to its special properties such as high energy storage density, low pumping power requirements, and high heat transfer rates between the wall and the suspension a lot of research work has been conducted on the PCM suspension flow. NE/MEPCMS can serve as both the energy storage and heat transfer media because of the relatively large surface area to volume of NE/MEPCM, in addition, the agglomeration of NE/MEPCM can be avoided due to the encapsulation (Chen et al., 2014). Roy and Sengupta (1991) used n-eicosane and stearic acid as phase change material for MEPCMS, the microcapsules were manufactured with two different wall thickness; they found that the microcapsules with thicker walls were able to withstand repeated thermal cycling past the melting point. In another study Wang et al. (2007) demonstrated that the heat transfer coefficients measured for MEPCM slurry are significantly higher than for those of single-phase fluid flow.

2.7 Summary

The concept of solid-liquid phase change materials as the latent heat materials for thermal energy storage was introduced in this chapter. The important aspect of high

heat content at narrow ranges of temperature supports the use of PCM in solar applications, but various other thermo-physicals, kinetic and chemical properties have also been identified as essential to the proper utilization of PCMs. The lack of certain desired properties can be overcome through appropriate system design. The classification of PCMs into organic, inorganic and eutectics has been presented.

Solid-liquid PCMs are found to have poor heat transfer properties and hence are not used directly as a heat transfer medium. Encapsulation of PCMs was introduced as one of the most significant methods to overcome the hindrances of PCMs. The concept and classification of EPCMs were presented by introducing previous researches that have been done. The importance of choosing an appropriate shell material was discussed. The majority of PCM systems encountered in the literature have been studied for the encapsulated PCMs in the organic polymer shell materials. The difficulties of using polymer materials as the shell material like low thermal conductivity, flammability and complex synthesis process, etc were discussed.

The following chapters describe the novel materials and NE/MEPCMs with inorganic shell materials employed in this study to enhance the performance of NE/MEPCMs.

CHAPTER 3

MATERIALS AND METHODS

3.1 Introduction

In this chapter the theory of fundamentals and technologies of manufacturing the NE/MEPCMs within three different kinds of metal oxides is brought up. The processing techniques including material selection, determination of specific parameters and material pretreatment are thoroughly discussed. A full factorial experimental design and its principals are determined.

Characterization of the materials and their preparation methods are addressed in this chapter. A number of modern characterization techniques were adopted to study the structure and morphology features of novel NE/MEPCMs. These techniques including Field Emission Scanning Electron Microscopy (FESEM) and Transmission Electron Microscopy (TEM) for surface and inner structure observation; Fourier Transmittance Infrared Spectra (FT-IR), X-ray Diffractometry (XRD), Differential Scanning Calorimetry (DSC), Thermal Gravimetry (TGA). These instruments were applied to the objective evaluation of chemistry and identification of physical structure. The thermal cycling test was also introduced to investigate the thermal performance of the prepared NE/MEPCMs. The thermal conductivity of the prepared PCMs were measured by two methods and explained in this chapter. The materials research for TES applications and some fundamental aspects that should be considered was followed in this research which is shown in Figure 3-1.

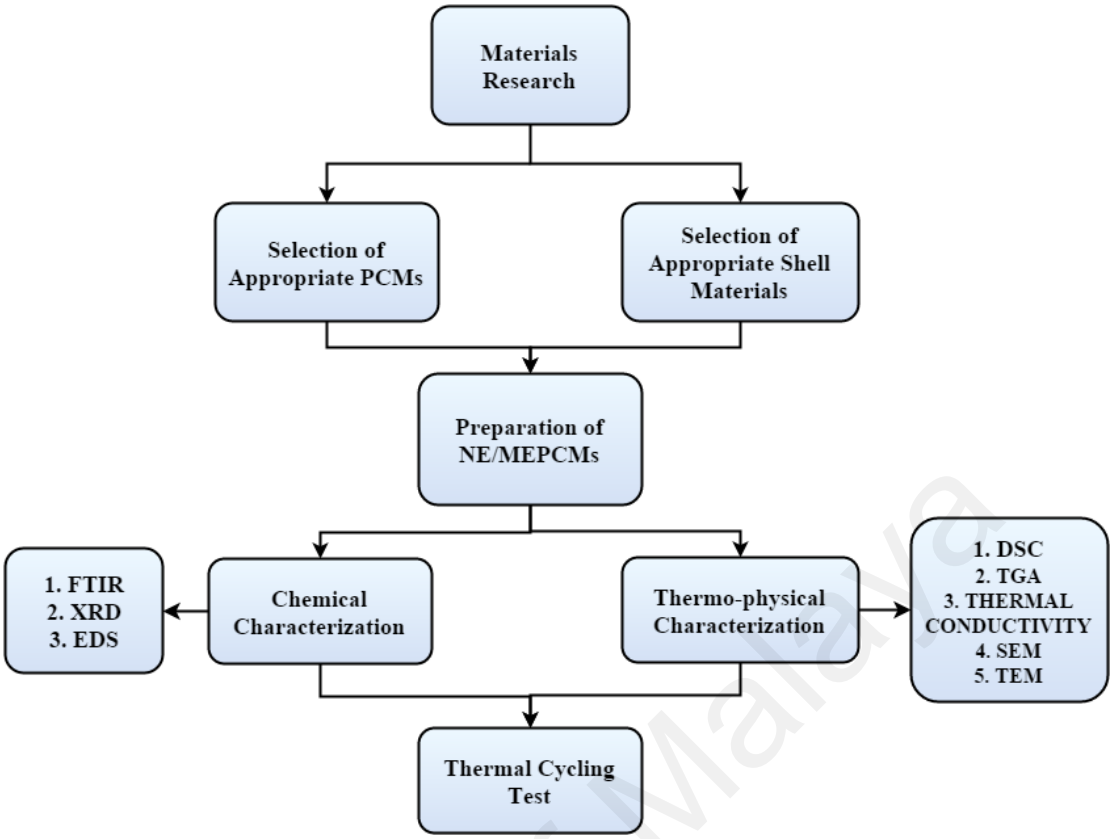

Figure 3-1: NE/MEPCMs preparation and characterization process

3.2 The Selection of Appropriate PCMs as the Core Material

For choosing core materials, there are several rules that should be followed for increasing the efficiency of the TES system (CHAPTER 2). However, it is impossible to find a kind of material that can meet all the requirements. Therefore; the most important parameters such as appropriate melting temperature, high latent heat and high thermal stability were considered to choose the appropriate PCM candidates for the solar application which is one of the objectives in this project. For outdoor conditions in solar applications, the transition temperature should be in the range of 50℃ to 75℃ in most cases. Among the PCMs, stearic acid and palmitic acid as kinds of fatty acids are the materials that can meet these required properties. The melting points of them are between 52℃ and 70℃, which is just in the temperature range of the solar energy

systems. The required materials for our experiments were procured from Fisher Scientific, Inc.

3.2.1 Palmitic Acid

Renewed interest in the use of fats and oils for sustainable chemistry has led to the growing importance of materials prepared from them. Animal and plant based fats and oils are typically hydrolyzed to obtain mixtures of fatty acids that are purified and subsequently separated. The fatty acids are easily producible from common vegetable and animal oils. Thus it provides an assurance of continuous supply despite the shortage of fuel sources. Fatty acids have high heat of fusion values comparable to those of paraffin's. They also show reproducible melting and freezing behavior and freeze with negligible supercooling.

Generally, fatty acids are aliphatic carboxylic acid consists of a straight chain of an even number of carbon atoms, with hydrogen atoms along the length of the chain and at one end of the chain joined to terminal carboxyl (−COOH) group at the other end. That carboxyl group makes it an acid (carboxylic acid). If the carbon-to-carbon bonds are all single, the acid is saturated; if any of the bonds is double or triple, the acid is unsaturated and is more reactive. The saturated fatty acids are white, waxy, natural fatty acids which are fairly insoluble in water but can be somewhat soluble in alcohol.

Palmitic acid (also called n-hexadecanoic acid; 1-pentadecanecarboxylic acid; cetylic acid; hexadecylic acid) is a saturated fatty acid that is commonly found in both animals and plants. As its name indicates, it is a major component of the oils from palm trees, such as palm oil, palm kernel oil and coconut oil, but can also be found in meat and dairy products. Its chemical formula is $CH_3(CH_2)_{14}COOH$. The chemical structure of palmitic acid (PA) as an example of saturated fatty acid and also the unsaturated PA

as an unsaturated fatty acid are shown in Figure 3-2. The thermo physical properties of the used palmitic acid are listed in Table 3-1.

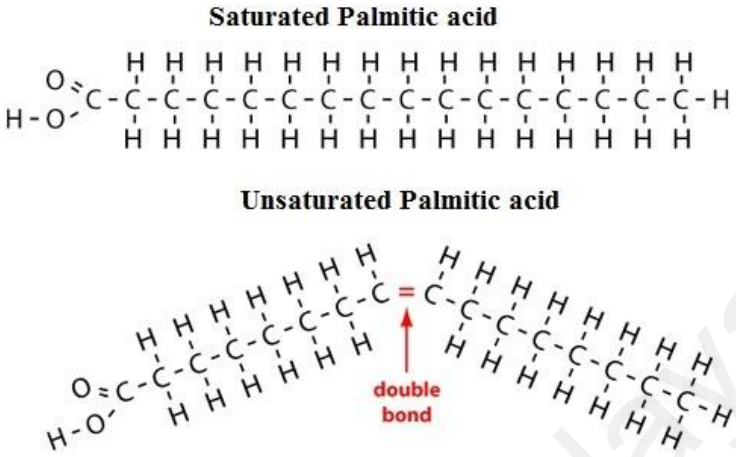

Figure 3-2: Chemical structure of saturated palmitic acid and unsaturated palmitic acid

Table 3-1: Thermo-physical properties of the palmitic acid

Name	Palmitic acid
Purity	98%
Molecular weight (g/mol)	256
Density (g/cm3)	at 20℃ 0.852 at 62℃ 0.852
Solubility	insoluble in water, soluble in amyl acetate, alcohol, CCl_4, C_6H_6 and very soluble in $CHCl_3$
Melting Point (℃)	59-63
Boiling point (℃)	351
Thermal conductivity (W/m.K)	0.21-0.30
Thermal capacity ΔH (J/g)	180-208
Specific heat capacity C (J/mol.K)	at 25℃ 1.8069

3.2.2 Stearic Acid

Stearic acid (also called octadecanoic acid, 1-heptadecanecarboxylic acid, cetylacetic acid, stearophanic acid) is a white, waxy, natural acid and is one of the most common long-chain saturated fatty acids, found in animal and vegetable fats. It is much more abundant in animal fat than in vegetable fat. The chemical formula of stearic acid

is $CH_3(CH_2)_{16}COOH$. The chemical structure of stearic acid (SA) is demonstrated in Figure 3-3.

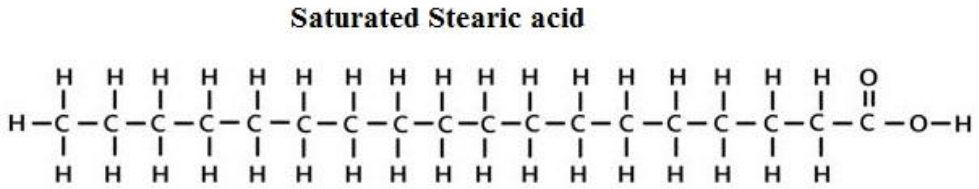

Figure 3-3: Chemical structure of saturated stearic acid

Apart from PCMs in thermal energy storage applications, stearic acid is also used as a lubricant, softener, accelerator activator and as an additive in industrial preparations such as the manufacture of metallic stearates, pharmaceuticals, soaps, cosmetics, and food packaging. Thermo physical properties of the used stearic acid are listed in Table 3-2.

Table 3-2: Thermo-physical properties of stearic acid

Name	Stearic acid
Purity	99%
Molecular weight (g/mol)	284
Density (g/cm3)	at 25℃ 0.940 at 70℃ 0.847
Solubility	insoluble in water, Soluble in alkyl acetates,alcohols, $HCOOCH_3$, phenyls, CCl_4
Melting Point (℃)	54-58
Boiling point (℃)	350
Thermal conductivity (W/m.K)	0.17-0.25
Thermal capacity ΔH (J/g)	170-195
Specific heat capacity C (J/mol.K)	at 25℃ 1.765

3.3 The Selection of Shell Materials

The coating materials used in the encapsulation of PCMs have an important effect on the efficiency of the prepared materials, therefore there are also some characteristic that should be considered in choosing the shell material. According to the required properties of the shell material and the disadvantages of using polymeric organic materials which is noted in CHAPTER 2, inorganic materials were chosen as the shell material. Among the inorganic materials, metal oxides have high thermal conductivity, thermal stability and mechanical strength. So silicon dioxide, titanium dioxide and aluminium oxide were chosen for use as shell material in the encapsulated PCMs.

There are several methods to fabricate NE/MEPCMs, which can be divided into three categories:

1. Physical methods: pan coating, spray drying, air-suspension coating, centrifugal extrusion, vibrational nozzle, solvent evaporation, etc.
2. Chemical methods: interfacial polymerization, suspension polymerization, emulsion polymerization, etc.
3. Physico-chemical method: ionic gelation, coacervation, sol-gel method, etc.

Chemical methods can cause environmental and health problems but physical methods have little negative influence on the environment. However, they are not capable of producing MEPCMs smaller than 100 μm. The other disadvantages of these methods are that the temperature of their reaction should be controlled and the produced NE/MEPCMs have poor stability and have non uniform particle size distribution (Chen et al., 2014). Physico-chemical techniques are based on phase separation in a colloidal system, wherein a soluble shell material aggregates around the core material to form a solid wall. The produced nano/microcapsules via physico-chemical methods have a small size, uniform size distribution, tight shell and good stability (Fang et al., 2014).

Among the physico-chemical methods, nano/microcapsules within high thermal conductivity inorganic shell materials can be produced with the sol-gel method (Jamekhorshid et al., 2014). The sol-gel method has some advantages compared to other methods such as providing high purity homogeneous materials; offering an easy way for the introduction of trace elements; allowing the use of chemical techniques for reaction control; allowing the formation of a "pre"- inorganic network in solution and also allowing the densification to inorganic solids at comparatively low temperatures (due to the "pre"-inorganic network). Therefore; in this project a sol-gel method was utilized to prepare the NE/MEPCMs.

3.3.1 Sol-Gel Method

The sol-gel process has become known as the most practical method in recent years for preparing chemically homogeneous coatings and powders (typically a metal oxide) with a variety of useful applications such as coating and ceramic engineering (Brinker & Scherer, 2013; Hayat et al., 2011; Tredwin et al., 2013). The sol-gel method was developed in the 1960s mainly due to the need of new synthesis methods in the nuclear industry. The term "sol–gel" is an abbreviation for "solution-gelling" and denotes a cheap and low-temperature technique which involves the controlled hydrolysis and condensation of molecular precursors such as a metal alkoxide, or metal salt.

The sol-gel processes can be classified into two different routes depending on the nature of the precursors. The precursor is a solution of: a) an inorganic salt or b) a metal alkoxide. The chemistry of transition metal ions can be rather complicated because of the formation of a large number of oligomeric species, depending on the oxidation state, the pH or the concentration (Klein, 2013). In this route the counter anions, which are able to coordinate the metal ion giving rise to a new molecular precursor with different chemical reactivity. These ions can influence the morphology, the structure and even the

chemical composition of the resulting solid phase. Also the removal of these anions from the final metal oxide product is often a problem. Many of these issues can be avoided by using metal alkoxides as precursors. They are often soluble in organic solvents, providing high homogeneity, and can easily be converted to the corresponding oxide. Some alkoxides, which are widely used in industry, are commercially available at low cost (Si, Ti, Al, Zr, etc), whereas others are hardly available, or only at very high cost (Mn, Fe, Co, Ni, Cu, Y, Nb, Ta, etc). In this project the low cost alkoxides of silicon, titanium and aluminium were utilized to prepare the NE/MEPCMs. The sol-gel conversion of metal alkoxides involves main processes as follows (Brinker & Scherer, 2013):

a) The hydrolysis:

In this step, metal alkoxide as the precursor mixes uniformly with the solvent to form a homogeneous sol. The reaction is called hydrolysis, because a hydroxyl ion becomes attached to the metal atom as follows:

$$M(OR)_n + xH_2O \rightarrow M(OR)_{n-x}(OH)_x + xROH \quad (3\text{-}1)$$

$$(\equiv M - OR + H_2O \rightarrow \equiv M - OH + ROH)$$

$$R = \begin{cases} i - Pr = \text{isopropyl group } (CH(CH_3)_2) \\ Et = \text{Ethyl group } (C_2H_5) \end{cases}$$

$$M = \text{metals like } (Si, Al, Ti, Zr, Nb, K, \dots)$$

Through the hydrolysis reaction, the alkoxide groups ($-OR$) are replaced via the nucleophilic attack of the oxygen atom of a water molecule under release of alcohol and the formation of a metal hydroxide. In this project tetraethoxysilane ($SiC_8H_{20}O_4$-TEOS), titanium tetraisopropoxide ($C_{12}H_{28}O_4Ti$, TTIP) and aluminium isopropoxide ($C_9H_{21}O_3Al$-AIP) were used as the alkoxide for preparing SiO_2, TiO_2 and Al_2O_3, respectively.

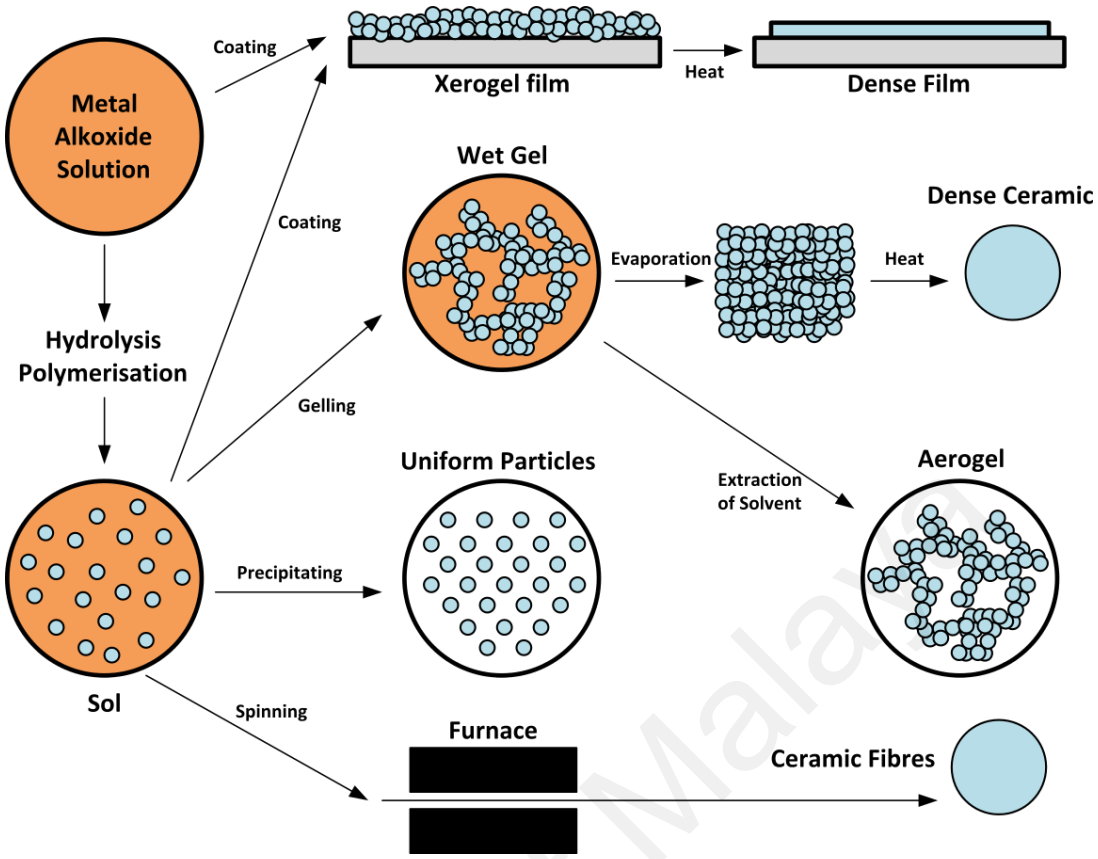

Figure 3-4: the sol-gel process schematic of preparing metal oxides (Samiey et al., 2014)

b) The polycondensation:

Hydrolysis leads to a sol, a dispersion of colloidal particles in a liquid, and further condensation results in a gel, an interconnected and rigid inorganic network enclosing a continuous liquid phase. Condensation reactions between two hydroxylated metal species lead to M−O−M bonds under release of water (oxolation), whereas the reaction between a hydroxide and an alkoxide leads to M−O−M bonds under release of an alcohol (alkoxolation). The main reactions of this step are as the reactions below (Brinker & Scherer, 2013):

$$(OR)_{n-1}M-OH+HO-M(OR)_{n-1}\rightarrow(OR)_{n-1}M-O-M(OR)_{n-1}+H_2O \quad (3\text{-}2)$$

$$m(OR)_{n-2}M(OH)_2\rightarrow[(OR)_{n-2}M-O]_m+mH_2O$$

$$m(OR)_{n-3}M(OH)_3\rightarrow[(OR)_{n-3}M-O]_m+mH_2O+mH^+$$

$$(\equiv M-OH+HO-M\equiv\rightarrow\equiv M-O-M\equiv+H_2O)$$

$$(OR)_{n-x}(HO)_{x-1}M-OH+ROM(OR)_{n-x-1}(OH)_x \quad (3\text{-}3)$$

$$\rightarrow(OR)_{n-x}(OH)_{x-1}M-O-M(OR)_{n-x-1}(OH)_x+R-OH$$

$$(\equiv M-OR+HO-M\equiv\rightarrow\equiv M-O-M\equiv+ROH)$$

c) Drying step:

Then the gel with three-dimensional network structure formed the final oxide structure after aging and drying of the sol.

Figure 3-4 illustrates the sol-gel process to produce different structure types of metal oxides. The sol-gel process is dynamic, and may be steered in the desired direction by adjusting the proper parameters. Parameters which influence the sol-gel process are such as: type of precursor, type of catalyst used, type of solvent, temperature, pH value, relative and absolute concentrations of the reactants. Aqueous sol–gel chemistry is rather complex, mainly due to the high reactivity of the metal oxide precursors and the double role of water as ligand and solvent. Therefore; slight changes in experimental conditions cause the final oxide material to have changes in structural and morphological aspects. One possibility to decrease and to adjust the reactivity of the precursors is the use of organic additives like carboxylic acids, β-diketones or functional alcohols, which act as chelating ligands and modify the reactivity of the precursors. In the synthesis process of this project absolute ethanol was used as the organic solvent. Another alternative strategy involves the slow release of water by chemical or physical processes, allowing control over the local water concentration and thus over the hydrolysis of the metal oxide precursors. Additionally, because the ratio of hydrolysis and condensation determines the stability of the sol-gel formulation and both of these

processes are strongly dependent on the pH value, addition of bases typically causes a destabilization of the formulation and therefore a significant reduction of its lifetime. Bases are known to catalyze the post-condensation step of a sol-gel process and thereby also allow a reduction of the curing temperature (Jamekhorshid et al., 2014; Kaneko et al., 2002; Macwan et al., 2011).

3.3.2 Silicon Dioxide (SiO_2)

Silicon dioxide (SiO_2) also called silica, is recognized for its wide applications and advantages. SiO_2 can be considered as a good inorganic supporting material candidate because of its non-toxicity, excellent thermal stability, good mechanical properties, low thermal expansion coefficient, desirable thermal conductivity, high melting point and specific surface area and fire resistance. The physical forms of silica can be grouped as crystalline, amorphous, synthetic amorphous and impure forms (as in quartz, opal, and sand) (Joo et al., 2009; Libor & Zhang, 2009). The properties of silica are noted in Table 3-3.

Table 3-3: The properties of silica

Property	Value
Molar mass (g/mol)	60.08
Density (g/cm^3)	2.17-2.65
Melting Point (℃)	1600
Boling Point (℃)	2300
Specific Heat (J/kg.K)	680-730
Thermal Expansion (10^{-6}/K)	0.55
Thermal Conductivity (W/m.K)	1.3-3

At present, there are quite a few methods for preparing nano scale silicon dioxide, such as precipitation, sol-gel, micro-emulsification, as well as vacuum

distillation and condensation. However, sol-gel is easy to control, and the obtained particles are evenly distributed (Gao & Yang, 2010; Zhang et al., 2004a). The best known silicate ester to produce silicon dioxide is tetraethyl orthosilicate (TEOS) which was used in this project. Tetraethyl orthosilicate (TEOS; $Si(OC_2H_5)_4$) is a colorless liquid with a sharp, alcohol-like odor. The substance is classified as flammable on the basis of its flash point of 45°C. It is not explosive and not oxidizing. TEOS is also called Tetraethoxysilane, Tetraethyl silicate or Silicon tetraethoxide and has a molecular weight of 208.3275 g/mol and a density of 0.94 g/cm^3 (Choi et al., 2003; Glaser & Pantano, 1984; Nakamura & Matsui, 1995). The structural formula of TEOS is presented in Figure 3-5.

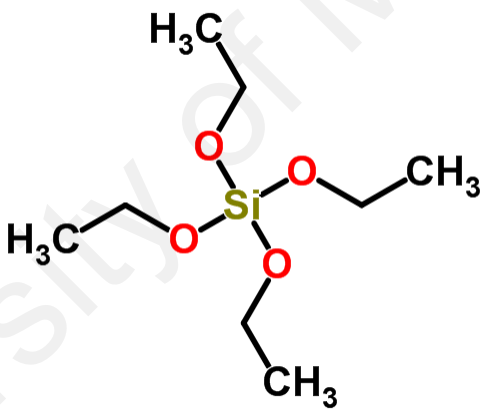

Figure 3-5: The structural formula of TEOS

3.3.2.1 Preparation of Palmitic Acid/Silicon Dioxide NE/MEPCMs

Preparation of palmitic acid emulsion: 0.4 g sodium dodecyl sulfate ($NaC_{12}H_{25}SO_4$) (SDS) as surfactant was dissolved in 200 mL distilled water at 70°C (more than the melting point temperature of PA); 20 g PA was then added into this solution which was stirred continuously with a magnetic stirrer at a rate of 1000 rpm for 2 hr.

Preparation of silica nanoparticles: 20 g TEOS and 180 mL absolute ethanol (C_2H_6O) (99.9%) as the solvent were mixed with 54 mL distilled water and the pH of the solvent was controlled by adding ammonium hydroxide (NH_4OH). The mixture was stirred with a magnetic stirrer at a rate of 500 rpm for 30 min. The pH of the solution was controlled at 11(SI1), 11.5(SI2) and 12(SI3) in three different beakers. When the hydrolysis reaction of the silica was completed, the resultant sol was used as the encapsulation precursor.

Preparation of nanocapsules: The sol was added drop wise into the PA emulsion which was stirred at a rate of 500 rpm for 4 hr. The temperature of the emulsion was controlled at 70℃. Then the emulsion was cooled to room temperature, washed with distilled water and centrifuged at a rate of 6000 rpm. The formed white powder was collected and dried at 50℃ for 10 hr; then it was washed with toluene to remove the residual PA which may not have been encapsulated. Finally, the toluene solution was centrifuged again and the white powder was collected and dried at 50℃ for 24 hr. The prepared samples are listed in Table 3-4.

Table 3-4: Specifications of prepared materials

Sample code	pH value
SI1	11
SI2	11.5
SI3	12

3.3.3 Titanium Dioxide (TiO_2)

Titanium dioxide (TiO_2), titania is a white solid inorganic substance which occurs naturally in several kinds of rock and mineral sands. It is well known that titania occurs in different forms such as amorphous form, brookite, tetragonal phases, anatase and rutile. Titanium dioxide is one of the most widely studied transition metal oxides

due to its nontoxic nature, chemical and thermal stability, non-flammability, high thermal conductivity and commercial availability at a low cost. This substance has become the subject of many investigations for energy and environmental applications, such as hydrogen generation by water splitting, photocatalytic water purification, supporting material for thermal energy storage, dye-sensitized solar cells, and optical coatings (Lekeufack et al., 2010). Some of the properties of titania are mentioned in Table 3-5.

Table 3-5: Properties of titania

Property	Value
Molar mass (g/mol)	79.86
Density (g/cm^3)	3.78-4.23
Melting Point (℃)	1843
Boling Point (℃)	2972
Specific Heat (J/kg.K)	683-697
Thermal Expansion (10^{-6}/K)	8.4-11.8
Thermal Conductivity (W/m.K)	1.8-11.7

Many methods have been established for synthesizing titania. From these methods, sol–gel process based on the controlled hydrolysis and condensation of appropriate precursors (mostly titanium alkoxides or chlorides), has notable advantages such as high purity, good uniformity of the product materials, low temperature synthesis and easily controlled reaction condition (Macwan et al., 2011). Titanium (IV) isopropoxide (TTIP) with molecular formula of $C_{12}H_{28}O_4Ti$ and a molecular weight of 284.21532 g/mol (Figure 3-6), is one of the most attractive alkoxides for preparing the titania. TTIP, which is also called tetraisopropyl titanate, was used in this project for synthesizing the shell material of titanium dioxide.

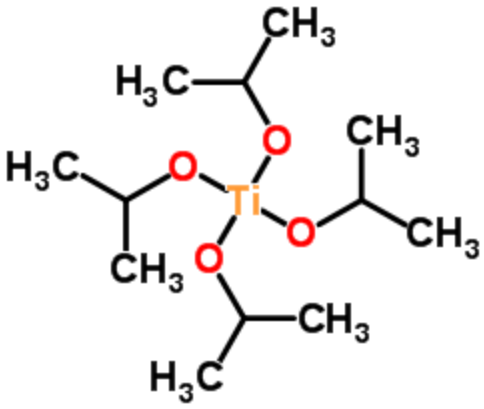

Figure 3-6: The structural formula of TTIP

3.3.3.1 Preparation of Stearic Acid/TiO_2 NE/MEPCMs

In this part the following method was followed to prepare the stearic acid/TiO_2 nanocapsules. In the synthesis procedure, an oil/water (O/W) emulsion was prepared by mixing 0.3 g of SDS and 50 mL of distilled water using a magnetic stirrer at the rate of 1000 rpm. Once the temperature of the mixture stabilized at 70℃, 3 g of SA was added to the mixture, and the emulsion was stirred for 1 hr at a constant temperature of 70°C. After the SA was uniformly dispersed in the emulsion, 15mL of absolute ethanol was added to the mixture. Due to the high hydrolysis rate of TTIP compared to the TEOS, the ethanol was added as the solvent in both steps to control the hydrolysis rate.

The precursor solution was prepared in a separate beaker by mixing 15mL of anhydrous ethanol with TTIP in the ratios listed in Table 3-6 for 15 min. Afterward, ammonium hydroxide (28%) was used to adjust the pH to 10, 10.8, and 11.5.

Nanocapsule formation was achieved in the last phase by adding the precursor solution dropwise into the SA emulsion while the emulsion was stirred continuously at a rate of 750 rpm and a temperature of 70℃. After 2 hr, the mixture was cooled to room temperature and washed with distilled water several times, and the twelve different white powder samples were collected and dried in an oven at 50℃.

Table 3-6: Chemical composition of the O/W emulsion and precursor solution used for the fabrication of NEPCMs

		Precursor solution		
Sample number	SA/TTIP ratio (wt/wt)	TTIP (g)	Volume of absolute ethanol added (mL)	pH
ST1	50/50	3.00	15	10.0
ST2	60/40	2.00	15	10.0
ST3	70/30	1.28	15	10.0
ST4	80/20	0.75	15	10.0
ST5	50/50	3.00	15	10.8
ST6	60/40	2.00	15	10.8
ST7	70/30	1.28	15	10.8
ST8	80/20	0.75	15	10.8
ST9	50/50	3.00	15	11.5
ST10	60/40	2.00	15	11.5
ST11	70/30	1.28	15	11.5
ST12	80/20	0.75	15	11.5

3.3.4 Aluminium Oxide (Al_2O_3)

Aluminium oxide is a chemical compound of aluminium and oxygen specifically identified as aluminium (III) oxide called alumina and is very commonly occurring. The aluminium oxides, oxide hydroxides, and hydroxides can be summarized as follows (Wefers & Misra, 1987):

- Aluminium oxides: corundum (α-Al_2O_3)

- Aluminium oxide hydroxides ($Al_2O_3.xH_2O$): diaspore (α-AlOOH), boehmite (γ-AlOOH), akdalaite ($5Al_2O_3.H_2O$) (once believed to be $4Al_2O_3.H_2O$), also called tohdite

- Aluminium hydroxides: gibbsite (often designated as γ-$Al(OH)_3$, but sometimes as α-$Al(OH)_3$), bayerite (designated often as α-$Al(OH)_3$ but sometimes as β-$Al(OH)_3$)

Al_2O_3 is an electrical insulator but has a relatively high thermal conductivity, high chemical and thermal durability and environmental resistance. Its good properties make it the material of choice for a wide range of applications like coating materials (Li et al., 2006; Zhang & Lee, 2003). Some general properties of alumina are listed in Table 3-7.

Table 3-7: General properties of alumina

Property	Value
Molar mass (g/mol)	101.96
Density (g/cm^3)	3-4.1
Melting Point (˚C)	2270-2369
Boling Point (˚C)	2977
Specific Heat (J/kg.K)	451-955
Thermal Expansion (10^{-6}/K)	4.5-10.9
Thermal Conductivity (W/m.K)	12-38.5

Synthesis of alumina has been carried out by a wide variety of methods, including reactive sputtering, evaporation, anodization, sol-gel etc. To prepare alumina via sol-gel method aluminium alkoxides are the best choice because they are less reactive than the other precursors and their hydrolysis is easier to control (Yoldas,

1975). Aluminium alkoxides are solid or liquid compounds of covalent character. They are readily soluble in hydrocarbons, but sparingly soluble in alcohols. Hydrolysis with water occurs readily, giving aluminum hydroxide and the corresponding alcohol. Industrially, only the isopropoxide (isopropylate) and sec-butoxide (sec-butylate) are important (Kureti & Weisweiler, 2002; Vinogradov et al., 2010). Aluminium isopropoxide (AIP) is the chemical compound usually described with the formula Al(O-i-Pr)$_3$, where i-Pr is the isopropyl group (CH(CH$_3$)$_2$) (Lepot et al., 2008; Vinogradov et al., 2013). The AIP, with molar mass of 204.25 g/mol and density of 1.035 g/cm^3, was used to synthesize the alumina in this project (Figure 3-7).

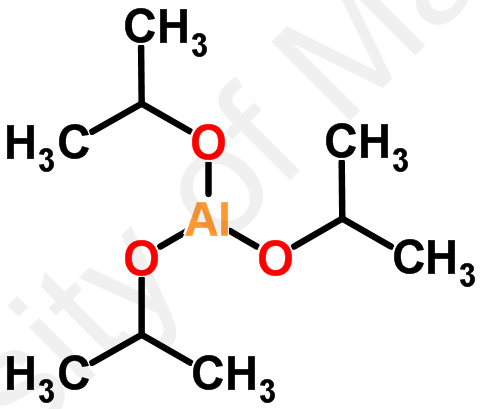

Figure 3-7: The structural formula of AIP

3.3.4.1 Preparation of Palmitic Acid/Aluminium Oxide NE/MEPCMs

PA was dissolved in preheated distilled water at 80℃ on a magnetic stirrer at 1000 rpm and SDS was added to obtain a clear emulsion. The oil/water emulsion was stirred continuously for 2 hr.

4 g AIP was separately dispersed in 40 mL of preheated distilled water at 75℃ and at 750 rpm on a magnetic stirrer. Afterwards, ammonia solution was added to obtain the desired pH value under stirring at 85℃. Different pH values were examined in preparing the precursor solution. Based on preliminary experiments which were done,

the pH value was adjusted to 10.5 to obtain properly produced materials. The sol was stirred for an additional 10 min to complete the hydrolysis and release the formed alcohol. Subsequently, 10 ml of the AIP/water homogenous sol was added dropwise to the oil/water emulsion throughout 3 hr at 80℃ and 500 rpm. Finally, white precipitates were collected and washed several times with distilled water and ethanol. The white powder was dried at 55℃ for 24 hr. Four samples were synthesized according to the specifications listed in Table 3-8.

Table 3-8: The compositions of the O/W emulsion and the solution of the AIP

Sample code	PA/AIP weight ratio (wt/wt)	PCM solution			Solution of AIP	
		PA(g)	SDS(g)	Distilled water(ml)	AIP(g)	Distilled water(ml)
S1	50/50	1	0.4	300	1	10
S2	60/40	1.5	0.6	450	1	10
S3	70/30	2.3	0.9	600	1	10
S4	80/20	4	1.6	750	1	10

3.3.5 Core Material-Shell Material Detach

The wall materials were recovered from the produced encapsulated PCMs for further evaluations and analyses by extraction of PCM core material with toluene. The dried, encapsulated material was treated briefly with toluene to dissolve any uncoated or partially coated particles. The washed and dried capsules were extracted with toluene for at least 3 h. Forty milliliters of toluene was used for each gram of NE/MEPCM capsules. This treatment completely extracted and dissolved fatty acids, leaving not dissolved wall material. After separation by filtration and further washing with toluene, the wall material was dried and weighed. As a check on completeness of extraction, the

weight of the fatty acid extracted was determined after evaporation of the toluene washing and filtrate.

3.3.6 Synthesis Process of NE/MEPCMs

The NE/MEPCMs were synthesized via polycondensation using a sol-gel route. According to the method described in 3.3.1, in the first step, the oily fatty acid was dispersed in an aqueous solution containing SDS as the surfactant. A typical O/W emulsion was obtained. In this case, the hydrophobic segments of the SDS were intermittently collocated with the hydrophilic segments of the oil molecules, and water molecules attached to the hydrophilic segments of the oil molecules. Thus, the hydrophobic SDS segments covered the surface of the fatty acid droplets. After formation of the oil micelles, absolute ethanol was added as an assistant emulsifier, which decreased the hydrolysis and condensation rate of the precursors in a subsequent step for optimizing NE/MEPCMs formation. A transparent solution of metal alkoxide and absolute ethanol was formed and used to modify the alkoxide. Ammonium hydroxide (which contained water molecules) was added as a catalyst to initiate the hydrolysis reaction, and a transparent sol formed. In the final phase, a transparent sol of metal oxide was added dropwise to the O/W emulsion, and the metal oxide precursors were attracted to the surface of the fatty acid micelles via the hydrogen bonding interaction between the metal oxide precursors and hydrophilic sections of the SDS. Polycondensation of the M–OH bonds then occurred in the presence of water molecules under alkaline conditions, and a metal hydroxide gel was formed around the SA micelle. Polycondensation of the metal hydroxide resulted in the fabrication of compact metal oxide shells over the surface of the SA droplets. Figure 3-8 is a schematic of the entire NE/MEPCMs formation process generally for the prepared materials.

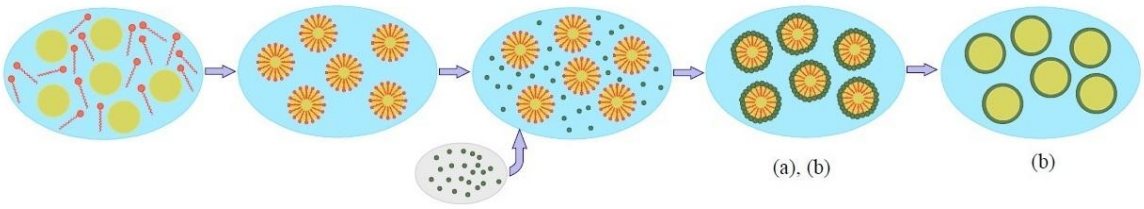

(a):

PA/Silica:

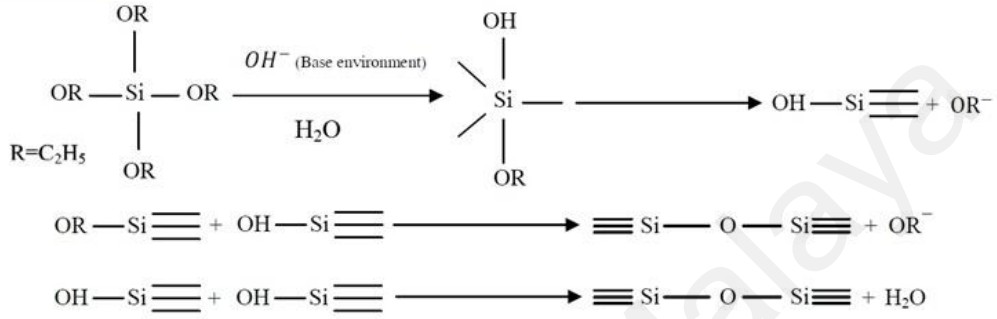

SA/Titania:

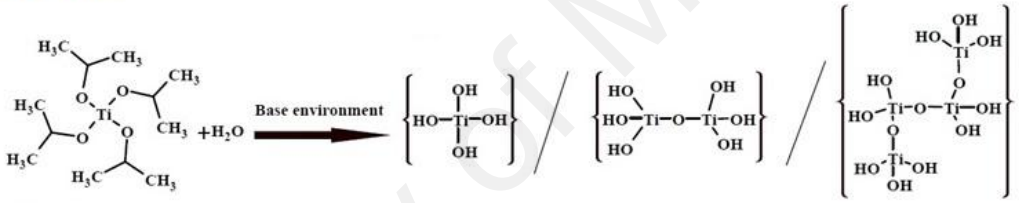

Titanium isopropoxide

PA/Alumina:

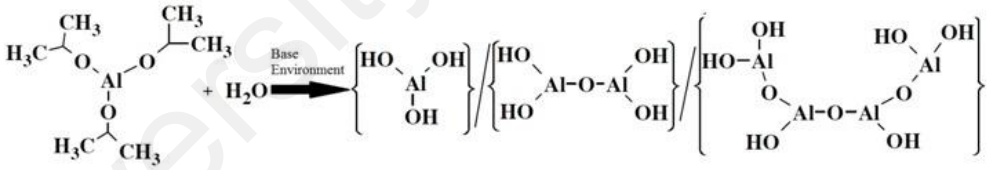

(b):

PA/Silica:

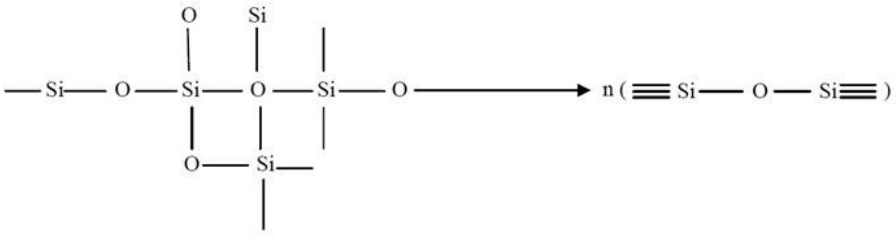

SA/Titania:

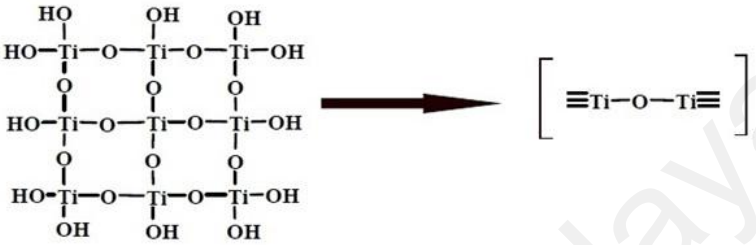

Ti OXO cluster

PA/Alumina:

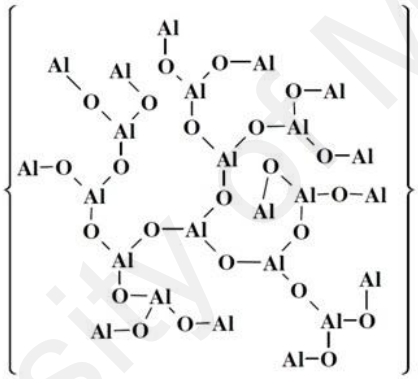

Figure 3-8: Schematic of the encapsulation of metal oxide shell with the PCM cores

3.4 Properties Characterization Methods

When using encapsulated PCMs for designing a TES system it is important to ensure that the encapsulation or containment of PCM meets some requirements including: thermal and structural stability, suitable thermo-physical properties such as appropriate melting temperature, high latent heat of fusion, provide sufficient surface and high thermal conductivity for heat transfer, and high encapsulation efficiency (Yinping & Yi, 1999). There are a lot of analytical techniques and standard instruments for evaluating the properties of NE/MEPCMs. In this project after preparing the NE/MEPCMs properly through the above mentioned procedures the objective

characterizations of the prepared materials, which are all in powder form, were accomplished by using a series of modern instruments for materials analysis. The characterization instruments which were utilized in this project are noted in Table 3-9.

Table 3-9: The instruments utilized for the characterization of the prepared NE/MEPCMs

Instruments Name	Abbreviation	Instrument Details	Measured Features
Fourier Transmittance Infrared Spectra	FT-IR	PERKIN ELMER SYSTEM 2000	Chemical Structure
X-Ray Diffraction And Scattering	XRD	EMPYREAN-PANALYTICAL	System Physical Structures
Energy Dispersive X-ray Spectrometry	EDS	CARL ZEISS-AURIGA 60 and FEI QUANTA 200F	Surface Elemental Composition
(Field Emission) Scanning Electron Microscope	FESEM and SEM	CARL ZEISS-AURIGA 60 and FEI QUANTA 200F	Surface Morphology
Transmission Electron Microscopy	TEM	CARL ZEISS-LIBRA120	Inner Morphology
Differential Scanning Calorimetry	DSC	METTLER TOLEDO 820C	Thermal Features
Thermal Gravimetry	TGA/DTG	METTLER TOLEDO SDTA 851	Thermal Stability
Thermal Conductivity	KD2-PRO	DECAGON DEVICES	Thermal Features
	LFA	NETZSCH LFA 447	
Thermal Cycling	-	IN HOUSE	Reliability

After drying the prepared materials the morphology was observed to ensure a core-shell structure was obtained. The morphology characteristics and the elemental analysis of the prepared materials were observed and analyzed by a high-resolution Scanning Electron Microscope, Transmission Electron Microscope and Energy Dispersive X-ray Spectrometry. The chemical structure and the crystallography of the capsules were analyzed by a Fourier Transformation Infrared spectrometer and an X-ray

Diffractometer. Followed by the chemical and physical characterization of the material, the thermo-physical properties of the capsules-which are the main objective properties of the PCMs-were investigated by the Differential Scanning Calorimeter and Thermogravimetric Analyzer. Ultimately, a thermal cycling test was designed to study the thermal reliability of the prepared NE/MEPCM capsules. The characterization methods are introduced below, concisely.

3.4.1 Fourier-Transform Infrared Spectroscopy (FTIR)

Chemical interaction between the core PCM and the supporting shell material were studied by observing the changes in Fourier Transform Infrared spectrum of the materials. FTIR spectroscopy is closely related to dispersive spectroscopy, but the actual technique used is different. In dispersive spectroscopy, a monochromatic beam of light is shone at a sample in different wavelengths and the absorption of light is measured each time. In FTIR spectroscopy, a beam of light is passed through a series of mirrors that cause the beam's individual wavelengths to hit each other in a way that allows a sample to absorb some wavelengths, while others are blocked. When IR radiation is passed through a sample molecule bonds absorb energy and vibrate at a certain frequency. When molecules undergo transitions between quantum states corresponding to two different internal energies, spectra emission or absorption will take place. The energy difference ΔE, is related to the frequency of radiation emitted or absorbed by the quantum state as given by Bohr Equation:

$$\Delta E = hv \tag{3-4}$$

where h is Planck`s constant, $h=6.6262\times10^{-34}$ Js, and v is the frequency. Infrared frequencies in the wavelength range of 1~50μm ($10000cm^{-1}$ ~$200cm^{-1}$) are associated with molecule group vibration and vibration-rotation spectra. Each bond present in a molecule group is capable of performing a number of different modes of vibration, such as stretching and bending, scissoring, rocking, wagging and twisting. A transmittance or

absorbance is measured and a computer infers the transmission and absorption rate of each wavelength within the beam. The resulting spectrum represents the molecular absorption and transmission, creating a molecular fingerprint of the sample. This fingerprint of the sample with absorption peaks corresponds to the frequencies of vibrations between the bonds of the atoms making up the material. Because each different material is a unique combination of atoms, no two compounds produce the exact same infrared spectrum. Therefore, infrared spectroscopy can result in a positive identification (qualitative analysis) of every different kind of material. In addition, the size of the peaks in the spectrum is a direct indication of the amount of material present (Pasquini, 2003).

The FT-IR transmittance of the prepared and the precursor materials were obtained by using the instrument of Perkin Elmer Spectrum 100 in a wave number range of 400~4000 cm^{-1} at a resolution of 4 cm^{-1} at room temperature.

3.4.2 X-Ray Diffractometry (XRD)

Typically X-ray is an electromagnetic radiation having a wave length of around 1Å (in between ultraviolet and gamma-rays) which is of the same order as the distance between the atoms in the materials. Therefore; X-rays are an ideal probe capable of investigating the crystalline structures of the materials. XRD can also be used to show the crystallization properties of the encapsulated PCMs (Fan et al., 2004; Fang et al., 2010b; Fang et al., 2008) which is very important because of the ability to prove whether PCMs have been embedded within the layer of the shell materials or not especially in the synthesis process performed in this project. The interaction of X-ray beam with a crystal results in a diffraction pattern that identifies the material and corresponding phase. The information obtained from the diffraction pattern includes the material properties such as crystalline phase composition, stress, strain and growth orientation, etc. The phenomenon behind the generation of diffraction pattern can be

described as below. When an X-ray beam having wave length λ strikes the solid crystal with an angle θ, the resulted scattered radiation can be determined by Bragg's law (Will, 2006):

$$n\lambda = 2d\sin\theta \quad (3\text{-}5)$$

Where n is called the diffraction order and d denotes the distance between the parallel planes inside the crystallites. It is remarkable that the set of d-planes is unique for each and every material. In this work the dried samples were put into a holder in a dense and plate state. The X-ray diffraction data were taken by the EMPYREAN-PANALYTICAL XRD system diffractometer equipped with Cu, Kα radiation (Kα =1.54178 Å) having a generator voltage of 40 kV and a current of 10 mA. The XRD patterns were obtained in the range of $2\theta=5\sim70^{o}$ and a scanning speed of 0.02^{o}/second.

3.4.3 Scanning Electron Microscopy (SEM)

Scanning electron microscopy is the most widely used versatile instrument to evaluate the morphological characteristics of NE/MEPCMs such as shape, particle size and outer structure. SEM belongs to the family of microscopes, but it uses a beam of electrons in lieu of light in order to make an image. The beam of electrons passes through electromagnetic lenses and strikes the surface of the sample. The bombardment of electrons does not cause any damage to the samples but generate signals. These signals include secondary and backscatter electrons (that produce SEM images) and photons (characteristic X-rays that are used for elemental analysis-EDS). SEMs always have at least one detector (usually a secondary electron detector), and most have additional detectors. The detector collects the secondary/backscattered electrons ejected from the sample and converts them into a signal. Finally this signal is displayed on a screen. SEM has the ability to capture images from visible to a few nanometers (Goldstein et al., 2012; Zhou et al., 2007). In SEM the nature of the sample determines the necessary preparation of the sample. Unfortunately, some materials such as some

polymers present specific problems making them inappropriate. Therefore proper sample preparation is necessary. These kinds of samples are coated with a thin layer of conducting material, commonly carbon, gold, or some other metal or alloy. While metal coatings are the most effective materials for high resolution electron imaging, the gold coating was done for just some prepared samples in this project according to their unsuitability nature for SEM imagining. To study the morphology and surface appearance of microcapsules in this project, a high-resolution FEI Quanta 200F SEM and a CARL ZEISS-AURIGA 60 FESEM (Field Emission Scanning Electron Microscopy) were used at room temperature.

The size of PCM capsules affects the heat transfer characteristics of the PCM. The prepared capsules size analysis was also performed by SEM image observation and image analyzer software (DIGIMIZER software-Version 4.1.1.0). The mean diameter and standard deviation were determined from the data set of measurements for each specimen. Histograms were plotted by the statistical analysis of the data in MINITAB-16.2.2 software.

3.4.4 Transmission Electron Microscopy (TEM)

The SEM has limitations in the visualization of the internal structure of nano/microcapsules; therefore Transmission Electron Microscopy (TEM) as an imaging technique was also used. TEM is also an imaging technique using a beam of electrons transmitting through a specimen, and then an image is formed. The maximal penetration thickness of an electron beam for TEM test is about 100 to 500nm depends on the nature of the sample material.

This core-shell structure of nano/microcapsules were observed using TEM (CARL ZEISS-LIBRA120) with an accelerating voltage of 120kV and a vacuum ratio

of 10^{-7} Torr. The samples used for TEM were prepared by drying a drop of aqueous suspension placed on a carbon coated copper grid.

3.4.5 Differential Scanning Calorimetry (DSC)

Differential Scanning Calorimetry (DSC) is one of the most widely used indicators reflecting the heat storage properties such as melting temperature and the latent heat capacity of the NE/MEPCMs. Rudd (Rudd, 1993) indicates that DSC can adequately predict the thermal performance of PCMs by carrying out large scale and small scale tests of PCMs. He recommended DSC test as standard for the measurements of PCM thermal performance.

In DSC analysis, a weighed small amount of sample is placed in a small aluminium crucible to put in an insulated chamber. The sample and a reference (which is usually an empty small crucible) are maintained at nearly the same temperature throughout the measurement process. When the sample and the reference are heated at a constant heating rate a physical transformation such as phase transitions occurs in the sample but not in the empty reference pan, therefore the heat flow required to keep the temperature constant between the sample and the reference is measured as a function of the temperature (Figure 3-9).

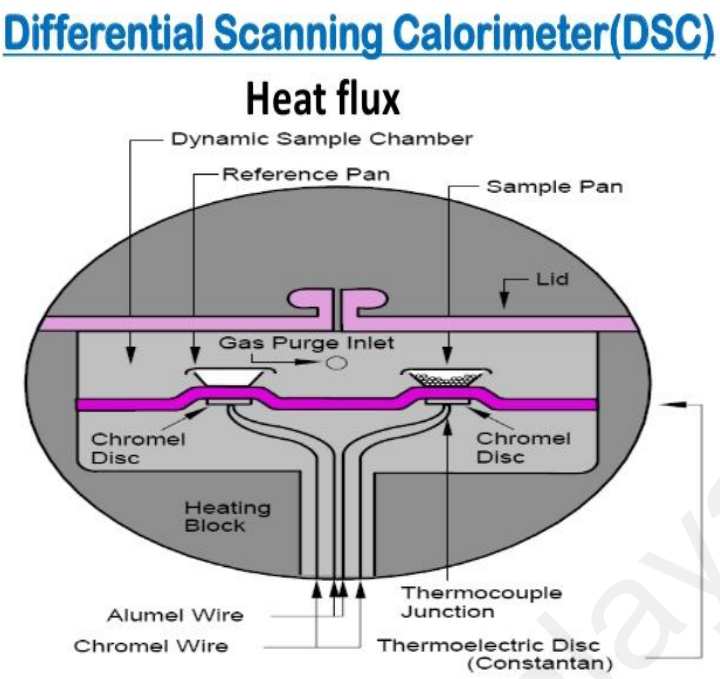

Figure 3-9: Differential scanning calorimeter (Memon, 2014)

The differential heat flows are plotted against temperature, which is called the DSC curve. The heat flow has a unit of energy per unit time per unit mass, usually in units of Wg^{-1}. Figure 3-10 demonstrates typical DSC curves of the melting and crystallization transitions. Changes in the sample are associated with absorption or evolution of heat cause a change in the differential heat flow which is then recorded as a peak. An endothermal or exothermal peak in the DSC thermogram denotes the melting or crystallization temperature of the tested material. The characteristic temperatures from DSC measurements are: initial peak temperature (T_i), the extrapolated peak onset temperature (T_{ei}), the extrapolated end temperature (T_{ef}), the peak temperature (T_p) and the end peak temperature (T_f) (Hatakeyama & Quinn, 1999). The extrapolated peak onset temperature is defined as the intersection between the tangent to the maximum rising slope of the peak and the extrapolated sample baseline (He et al., 2004). It is noteworthy that the user can choose different types of baseline such as linear, sigmoidal horizontal, sigmoidal tangent and extrapolated to calculate the thermal energy stored in the unit weight of PCM. Enthalpy or the thermal heat stored in the capsules which is the

latent heat of the core PCM of phase change is also usually tested by DSC. The enthalpy represents the thermal capacity of a material in which the higher the enthalpy of a material, the better the thermal storage capacity and thermal regulating property that can be provide. The thermal heat stored in the unit weight of PCM is derived by calculating the area under the peak by the software automatically (Rady, 2009; Song et al., 2008).

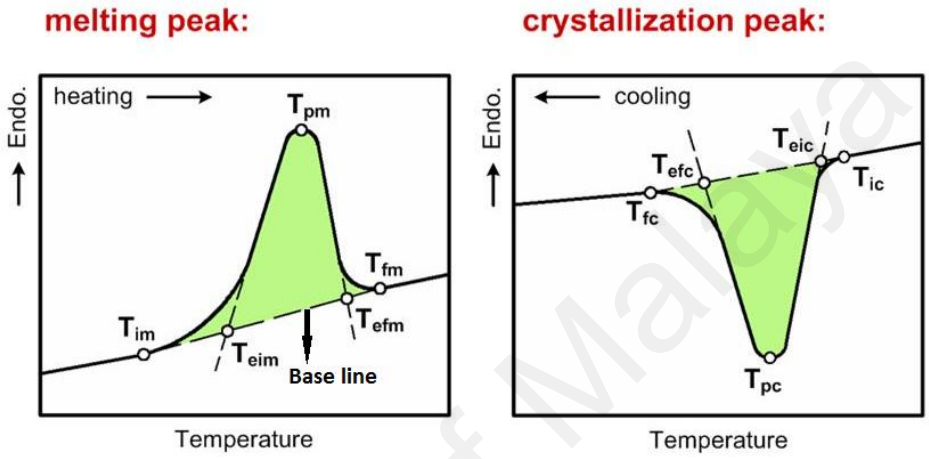

Figure 3-10: Typical DSC curve

The sample mass and the rate of scanning through a temperature range are important in the DSC analysis. The scanning rate commonly varies from 0.1 to 40℃/min, above which the effects of non-linearity becomes dominant and the calibration parameters are no longer applicable. The processes of material change, such as melting or solidifying, require time for heat transfer and atom or molecule diffusion. Increase of scanning rate will result in an increase of temperature gradient in the sample and the instrument, thus making it difficult for the sample to reach equilibrium therefore better resolution and more accurate measurement can be obtained at lower temperature rates (Verdonck et al., 1999). The mass of the sample should also be considered before choosing a rate. Low-mass samples (<10-30 mg) are also preferred because a low-mass sample can quickly reach temperature equilibrium throughout its volume but a large-mass sample will have an undesirable internal temperature gradient and this will affect

the accuracy of the curve. However; small samples can have faster rates, while heavier samples should have a slower rate in order to allow for uniformity of temperature distribution in the sample and improved resolution (Bershteĭn & Egorov, 1994).

In the present study, the thermal properties for each prepared sample of NE/MEPCMs, including the core PCMs and shell material, were measured using a METTLER TOLEDO 820C (Error ± 0.25-1℃) at a heating rate of 5℃ /min in a purified nitrogen atmosphere. The nitrogen atmosphere is used to remove any corrosive gases from the sample and to minimize the risk of condensation inside the DSC instrument when the temperature gets below the air dew point. The samples with 5-10 mg in weight were put in an aluminium vessel; then sample and reference vessels were hermetically sealed and were heated from 30 to 100℃. The temperature was maintained at 100℃ for 5 minutes and then cooled down to 30℃ to finish one measurement cycle.

Super-cooling is one of the physical properties of phase change materials. It refers to the phenomenon that a material crystallizes at a temperature below its melting point. Since super-cooling leads to reduced crystallization temperature; the latent heat will be released at a lower temperature or in a wider temperature range. This limits the application of PCM capsules in thermal regulation functions. The super-cooling phenomenon should be understood and controlled effectively.

The degree of super-cooling (ΔT), can be derived from the DSC outcomes by using the following equation (Cao & Yang, 2014):

$$\Delta T = T_m - T_c \tag{3-6}$$

Where T_m and T_c are the melting and crystallization peak temperatures, respectively.

As was discussed previously, the phase change enthalpy is an important factor representing the phase change properties and reflects the melting of the fatty acid content of NE/MEPCMs. Therefore, it is reasonable to believe that there is a close connection between the phase change enthalpies and the encapsulation ratio of encapsulated PCM as well as its encapsulation efficiency. Zhang and Wang (2009) suggested evaluating the phase-change performance of encapsulated PCMs by using the encapsulation ratio (E_r) and encapsulation efficiency (E_e) of NE/MEPCMs which are calculated by the following equations:

$$E_r = \frac{\Delta H_{m,MEPCM}}{\Delta H_{m,PCM}} \times 100\% \quad (3\text{-}7)$$

$$E_e = \frac{\Delta H_{m,MEPCM} + \Delta H_{c,MEPCM}}{\Delta H_{m,PCM} + \Delta H_{c,PCM}} \times 100\% \quad (3\text{-}8)$$

Where $\Delta H_{m,MEPCM}$ and $\Delta H_{m,PCM}$ are the melting enthalpies of prepared nano/microcapsules and pure PCM, and $\Delta H_{c,MEPCM}$ and $\Delta H_{c,PCM}$ are the crystallization enthalpies of the nano/microcapsules and pure PCM, respectively.

It is notable that the encapsulation ratio and encapsulation efficiency are associated with the mass ratio of core/shell, which describes the PCM loading inside the capsules. The encapsulation ratio describes the efficient encapsulation of PCM within the shell materials while the PCM loading content is considered as the dry weight percent of core material. Therefore, the encapsulation ratio demonstrates an effective property of the PCM inside the capsules for heat energy storage and thermal regulation. Encapsulation efficiency is defined as the percentage of core active materials that are fully encapsulated by shell. This represents an effective performance of the PCM inside the shell materials for latent heat storage. Higher encapsulation efficiency is desirable due to its higher mechanical strength and leak proof characteristics. The encapsulation efficiency seems to be more rational to evaluate the working efficiency and release

capabilities of encapsulated PCM than the encapsulation ratio, because it is derived from the phase-change enthalpies involved in both crystallization and melting processes (Zhang et al., 2004b).

Moreover, the thermal storage capability (φ) of the prepared encapsulated PCMs also were evaluated by using subsequent equation:

$$\varphi = \frac{E_e}{E_r} \times 100\% \tag{3-9}$$

Where E_e and E_r are the encapsulation ratio and encapsulation efficiency of NE/MEPCMs, respectively, that are calculated from equations (3-7) and (3-8). It is important to mention that the high thermal storage capabilities of the NE/MEPCMs indicated that nearly all of the capsules stored latent heat effectively through the phase change.

There are not many studies on the estimation and calculation of the shell thickness of the NE/MEPCMs. However; as the structure of the capsules could be thought to be a core/shell type structure and the encapsulation ratio presents the percentage amount of the core PCM content in the shell material, the shell thickness of the NE/MEPCMs can be calculated from (Tseng et al., 2005):

$$\frac{m_{PCM}}{m_{PCM} + m_{Shell}} = E_r = \frac{(4/3)\pi . R_{PCM}^3 . \rho_{PCM}}{(4/3)\pi . R_{PCM}^3 . \rho_{PCM} + (4/3)\pi(R^3 - R_{PCM}^3) . \rho_{Shell}} \tag{3-10}$$

$$= \frac{1}{1 + \left[(R/R_{PCM})^3 - 1\right](\rho_{Shell}/\rho_{PCM})}$$

$$R_{PCM} = R \Big/ \sqrt[3]{(\frac{1}{E_r} - 1) \times \frac{\rho_{PCM}}{\rho_{Shell}} + 1}$$

$$R_{Shell} = R - R_{PCM}$$

Equation (3-10) shows that the weight ratio of core PCM to the whole capsule is related to the sizes, where capsule radius R (that is obtained from SEM/TEM analysis) is the sum of core PCM radius (R_{PCM}) and the shell thickness (R_{Shell}).

3.4.6 Thermal Gravimetry and Derivative Thermogravimetric (TGA and DTG)

Thermogravimetric analysis (TGA) is a powerful technique for characterization of decomposition or weight loss properties and thermal stability of materials under different conditions, and to examine the kinetics of physical-chemical processes occurring in the materials. In the thermal gravimetry analysis the change in the sample mass is analyzed while the sample is subjected to a temperature programme.

In the TGA analysis, a sensitive balance is used to measure the changing in weight of a sample as a function of temperature. Typical applications in material characterization of thermal gravimetry (TG) include the assessment of thermal degradation properties and thermal stability, decomposition temperature, material composition, oxidative degradation characteristics, quantitative weight losses, chemistry reaction kinetics and purity determination etc. Derivative thermogravimetric (DTG) analyses can be calculated by the differential of change in sample weight over time. DTG data denotes the rate of change in weight (dm/dt) of a sample which is heated in a controlled manner.

In the present study, the samples were heated from the ambient temperature (20-30℃) to 600℃ in nitrogen atmosphere with a gas flow rate of 50mL/min at the heating rate of 10℃/min. The weight of different samples was 8~15 mg in all cases. During the heating period, both the weight loss and temperature data were recorded. METTLER TOLEDO-SDTA 851 equipment was used in the test with the testing range of 25 to 1300℃.

3.4.7 Thermal Conductivity

It is well-known that the low thermal conductivity of PCM increases its thermal response time for storage and release of latent heat. Thus, enhancing the thermal conductivity of PCMs is a major aim in designing a nano/microencapsulated material which attracts a vast attention. Measuring these thermo-physical properties was a challenge for a long time since different methods and techniques presented different results. Thus, the method which is going to be used is significant to lower the measurement error and uncertainty as much as possible. In this study, two thermal conductivity measurement methods were employed including Transient hot-wire techniques and laser flash method.

Generally, Fourier's law for conduction heat transfer can be utilized to measure thermal conductivity of a material. A temperature difference can cause heat transfer through materials which is known as conductive heat transfer. Thermal conductivity is the property of the material which relates heat flux to temperature gradient and can differ from one material to another. It can be calculated from the following equation:

$$k = (q/A)/(\Delta T/L) \tag{3-11}$$

Where, k is thermal conductivity, q is magnitude of heat transmission, ΔT is temperature difference, A is cross sectional area and L is the length (Ehsan Bitaraf et al., 2012). To simplify calculations, a one-dimensional temperature field and steady state flow are considered.

3.4.7.1 Transient Hot-Wire Method (THW)

This is the most regular and the oldest method of measuring thermal conductivity. This technique has been well developed and widely used for measurements of the thermal conductivity of solids, and in some cases, the thermal diffusivity of fluids with a high degree of accuracy. Comparing other methods, the most

attractive advantage of the technique is its very fast measurement with high accuracy and the simplicity of the conceptual design of the apparatus of it as well. The transient hot-wire technique was first introduced by (Carslaw & Jaeger, 1986). It has been used to measure thermal conductivity of powders at the beginning. However, it has been improved by many researchers. The THW method is based upon using a long, thin platinum wire as a dual line heat source and temperature sensor. This is possible due to the relatively unique relationship between the temperature and thermal characteristics of platinum. The platinum filament is fully placed within the material for which the thermal conductivity is to be determined, and a step increase in the electrical power supplied to the wire is introduced. This allows the platinum wire to heat up due to resistive heating. The excess heat from the hot filament is rejected to the surrounding material through conduction. Simultaneously, while this heating occurs, the relative change in resistivity of the wire is being measured through a two or four wire resistive measurement system. The surface temperature of the hot wire and therefore the temperature of the immediate surrounding can be calculated based upon this approach. The measured value of total input power, and power lost to the surrounding, combined with the overall change in resistivity of the platinum wire due to electrical heating are collected; these values, in conjunction with the measured experimental time and dimensional parameters of the hot wire setup, can be used to back calculate the thermal conductivity of the material of interest.

In this study a KD2-Pro system was used to measure the thermal conductivity of some NE/MEPCMs. The KD2 Pro resolves to 0.001℃ in temperature by utilizing special algorithms to analyze measurements made during a heating and a cooling interval. Algorithms also separate out the effects of the heat pulse from ambient temperature changes. The prepared samples were placed in a proper container in a

circulating bath while the temperature was controlled and a dual needle apparatus was used to measure the thermal conductivity of the samples.

3.4.7.2 Laser Flash Technique (LFA)

For the precise and reliable measurement of thermophysical properties like the thermal diffusivity and thermal conductivity, the Laser Flash technique (LFA) has proven itself as a fast, versatile and precise absolute method. The Laser Flash technique is based on the measurement of the thermal transient of the rear surface of the sample when a pulsed laser illuminates the front and it avoids interferences between the thermal sensor and the heat source. The physical model of the Laser Flash measurement supposes to have a single pulsed heat source (delta like), for example a laser shot, on the sample front surface. The study of the thermal transient of the rear surface provides the desired thermal information. The temperature of the rear face is measured with an infrared detector and it can be expressed mathematically as a function of several variables that are grouped into dimensionless parameters. These variables include sample geometry, thermal diffusivity and heat loss from the sample (Mirmohammadi & Behi, 2012).

The laser flash technique (Netzsch LFA 447 NanoFlash) was used to measure the thermal diffusivity of samples at 35 and 80℃. The thermal conductivity may also be derived from the thermal diffusivity when the specific heat and the sample bulk density are known as shown in equation (3-12):

$$k = \alpha . \rho . C_p \tag{3-12}$$

Where k is the thermal conductivity (W/ (m.K)), α is thermal diffusivity (m^2/s), ρ is density (kg/m^3) and C_p is specific heat capacity (J/(kg.K)).

3.4.8 Thermal Cycler

The most common application for PCM-based energy storage unit is solar applications. A solar thermal system with latent heat storage undergoes at least one melt/solidify thermal cycle per day. This can be considered as a normal cycle. Therefore an important parameter to consider while designing the encapsulated PCM based thermal system is the thermal, chemical and physical stability of the NE/MEPCMs after a number of repeated thermal cycles. A comprehensive knowledge of thermal reliability of the encapsulated PCMs is essential to ensure the long-term performance of the encapsulated PCMs as TES materials and its economic feasibility. Thermal cycling tests conducted under controlled conditions in the laboratory are called accelerated thermal cycling tests. A small amount of material is withdrawn after each prescribed number of thermal cycles for obtaining the thermo-physical properties of PCMs. A PCM is thermally stable for latent heat storage applications if it undergoes negligible changes in the melting point and latent heat of fusion after repeated operative thermal cycles.

To determine the thermal stability and reliability of the NE/MEPCMs during melting and solidifying, a thermal cycling test was done using a thermal cycling system of in-house design (university of Malaya). The thermal cycling system was designed to operate between 30 and 80℃. The schematic and picture of the thermal cycling system are shown in Figure 3-11. The tests were done using fan and heater as cooling and heating parts, digital Indicating Controller (Brian Child-P41) for controlling of melting and solidifying process, communication converter (Autonics-SCM-US48I) to transfer data to PC and controller program, relay (ANV) to control heater and power supplies for fans and heater. The cartridge heater was located behind the PCM container and a thermocouple was placed inside the PCM to check the temperature and transfer data to the digital Indicating Controller. First, the specified amount of PCMs was placed inside the container and the thermocouple was carefully placed inside the PCM to measure

temperature and send data to the communication converter. Second, by operating the program in PC cycling started and melting was done by heating up to 80℃ and then immediately freezing was started by switching off the heater and starting the fan till 30℃. The temperature variations of NE/MEPCMs were automatically recorded in a PC with an accuracy of ±0.1℃. The characterization analysis, including SEM, DCS and FTIR, etc were done before and after the thermal cycling and the outcomes were compared to investigate the thermal and chemical stability of the materials.

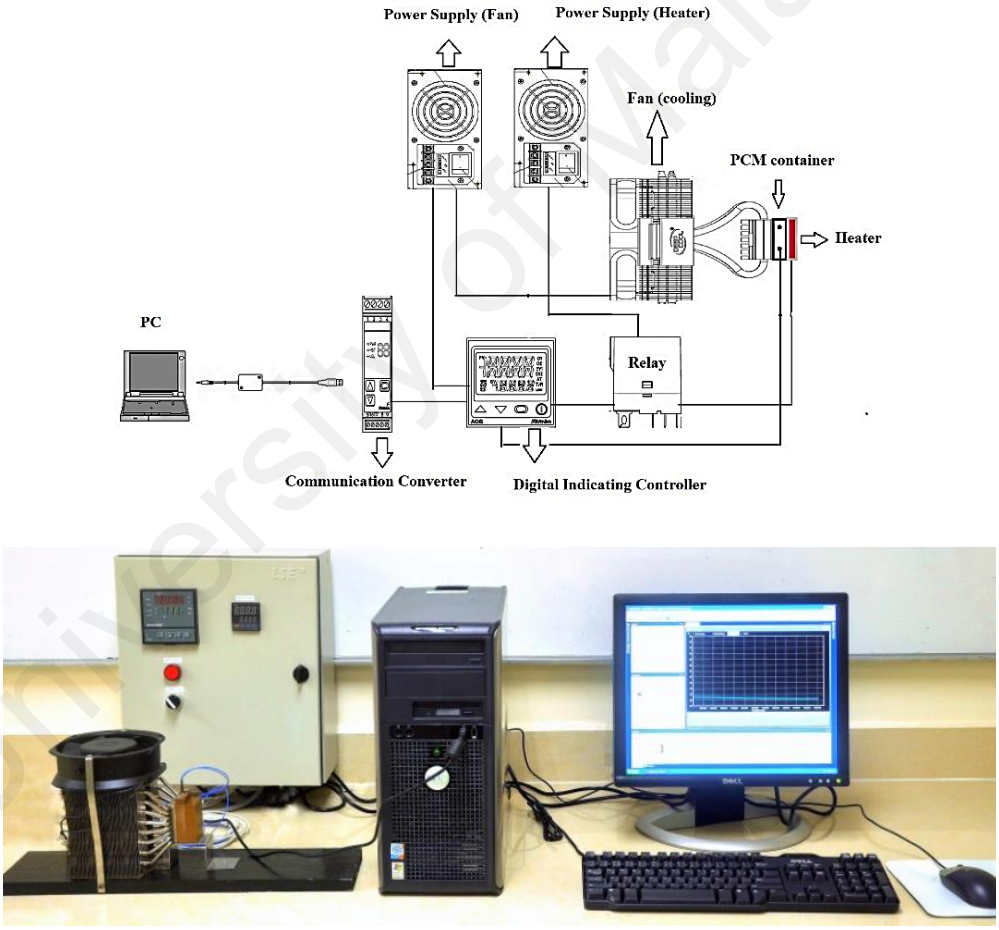

Figure 3-11: Accelerated thermal cycler

3.5 Summary

According to the benefits and superiority of sol-gel method, the NE/MEPCMs incorporated with metal oxides as the shell materials were prepared through the sol-gel method. Furthermore, experimental parameters have been determined according to the previous experience and the preliminary studies.

The prepared NE/MEPCMs were characterized by a series of modern analysis techniques and instruments. The chemical and the crystal structure of the NE/MEPCMs were analyzed using FTIR and XRD, respectively. SEM was used to observe the surface morphology and the diameter size of the NE/MEPCMs. EDS was employed for surface elemental analysis. The core/shell structure of the capsules was observed using a TEM. DSC was used to measure the thermal capacity and properties, super-cooling and melting enthalpy of the NE/MEPCMs. The thermal stability of capsules was determined using TGA. The thermal conductivity of the prepared NE/MEPCMs was measured by two methods (hot wire & laser flash) to investigate the effects of shell materials and encapsulation on thermal conductivity of the pure PCMs. The thermal cycling test was introduced to investigate thermal performance of the prepared encapsulated PCMs.

CHAPTER 4

RESULTS AND DISCUSSION

4.1 Introduction

In this chapter the chemical and thermo-physical properties of the prepared NE/MEPCMs are evaluated. The characteristics of the materials were appraised by some advanced analysis instruments and characterization technologies including FTIR, XRD, SEM, TEM, DSC, TGA, LFA, and THW. A thermal cycling test were also designed and applied to investigate the thermal reliability of the prepared NE/MEPCMs in a large number of heating-cooling processes.

4.2 Palmitic Acid/Silica Nanocapsules

In this research the sol-gel method was used to prepare the encapsulated palmitic acid as a phase change material in silica shell. The TEOS which is one of the best precursors was used to synthesize the silica shell. The influence of the pH on the properties of the materials as one of the most important parameters in sol-gel process is studied by changing the pH value during the preparation process for three different samples. The characteristics and the capability of prepared capsules were investigated by several characterization methods and the results will be described in the following sections.

4.2.1 FTIR Spectra of PA/SiO_2 NEPCMs

The FTIR spectra of all three samples were essentially similar. Figure 4-1 shows the FTIR results for palmitic acid, SiO_2 and PA/SiO_2 nanocapsules of sample SI3. Figure 4-1a represents the FTIR spectra of SiO_2. The peaks at 1044.5, 788.39 and 450.5 cm^{-1} signify the bending vibration of the Si–O functional group and the peak at 940.37 cm^{-1} is assigned to the Si–OH functional group. The absorption bands at 2600-3400 cm^{-1} and 1400-1700 cm^{-1} characterize the stretching and bending vibrations of the –OH

functional group of H_2O. Figure 4-1b displays the spectrum of the pure palmitic acid. The peaks at 2915.02 cm^{-1} and 2849 cm^{-1} include the symmetrical stretching vibration peaks of $–CH_3$ and $–CH_2$ in PA. The absorption peak at 1691 cm^{-1} is assigned to the C=O stretching vibration. The peak at 1293 cm^{-1} refers to the in-plane bending vibration of the –OH group of palmitic acid, the peak at 937.99 cm^{-1} corresponds to the out-of-plane bending vibration of the –OH functional group and the peak at 720.10 cm^{-1} shows the in-plane swinging vibration of the –OH functional group . Figure 4-1c indicates that the absorption peaks of the SiO_2 at 1044.5, 788.39 and 450.5 cm^{-1} can also be found in the nanocapsules spectra. Because the SiO_2 can only be formed on the interface of palmitic acid O/W emulsion, the FTIR results imply that the SiO_2 shell was formed on the surface of the palmitic acid droplet. The absorption peaks from the palmitic acid at 2915.02, 2849, 1691, 1293, 937.99 and 720.10 cm^{-1} are not changed within the nanocapsule spectra. These results show that there is absolutely no chemical interaction relating to the molecules of palmitic acid and SiO_2. The palmitic acid was encapsulated easily inside the shells of SiO_2 through the condensation and polymerization processes of the obtained SiO_2 precursors from the hydrolysis of the tetraethoxysilane.

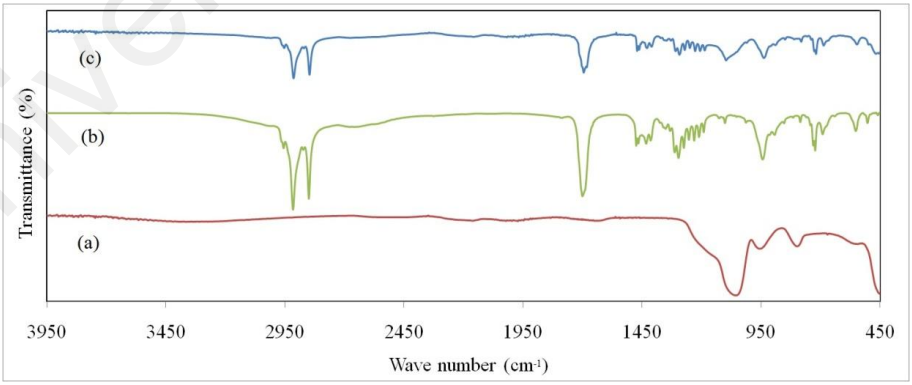

Figure 4-1: FTIR spectra of the (a) SiO_2, (b) PA, (c) PA/SiO_2 nanocapsules

4.2.2 XRD Patterns of PA/SiO_2 NEPCMs

Figure 4-2 shows the XRD patterns of the Palmitic acid, SiO_2 and nanocapsules of PA/SiO_2. As shown in Figure 4-2a, SiO_2 has a smooth peak at about 20°-25°. This indicates that the SiO_2 is non-crystalline with amorphous structure. Figure 4-2b implies that the XRD peaks at 21.8° and 24.3° are caused by palmitic acid due to its normal crystallization and Figure 4-2c shows that the XRD peaks of the palmitic acid in nanocapsules of PA/SiO_2 are also stated on the basis of the SiO_2 smooth peak. This indicates that the SiO_2 cannot be shaped inside the palmitic droplet; hence the palmitic acid was encapsulated within the SiO_2 shells (Zhang et al., 2004a).

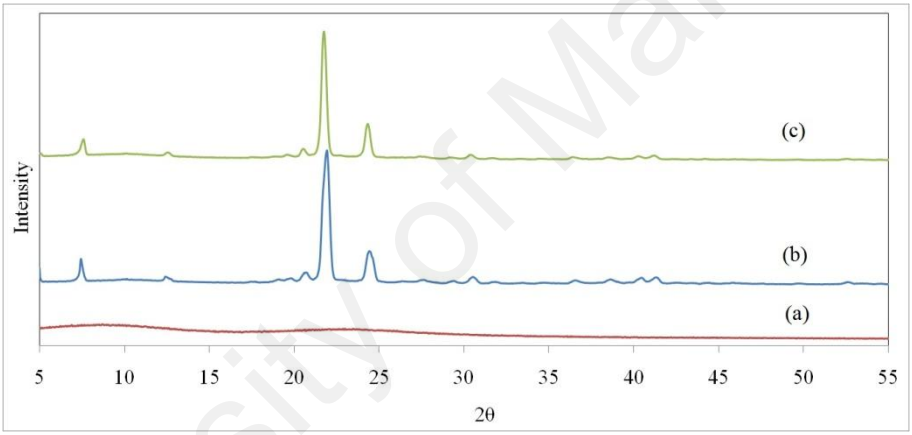

Figure 4-2: XRD pattern of (a) SiO_2, (b) PA, (c) PA/SiO_2 nanocapsules

4.2.3 Microstructure Analysis of PA/SiO_2 NEPCMs

The SEM photographs of three different samples of nanoencapsulated PCMs are shown in Figure 4-3. Figure 4-4 displays the particle size distributions. The SEM photographs of all three samples illustrate the spherical structure of nanocapsules and also their smooth surfaces. The homogeneous and uniform size distributions of nanocapsules are obvious. A comparison of the particle sizes of these three samples shows that increasing the pH value causes the diameter size of nanocapsules to be increased; this is confirmed by Figure 4-4. These graphs display the particle size distributions in the three different samples. As shown in Figure 4-4a, the mean diameter

size of PA/SiO_2 nanocapsules which are prepared in an environment with pH at 11 is 183.7 nm. The obtained mean diameter sizes of other samples are mentioned in Table 4-1. From Figure 4-4 and Figure 4-5 it can also be seen that there is a uniform size distribution for these nanocapsules at adjusted pH at 11 with a narrow size distribution and a small mean diameter. The ranges of diameter size of these three samples are also indicated in Table 4-1.

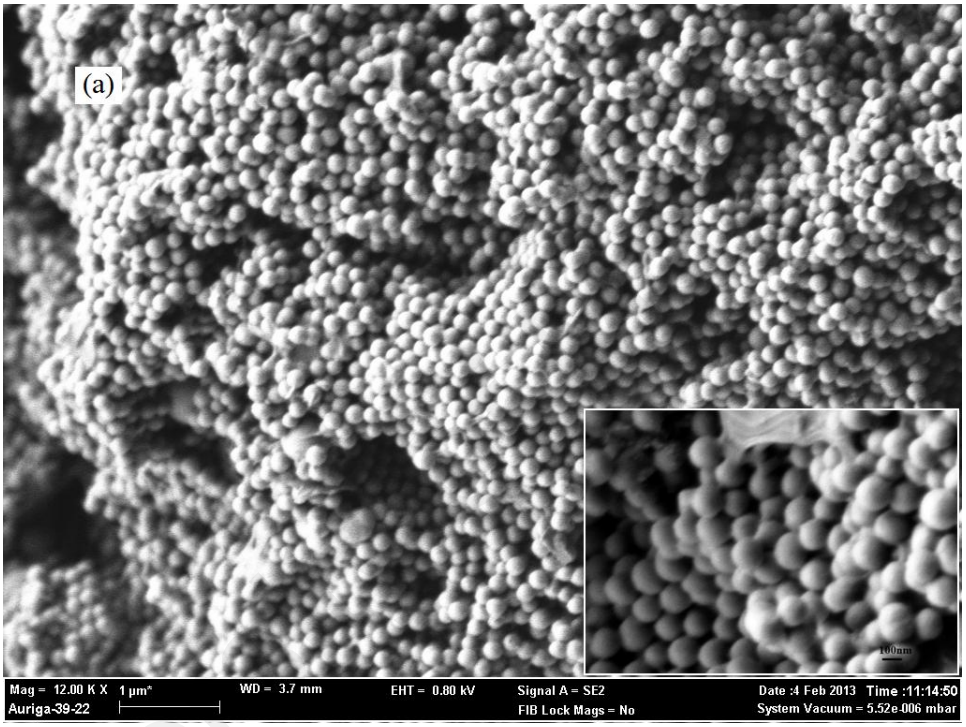

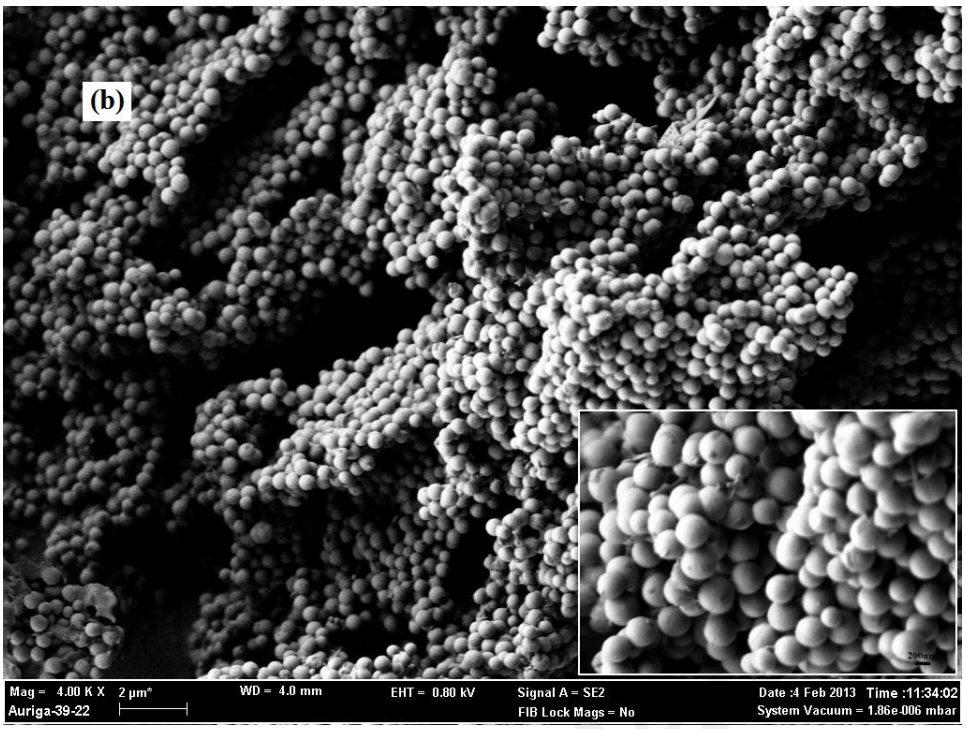

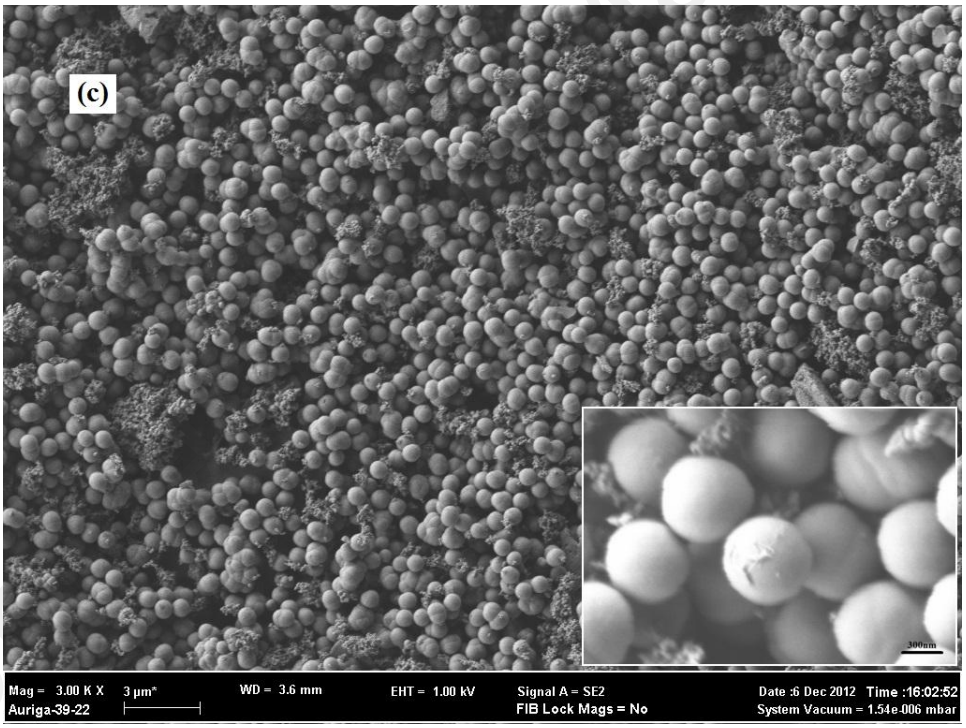

Figure 4-3: SEM of the PA/SiO_2 nanocapsules: (a) SI1, (b) SI2, (c) SI3

Table 4-1: Mean particle sizes and range of diameter sizes of PA/SiO_2 capsulated PCMs

Sample code	pH value	Range of diameter sizes of nanocapsules (nm)	Mean diameter size of nanocapsules (nm)
SI1	11	155-204	183.7
SI2	11.5	349-549	466.4
SI3	12	543-949	722.5

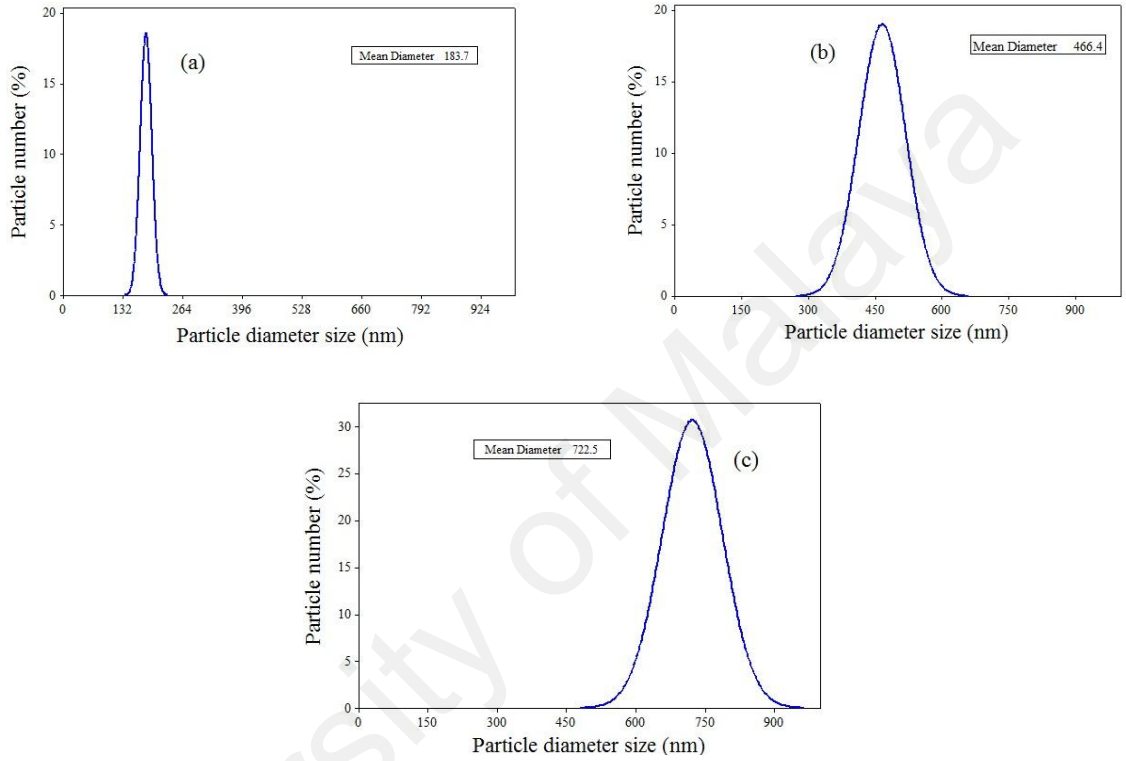

Figure 4-4: The particles size distributions of: (a) SI1, (b) SI2, (c) SI3

The EDS test result shown in Figure 4-5 confirms the existent elements in PA/SiO_2 nanocapsules. The silicon, oxygen and carbon element peaks appear in the graph. Silicon and oxygen are the components of silica and carbon and oxygen are the elements of the palmitic acid. As shown in the graph, there are no other elements in the samples.

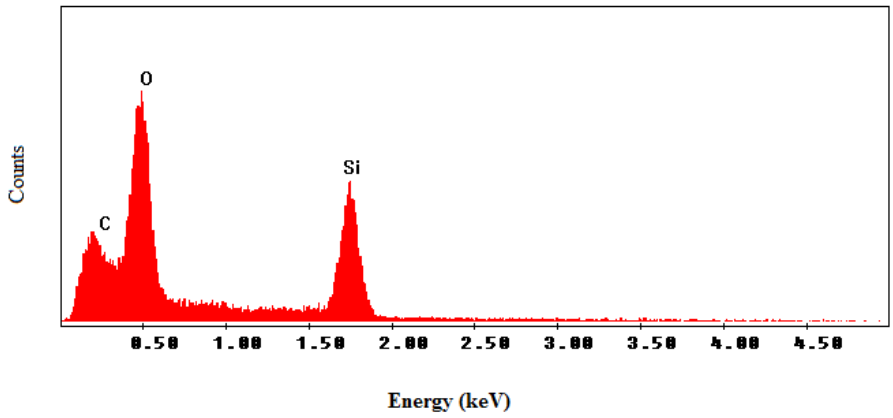

Figure 4-5: The EDS analysis of nanoencapsulated PA/SiO_2 of sample SI3

Transmission electron microscopy (TEM) was used for observing the core/shell structure of the nanocapsules. As can be seen in Figure 4-6, the core of palmitic acid (which is the dark part) is located in the shell of silica (which is the pale part).

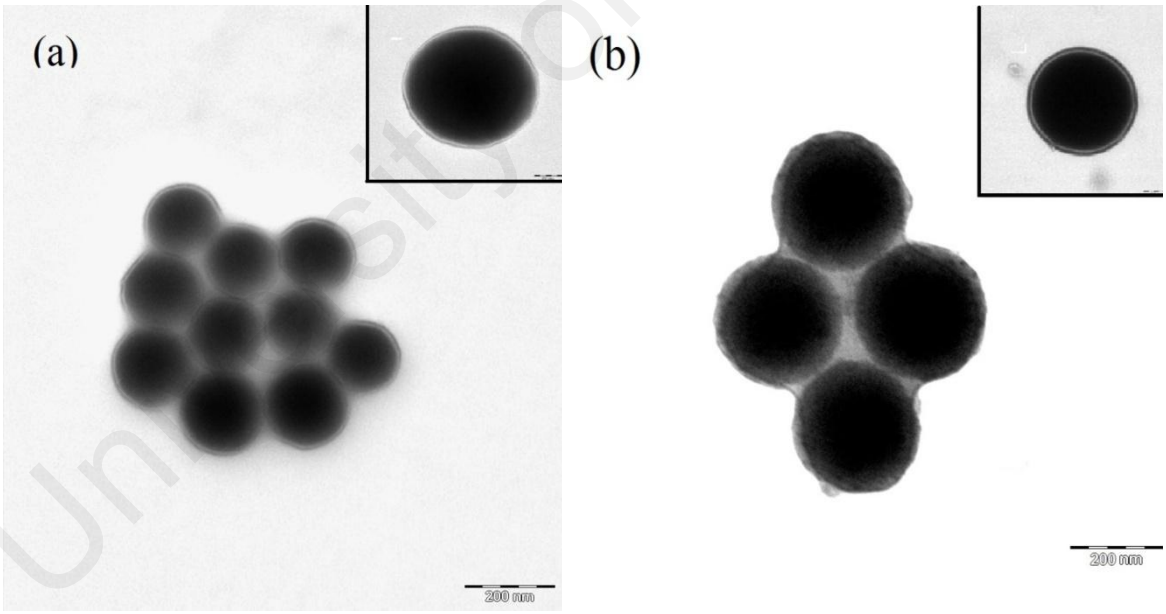

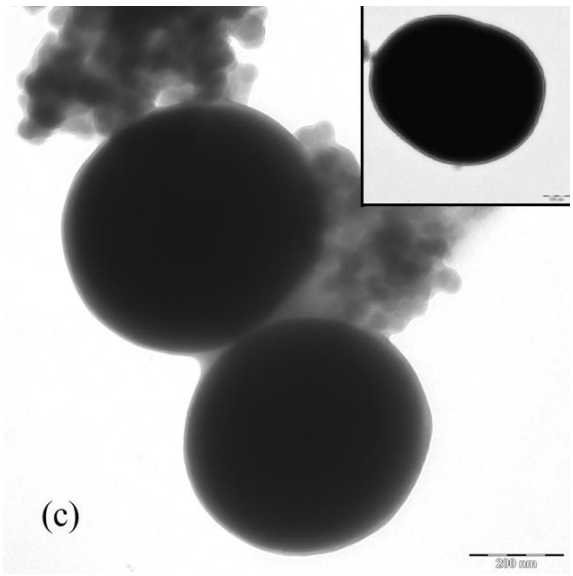

Figure 4-6: TEM images of nanoencapsulated PA/SiO_2 (a) SI1, (b) SI2, (c) SI3

4.2.4 Phase Change Properties of the PA/SiO_2 NEPCMs

The DSC curves of melting and solidifying of nanoencapsulated PA/SiO_2 in all three samples and pure PA are presented in Figure 4-7. The thermal properties based on the curves show that nanocapsules of SI1, SI2 and SI3 samples melt at 61.06, 60.92 and 61.6℃ and freeze at 62.91, 62.83 and 62.74℃, respectively, while pure PA melts at 62.2℃ and solidifies at 62.41℃. The melting and freezing latent heats of SI1, SI2, SI3 and pure PA are noted in Table 4-2.

Table 4-2: The thermal properties of the nanocapsules synthesized under different conditions

Sample	Melting			Solidifying			E_r (%)	E_e (%)	φ (%)
	T_{onset} (℃)	T_{peak} (℃)	ΔH_m (kJ/kg)	T_{onset} (℃)	T_{peak} (℃)	ΔH_C (kJ/kg)			
SI1	61.06	64.30	168.165	62.91	60.30	170.23	83.25	82.53	99.13
SI2	60.92	64.63	172.16	62.83	58.90	173.40	85.22	84.28	98.89
SI3	61.60	66.12	180.91	62.74	59.60	181.22	89.55	88.32	98.62
Pure PA	62.20	65.30	202.00	62.41	56.65	208.00	-	-	-

As noted in Table 4-2, nanocapsules in SI3 have higher latent heat value than the other samples in the melting and solidifying processes. For nanocapsule materials, absorbing/releasing thermal energy through phase change is only done by the core material. This indicates that with greater amount of core material, a higher latent heat storage capacity is achieved. According to this case, because of the larger mean diameter size of nanocapsules in SI3, the latent heat of melting and solidifying is higher than those in other samples.

The encapsulation ratio and encapsulation efficiency of nanocapsules in all three samples were calculated using equations (3-7) and (3-8) and are listed in Table 4-2. The encapsulation ratio reflects the effective content of fatty acid in the composite so by increasing the encapsulation ratio, the mechanical strength and leak proof characteristics of nanocapsules decrease. The great thermal storage capabilities of all three samples affirm the high thermal storage performance of the PCM core materials.

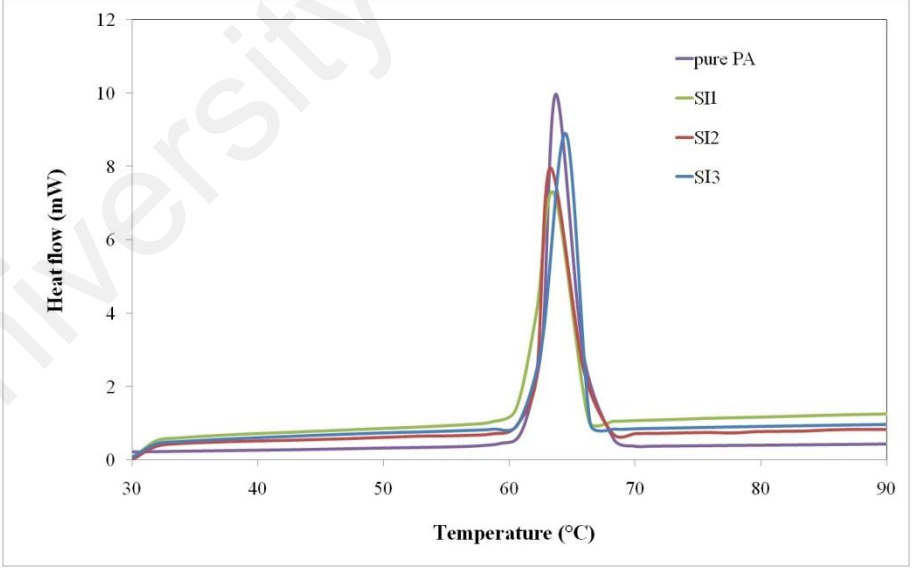

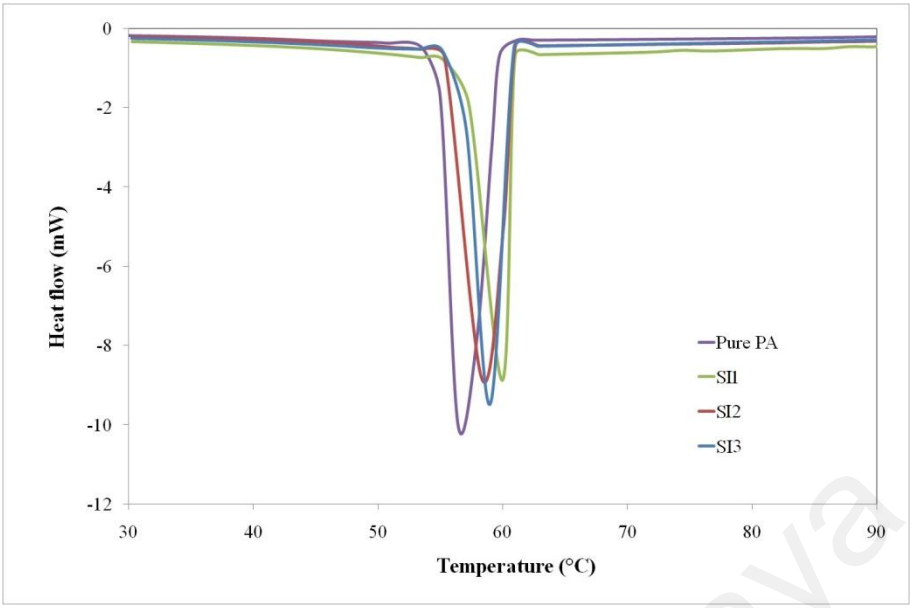

Figure 4-7: DSC curve of (a) melting, (b) solidifying processes of nanocapsules in samples: SI1, SI2, SI3 and pure PA

As is explained in CHAPTER 2 and CHAPTER 3 the supercooling of PCMs is one of their drawbacks. Therefore minimizing supercooling is one of the purposes of synthesizing the NE/MEPCMs. The supecooling of the three samples and pure palmitic acid are calculated by the DSC outcomes and by using the equation (3-6). The difference between the melting and solidification temperature of pure PA, SI1, SI2 and SI3 were 8.65, 4, 5.73, and 6.52℃, respectively which shows that supercooling degree of the NE/MEPCMs are smaller than pure PA during solidification process. The decrease of supercooling of capsules of sample SI1 compared to the other samples indicates that the decrease in the pH value of the shell material synthesis process according to the decrease in the particle size will positively affect the degree of supercooling in NEPCMs. This occurs because the contact surface area and the heat transfer rate of the capsules increase.

The mean shell thickness of the NEPCMs is also calculated by equation (3-10) by using the mean diameter size of the capsules from the SEM images. The density of the shell material found by Archimedes method is 2.1 g/cm^3. The estimated shell

thickness of the samples SI1, SI2 and SI3 are 3.95, 10.30 and 11.05 nm, respectively. The increment of the pH results in a higher silica shell thickness. The higher pH increases the hydrolysis and condensation rate, therefore a larger amount of shell growth in the synthesis period.

4.2.5 Thermal Stability of PA/SiO_2 NEPCMs

The TGA and DTG curves show the thermal stability which is one of the most important factors in thermal properties of PCM encapsulation. Figure 4-8 displays the TGA and DTG of SiO_2/PA nanocapsules. According to Figure 4-8a, pure palmitic acid and the other three samples degrade in one stage. Pure palmitic acid onset degradation is around 208℃ and the weight loss of the SI3 is larger than the other two samples, thus nanocapsules of sample SI3 are encapsulated in greater ratios. In addition, the degradation step of sample SI1 occurs at a higher temperature (around 236℃) than the other samples (around 220 and 230℃ for SI2 and SI3, respectively) which confirms that in lower diameter sizes of nanocapsules the thermal stability is superior. According to the DTG curves in Figure 4-8b, there is a little weight loss below 100℃; this is mainly due to the incomplete removal of water when drying the samples.

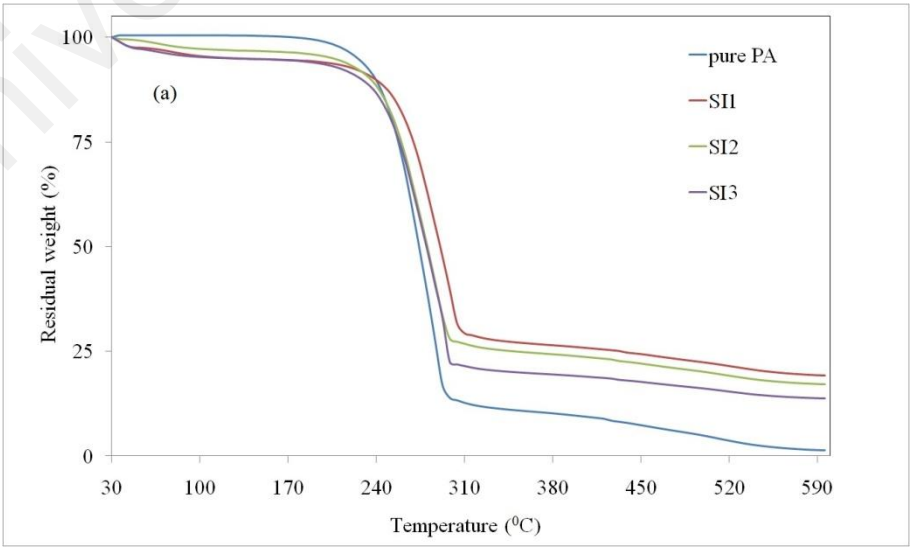

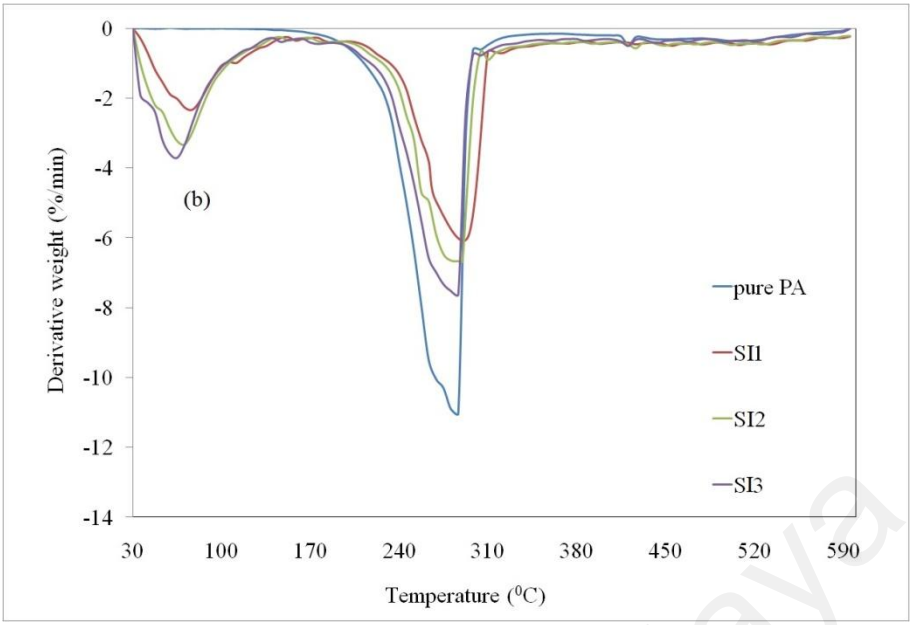

Figure 4-8: (a) TGA, (b) DTG curves of the nanocapsules of SI1, SI2, SI3 and pure PA

4.2.6 Thermal Reliability of PA/SiO_2 NEPCMs

The main issue in thermal energy storage materials is the stability of the thermal and chemical properties after a long term utility period. Accordingly, thermal cycling testing was performed to investigate properties of encapsulated PCMs after a large number of melting and freezing cycles. Thermal cycling test was done for 2500 cycles for three samples and the results indicate the supreme thermal reliability of all samples. The DSC results before and after thermal cycling for SI3 that had the highest encapsulation ratio are shown in Figure 4-9.

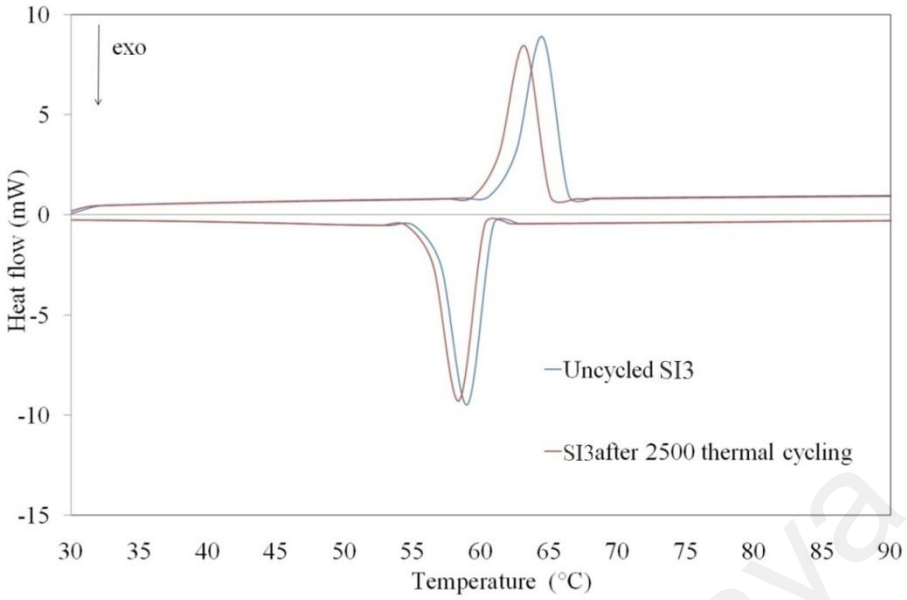

Figure 4-9: DSC curves for SI3 before and after thermal cycling

The melting and solidifying temperatures of encapsulated PCMs were changed from 61.6℃ to 60.1℃ and 62.74℃ to 61.63℃ after 2500 thermal cycling, respectively. Also, the latent heats of melting and freezing of encapsulated PCM were measured as 177.3 kJ/kg and 178.6 kJ/kg after 2500 thermal cycles, respectively. These results imply that there were no significant changes in temperatures and latent heats of encapsulated PCMs after a high number of thermal cycles. An SEM image of encapsulated PCMs of sample SI3 was also taken after thermal cycles to prove that the maintained its shape of capsules was stable during thermal cycling. Figure 4-10 shows that encapsulated PCMs have a perennial shape during thermal cycling.

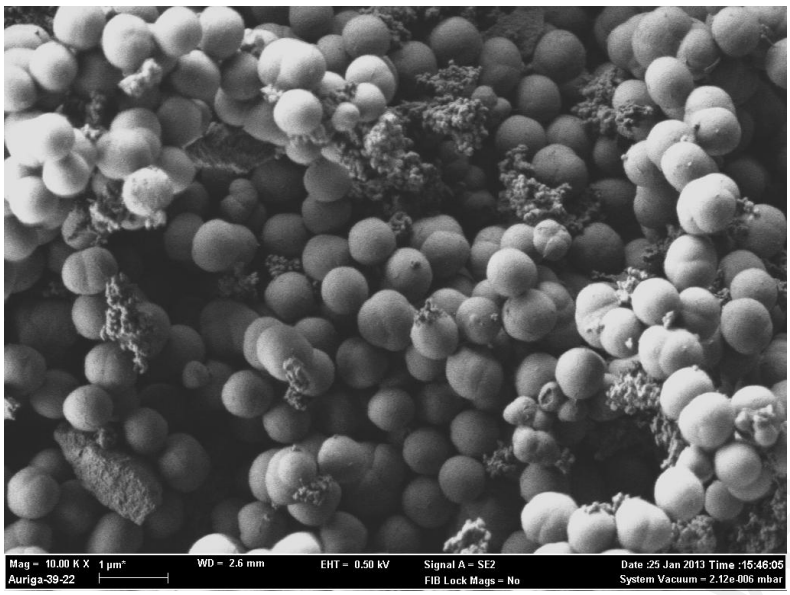

Figure 4-10: SEM image of encapsulated PCM of SI3 after thermal cycling

Figure 4-11 shows the FTIR spectra of encapsulated PCMs of SI3 before and after thermal cycling. It can be seen that there are no changes in the shape and frequency values of major peaks after the process, indicating that the chemical formation of the capsules was not affected after a high number of repeated melting/solidifying cycles.

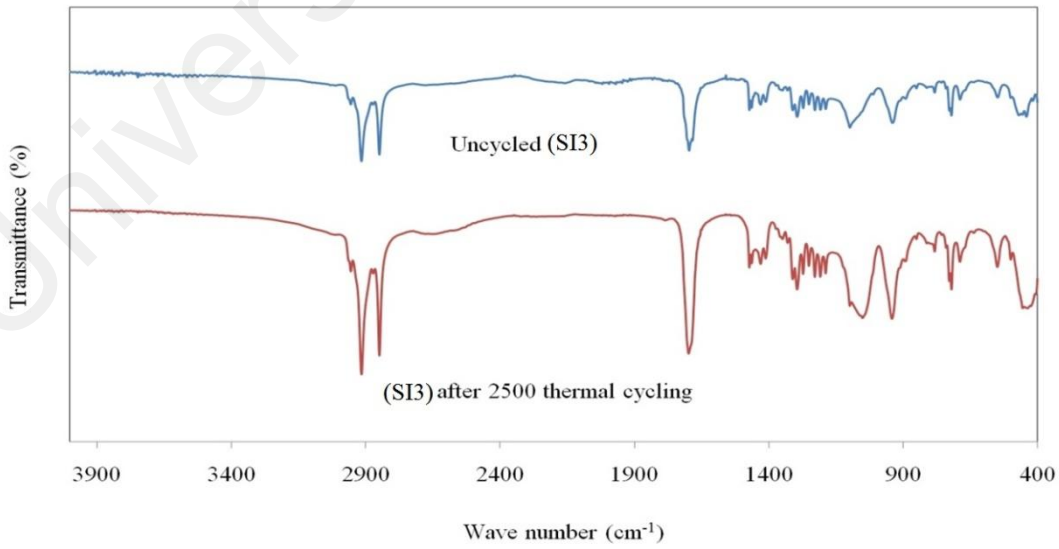

Figure 4-11: FT-IR spectra of encapsulated PCM before and after thermal cycling

4.2.7 Thermal Conductivity of PA/SiO_2 NEPCMs

The thermal conductivities of the pure PA and the encapsulated PCMs were measured by a thermal conductivity apparatus (KD-2 Pro) using the hot wire method. As is well known, PA has a low thermal conductivity which has significant effects on the rate of heating and cooling processes. The thermal conductivity of encapsulated PCMs was measured below and above the melting temperature of PA in thermal equilibrium condition. The results are presented in Table 4-3 for PA and SI1-SI3 which show that both in solid state (30℃) and molten state (80℃), the thermal conductivity of encapsulated PCMs is above than that of pure PA. The results prove that the thermal conductivity of the SI1 in both molten and solid regions was increased by more than three times compared to the PA thermal conductivity according to the high specific surface area of NEPCMs in sample SI1.

Table 4-3: Thermal conductivity of PA encapsulated within SiO_2 shell

Sample code	Thermal conductivity (W/m.K)	
	molten state (80℃)	Solid state(30℃)
PA	0.26	0.21
SI1	0.77	0.71
SI2	0.52	0.48
SI3	0.49	0.47

4.3 Stearic acid/Titania Nanocapsules

Titania attracts a wide attention in many applications due to its high thermal stability and chemical properties. In this study, by applying the sol-gel method the titania shell was fabricated around the stearic acid micelles by using SDS as surfactant. TTIP was used as the precursor for the titanium dioxide shell. The effect of pH value was studied by adjusting the pH value at 10-10.8 and 11.5 for different samples. The influence of SA/TTIP weight ratio on the thermo-physical properties of the

NE/MEPCMs is also investigated. The consequences of the characterization are demonstrated in subsequent sections.

4.3.1 FTIR Spectra of SA/TiO_2 NEPCMs

Chemical interaction between SA and TiO_2 would affect the latent heat storage performance of the NEPCMs; thus, chemical, structural and stability analyses are important in evaluating the performance of NEPCMs. FT-IR spectroscopy was used to investigate the interaction between SA and TiO_2, as shown in Figure 4-12. Figure 4-12a shows the spectrum of SA plus the prepared TiO_2 sol. In the pure SA spectrum, the registered peak at 2915 cm^{-1} corresponds to the symmetrical stretching vibration of the C–H_3 group, and the peak at 2848 cm^{-1} corresponds to the symmetrical stretching vibration of the C–H_2 group. The stretching vibration of the C=O group produces a strong absorption peak at 1692 cm^{-1}. The peaks at 1461 and 1290 cm^{-1} are allocated to the in-plane bending vibration of the functional O–H group in SA, and the peak at 926 cm^{-1} corresponds to the out-of-plane bending vibration of the O–H functional group. The peak at 719 cm^{-1} corresponds to the in-plane swinging vibration of the O–H functional group (Sarı et al., 2009b). In the TiO_2 spectrum, the absorption broad bands from approximately 2670 to 3800 cm^{-1} corresponds to the stretching and deformation vibrations of the –OH functional group in H_2O that are associated with absorbed water. The other peak at 1651 cm^{-1} corresponds to the stretching of titanium carboxylate that formed from the TTIP and ethanol precursors (Lee et al., 1998).

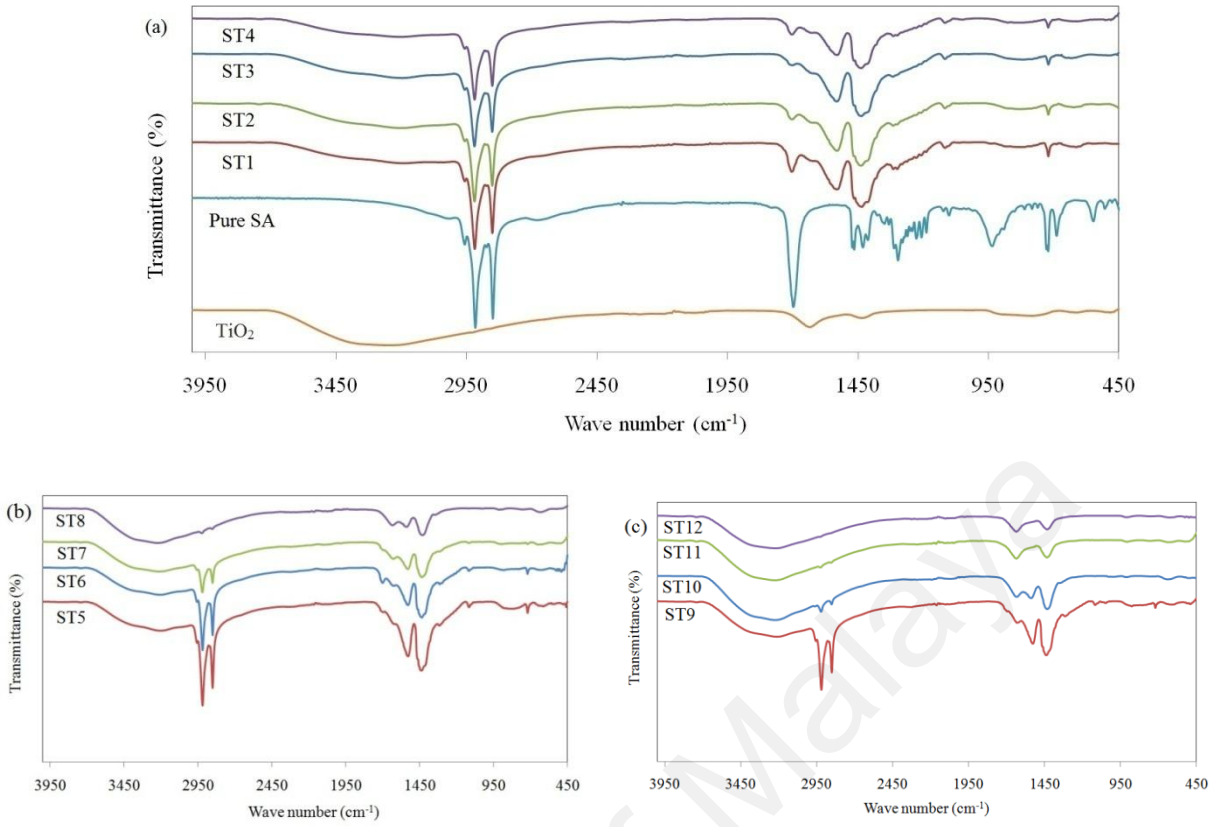

Figure 4-12: FTIR spectra of TiO_2, pure SA, and NEPCMs synthesised at (a) pH 10, (b) pH 10.8, and (c) pH 11.5

Figure 4-12a shows the spectra for the ST1-ST4 samples that were prepared at pH 10 for different SA/TTIP weight ratios: the characteristic peaks of SA and TiO_2 were clearly distinguishable in the spectra of nanocapsules, and no peak shifts were observed. Furthermore, the absorption peak at 1539 cm^{-1} in the spectra of the NEPCMs corresponded to the stretching vibration of the C=O from the small amount of titanium stearate that formed in the NEPCMs. The spectra of ST1-ST4 confirmed the successful encapsulation of SA by the titania shells. However, the characteristic peaks of SA did not appear in the spectra for the ST8 and ST10-ST12 samples (Figure 4-12b, c), which were synthesized at pH values of 10.8 and 11.5. This result indicated that the SA encapsulation was not successful for the conditions under which these samples were prepared. The SEM images of these samples also confirmed this result. This outcome may have occurred because of an accelerated hydrolysis rate at higher pH that did not

allow sufficient time for encapsulation. Thus, all of the imaging results and analyses on ST1-ST4 indicated that the NEPCMs were properly encapsulated at a pH of 10 and can be used to investigate the effect of the SA/TTIP weight ratios on the thermal properties of the NEPCMs.

4.3.2 XRD Crystallography of SA/TiO_2 NEPCMs

The XRD patterns of SA, the TiO_2, and ST1 are shown in Figure 4-13. The same XRD peaks were observed in the ST2, ST3, and ST4 patterns as for ST1 but at higher intensities because ST2, ST3, and ST4 contained higher amounts of SA than ST1. The SA peaks at 21.6° and 23.8° in Figure 4-13 corresponded to the regular crystal structure of SA. No distinct XRD pattern can be observed for TiO_2, indicating that the TiO_2 that was prepared by hydrolysis and condensation was non-crystalline and amorphous, which also explains the absence of the TiO_2 peaks from the NEPCM spectrum.

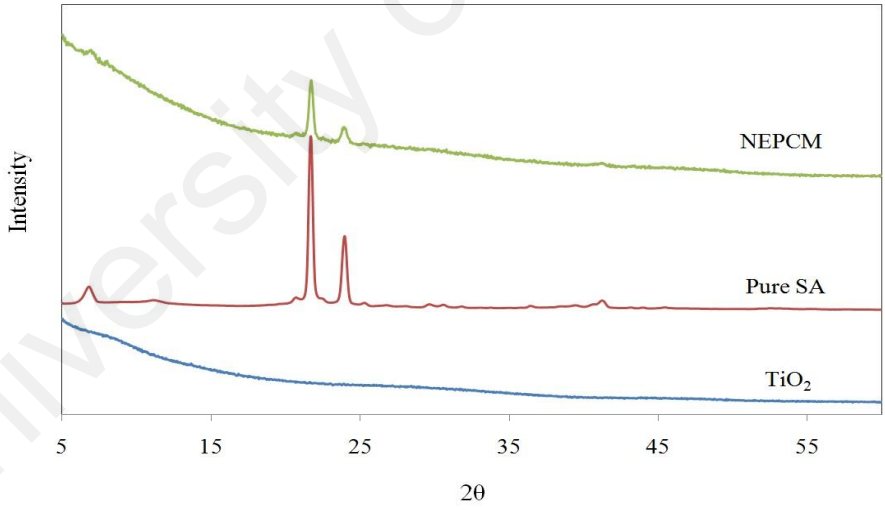

Figure 4-13: XRD patterns of the TiO_2, pure SA and SA/TiO2 NEPCMs

The NEPCM spectrum consisted of SA peaks superimposed on an amorphous bump for TiO_2. This result demonstrates that the crystal structure of the SA in the NEPCMs was not affected by the synthesis process and that SA was encapsulated in the TiO_2 shells, because TiO_2 could not form inside the SA droplet. The decreased intensity of the XRD peaks of SA for ST1 compared to that for pure SA indicated that the SA

crystallite size was smaller for the NEPCMs than for ST1, because SA crystal growth was inhibited by the small volume of the NEPCM capsules, which also increased the peak width.

4.3.3 Surface Morphology and Elemental Analysis of SA/TiO_2 NEPCMs

The particle size and shape of a substance can significantly alter its properties. Therefore, a morphological investigation using SEM was conducted to confirm the successful nanoencapsulation of SA within TiO_2. Figure 4-14a-d clearly illustrate that the nanoencapsulated SA had spherical shapes with smooth and compact surfaces. The particle size distribution (PSD) of the NEPCMs was estimated from the SEM images and is shown in Figure 4-14e. The mean diameter of the NEPCMs for sample ST1 was approximately 317.6 nm, whereas the mean diameter sizes of the ST2, ST3, and ST4 samples were 583.4, 620.1, and 946.4 nm, respectively. Figure 4-14a-d illustrate that the nanocapsules in ST1 were smaller, less aggregated and more uniform in size than the nanocapsules in ST2-ST4. This result was confirmed by the narrow and broad peaks for the ST1 and ST2-ST4 samples as shown in Figure 4-14e.

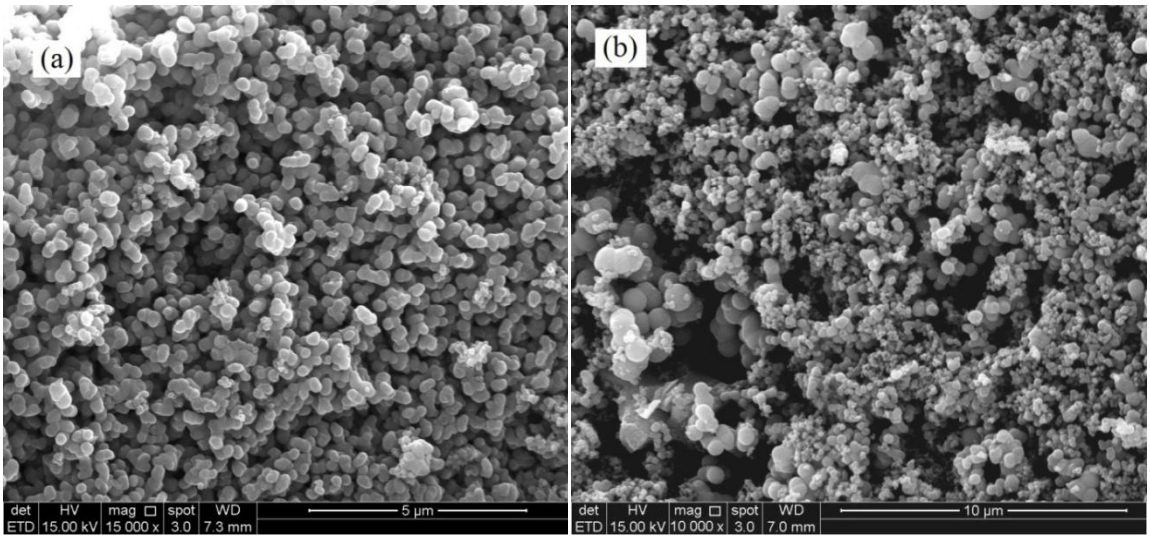

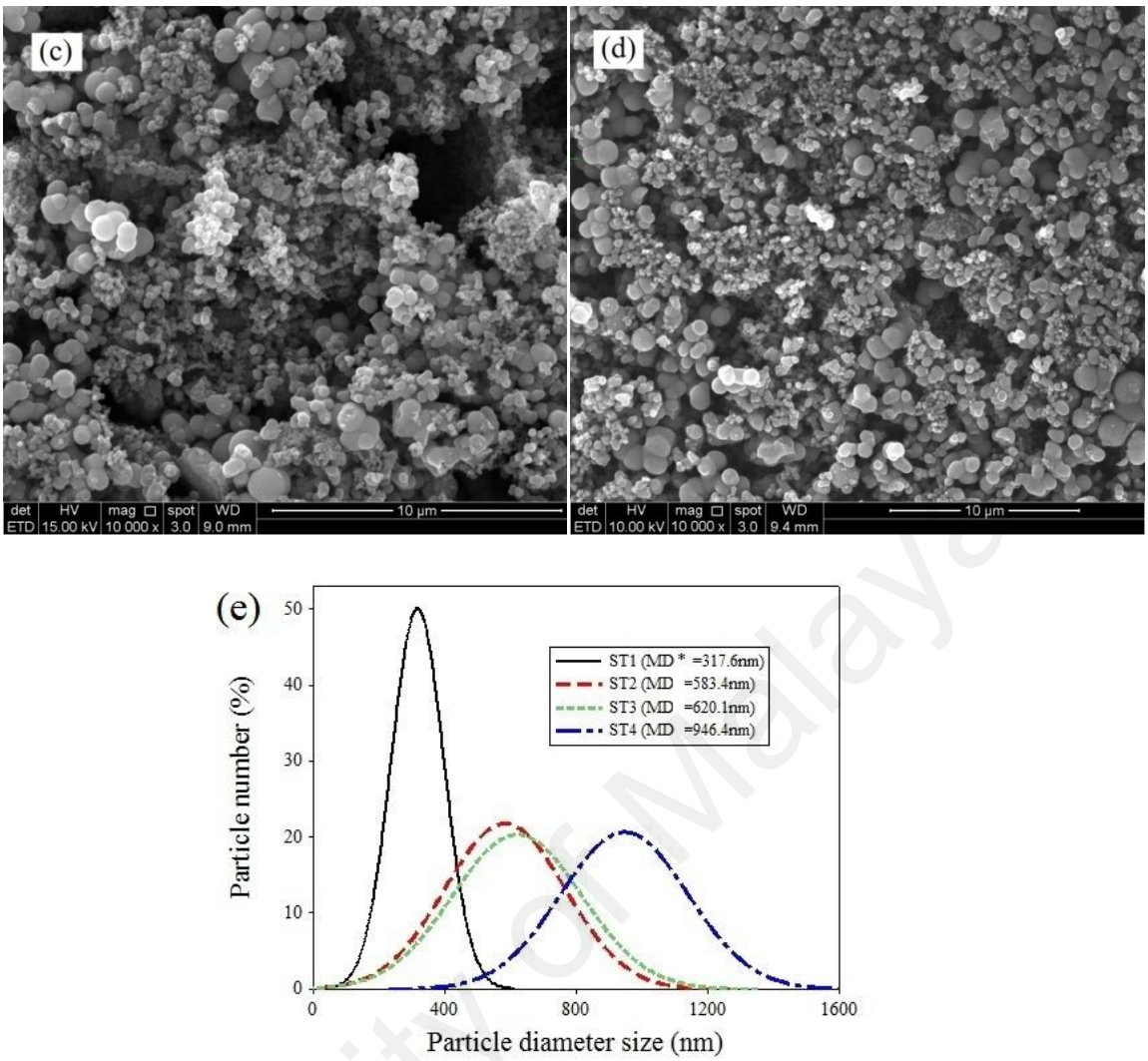

***MD= Mean Diameter**

Figure 4-14: SEM images for SA/TiO_2 nanocapsules for (a) ST1, (b) ST2, (c) ST3 and (d) ST4 and (e) particles size distributions of the prepared samples

In the sol-gel encapsulation method, the stirring rate and emulsifier amount are considered to be the two parameters that control the particle size distribution of the NEPCM products (Qiu et al., 2012). However, in our preparation scheme, all of the parameters were held constant except for the SA/TiO_2 ratio. The PSD in Figure 4-14e shows that this ratio was a major factor in determining the particle size and particle size distribution of the prepared samples.

A TEM analysis was performed to investigate the core-shell structure of the nanocapsules of SA with titania shells. The TEM image in Figure 4-15a shows the SA core (dark part) surrounded by a titania shell (pale part).

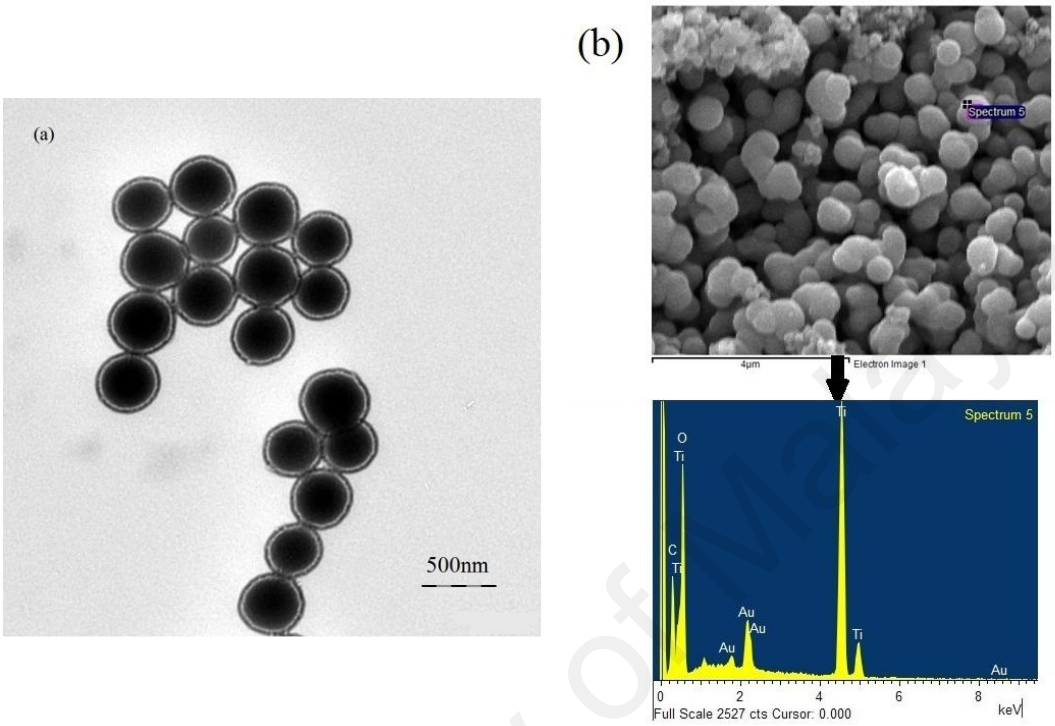

Figure 4-15: (a) TEM images and (b) EDS analysis of ST1

The EDS test results shown in Figure 4-15b confirmed the elements in the SA/TiO_2 nanocapsules. Titanium, oxygen and carbon element peaks appear in the graph. Titanium (Ti) and oxygen (O) are the components of titania, and carbon (C) and oxygen (O) are the elements of SA. The graph also indicates the presence of gold (Au), which resulted from the gold coating of the sample in preparation for the SEM and EDS analyses.

4.3.4 Thermal Performance of SA/TiO_2 NEPCMs

Phase-change properties are key parameters that affect the practical application of NEPCMs. Differential scanning calorimetry (DSC) is an appropriate technique for studying the phase change behaviour of pristine SA and NEPCMs. The DSC curves of

the melting and solidification processes of SA and the prepared NEPCMs for various SA/TTIP mass ratios are shown in Figure 4-16a, b, respectively. The relevant results are summarized in Table 4-4.

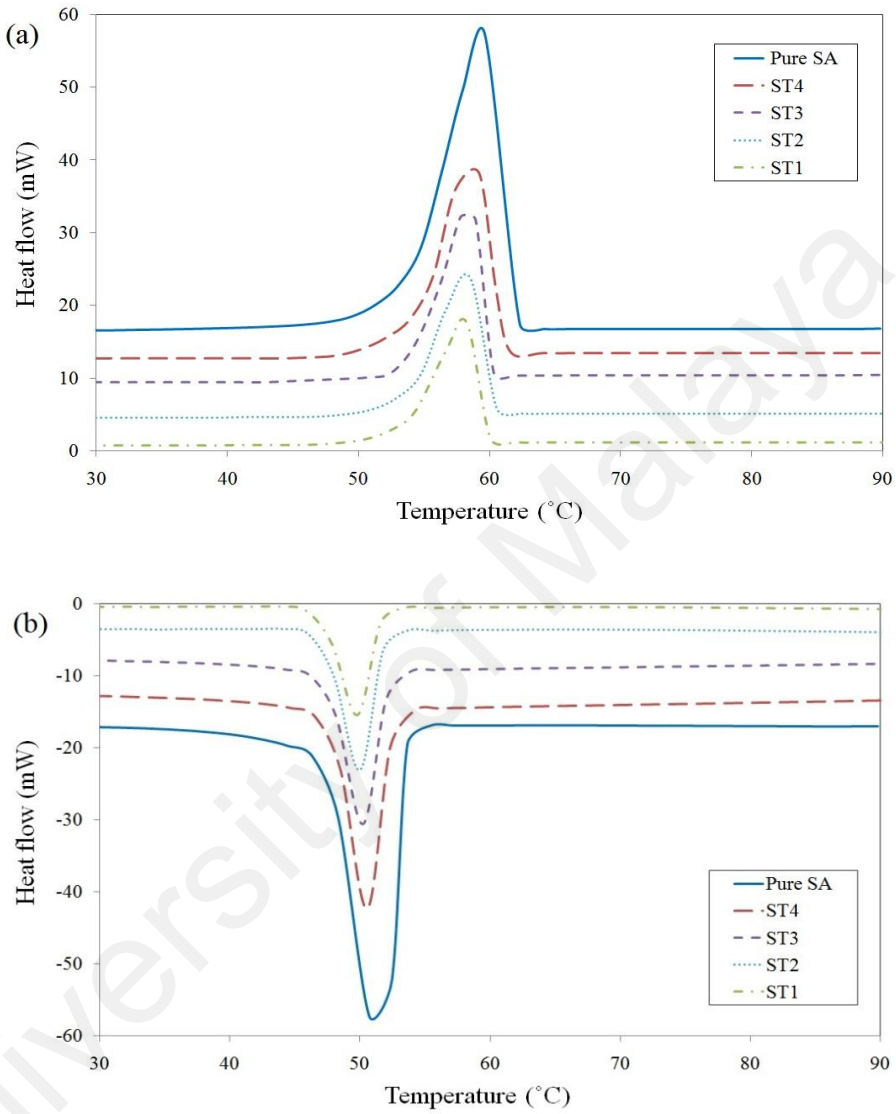

Figure 4-16: DSC thermograms of the (a) heating and (b) cooling of pure SA and the NEPCMs

Figure 4-16 and Table 4-4 illustrate that the melting and solidifying temperatures of pure SA were 55.32 and 53.31℃. The latent heat was 191.41 kJ/kg for melting and 172.93 kJ/kg for solidification. The thermal properties obtained from the curves indicated that nanocapsules in ST1, ST2, ST3 and ST4 melted at 54.35, 54.72, 54.83

and 55.04℃ and solidified at 51.64, 51.84, 52.03 and 52.36℃, respectively. The phase-change temperatures of the NEPCMs were close to each other and slightly lower than those of SA. Hence, in as much as the TiO_2 shell is an inert material, the similarity between the thermal properties of the NEPCMs and SA indicated that the absorption/release of thermal energy through phase change occurred in the core material. Thus, ST4 had the highest SA content and highest latent heat of all of the prepared samples.

Table 4-4: Phase-change properties of SA and NEPCMs

Sample	Melting			Solidifying					
	T_{onset} (℃)	T_{peak} (℃)	ΔH_m (kJ/kg)	T_{onset} (℃)	T_{peak} (℃)	ΔH_c (kJ/kg)	E_r (%)	E_e (%)	φ (%)
SA	55.32	59.40	191.41	53.31	51.22	172.93	-	-	-
ST1	54.35	58.23	58.12	51.64	49.80	50.59	30.36	29.84	98.32
ST2	54.72	58.46	87.95	51.84	49.97	74.76	45.94	44.66	97.23
ST3	54.83	58.72	99.02	52.03	50.20	84.93	51.73	50.49	97.61
ST4	55.04	59.14	123.96	52.36	50.54	109.43	64.76	64.06	98.93

The encapsulation ratio describes the efficient encapsulation of stearic acid within the titania shells. Stearic acid cannot melt if the nanocapsules are very small due to confinement. Therefore, the encapsulation ratio demonstrates an effective property of the SA inside the capsules for heat energy storage and thermal regulation. Also as the other important parameter, encapsulation efficiency describes the effective performance of the PCMs inside the capsules. Table 4-4 shows that the calculated SA contents in ST1-ST4 were 30.36 wt%, 45.94%, 51.73%, and 64.76%, which were lower than the

mass ratio during synthesis. This result indicates that a small amount of the SA was not encapsulated in the TiO_2 shell and was washed away in the preparation process. The encapsulation ratio and encapsulation efficiency are associated with the SA/TTIP weight ratio. A higher core/shell weight ratio was obtained because of the higher SA/TTIP weight ratio; therefore, the encapsulation ratio and encapsulation efficiency can be increased by increasing the SA/TTIP weight ratio. However, the high thermal storage capabilities of the NEPCMs indicated that nearly all of the nanocapsules stored latent heat effectively through the phase change. Additionally; the calculated mean shell thickness of prepared samples by using the obtained density of 2.9 g/cm^3 for titania shell material in equation (3-10), are 26.8, 59.6, 52.25 and 49.34nm for ST1, ST2, ST3 and ST4, respectively.

From Figure 4-16, we realize that the degree of supercooling in pure SA was slightly compared to that in the NEPCMs. However; the supercooling of all samples are in the appropriate range for TES applications.

4.3.5 Thermal Stability of SA/TiO_2 NEPCMs

Thermal stability is a significant factor for the practical application of NEPCMs. The thermal degradation temperature of NEPCMs was determined using TGA analysis. Figure 4-17 shows the thermogravimetry curves for pure SA and the prepared NEPCMs. The curves illustrate that the SA degraded in a single step over a temperature range of 150-250°C. The SA/TiO_2 nanocapsules exhibited two thermal degradation stages. The first stage occurred over a temperature range of 160-320°C and was associated with the evaporation of the SA content of the NEPCMs, whereas the second weight loss was observed between the temperatures of 320-450°C and was attributed to the removal of chemisorbed water molecules from inside the shell.

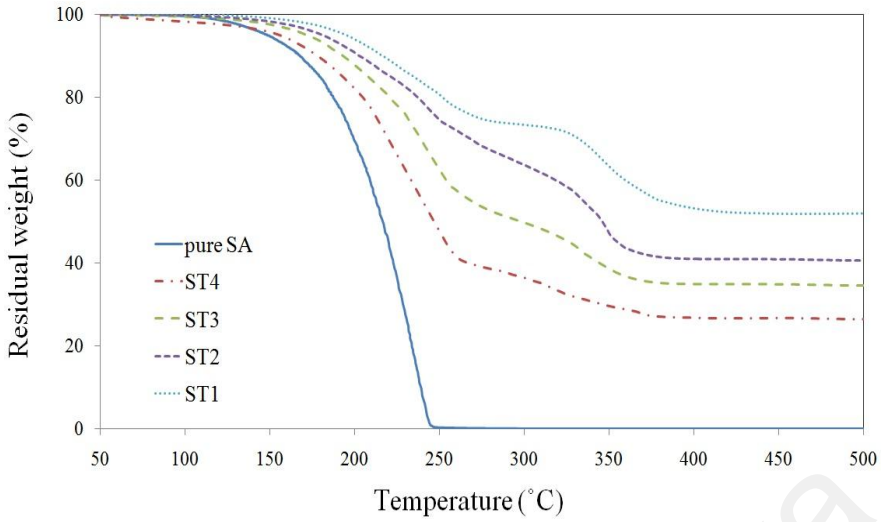

Figure 4-17: TGA curves for SA/TiO_2 nanocapsules

Figure 4-17 shows that all of the nanocapsule samples exhibited a maximum weight loss at higher temperatures than pure SA. However, the initial temperature of the first degradation step of the NEPCMs was reasonably above their working temperature or the melting temperature of them.

These results show that the titania shell increased the thermal stability of the nanoencapsulated SA and prevented leakage of the melted SA.

4.3.6 Thermal Conductivity of SA/TiO_2 NEPCMs

The low thermal conductivity of SA delays the thermal response during the storage and release of latent heat. Thus, the thermal conductivity of the prepared NEPCMs must be increased. The thermal diffusivity was measured by a laser flash method, and was calculated as described in CHAPTER 3.

The calculated thermal conductivities of the microcapsules and pure SA in the solid state (35°C) are shown in Table 4-5. The data in Table 4-5 indicate that the thermal conductivities of the SA/TiO_2 NEPCMs (ST1-ST4) were clearly greater than that of pure SA because of the high thermal conductivity of the TiO_2 shell.

Table 4-5: Thermal conductivity of encapsulated PCMs and pure SA

Sample	Thermal conductivity (W/m·K)	Thermal conductivity enhancement (%)
ST4	0.42	100.0
ST3	0.45	114.2
ST2	0.47	123.8
ST1	0.52	146.6
Pure SA	0.21	-

The thermal conductivities of nanoencapsulated SA depended strongly on the encapsulation ratio. Table 4-5 shows that the thermal conductivities of ST1-ST4 were increased by 146.6%, 123.8%, 114.2%, and 100%, respectively, over those of pure SA and the SA/TiO_2 nanocapsules.

We expected the NEPCM conductivity to increase as the SA loading decreased because of the increase in the weight percentage of the TiO_2 material. However, the thermal conductivities of the PCMs were at acceptable levels for thermal energy storage applications.

4.3.7 Thermal Reliability of SA/TiO_2 NEPCMs

Other highly significant limitations for the application of NEPCMs are the thermal and chemical stabilities of the NEPCMs after long-term use. There should be little or no difference in the thermal and chemical properties of NEPCMs after a large number of melting and freezing cycles. A thermal cycling test of 2500 cycles was performed to study the durability of ST4, which had a higher encapsulation proportion than the other samples. DSC and FT-IR spectra for the prepared NEPCMs were acquired before and after the thermal cycling test (Figure 4-18).

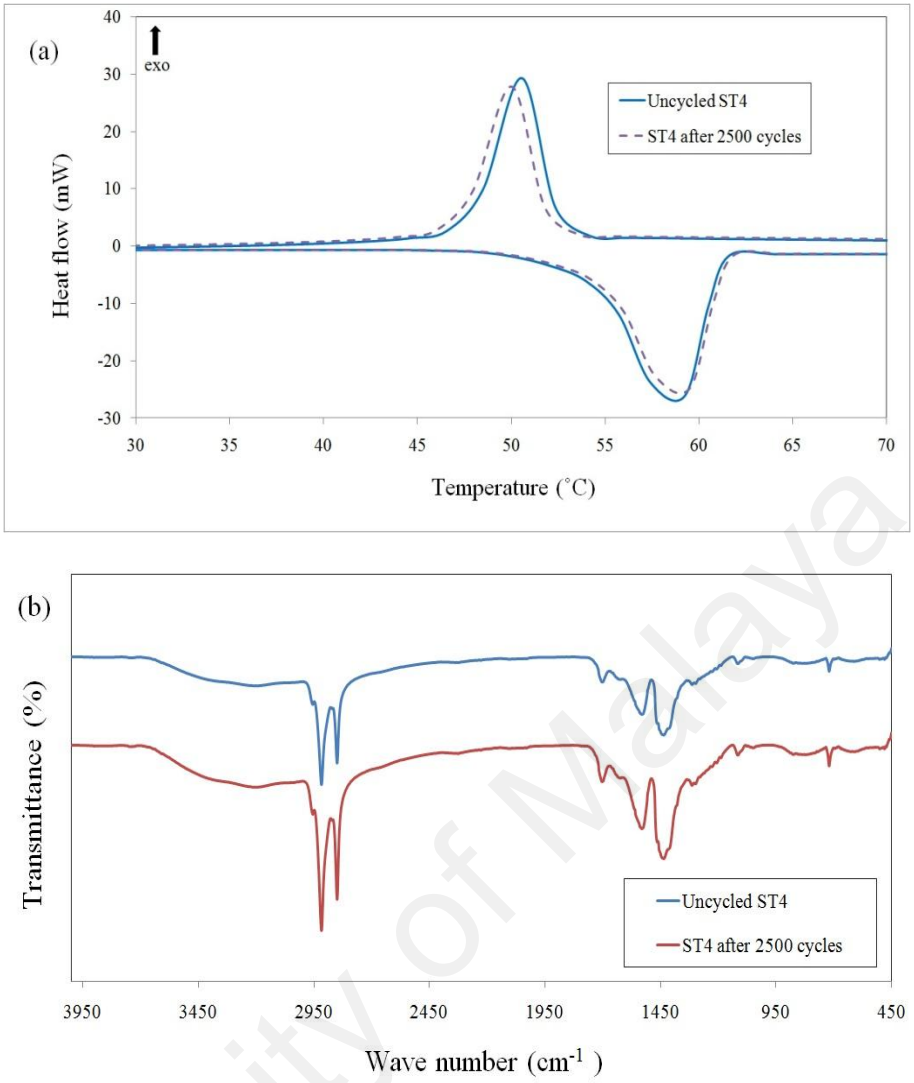

Figure 4-18: (a) DSC curves and (b) FT-IR spectra for ST4 before and after thermal cycling

Figure 4-18a shows that the melting and solidifying temperatures of ST4 changed only slightly from 59.14℃ to 59.41℃ and from 50.54℃ to 50.01℃, after 2500 thermal cycles. Furthermore, the latent heats of melting and freezing of the encapsulated PCM after 2500 thermal cycles were measured as 119.23kJ/kg and 105.68kJ/kg, respectively. The reduction in the latent heat values was within a suitable range for NEPCM applications. The FT-IR spectra for the NEPCMs before and after thermal cycling are shown in Figure 4-18b, after thermal cycling, no changes were observed in the shapes of the peaks and no new peaks appeared in the spectrum.

The properties of the NEPCMs after 2500 cycles indicate that the prepared NEPCMs exhibited good thermal and chemical stability for retaining a reversible phase change without any deterioration in the phase-change properties; thus, the NEPCMs can be repeatedly used for thermal storage.

4.4 Palmitic Acid/Alumina MEPCMs

The high thermal conductivity of alumina makes it a suitable candidate for encapsulating the PCMs. The AIP as one of the best alkoxides for preparing the alumina was used in this project to prepare PA/Alumina capsules. Different pH values were adjusted in the preparation process, but only at a pH of 10.5 microcapsules could be formed. The influence of the PA/AIP weight ratio on the properties of the MEPCMs were studied by characterizing the properties of four different samples with different PA/AIP weight ratios of 50/50,60/40,70/30 and 80/20. The characteristic descriptions are explained in the following sections.

4.4.1 Chemical Composition of PA/Al_2O_3 MEPCMs

The FTIR spectra of the prepared Al_2O_3 shell, pure PA, and prepared MEPCMs are displayed in Figure 4-19. Figure 4-19(a) shows broad absorption peaks at 3100–3700 cm^{-1} due to the O–H stretching of the absorbed water. The peaks at 450-700 cm^{-1} are allocated to the Al–O vibrations. The stretching modes of Al–O–Al linkages are observed at 624 and 700 cm^{-1}. The peak at 1080 cm^{-1} is due to the Al–O–H vibration modes of Al_2O_3.

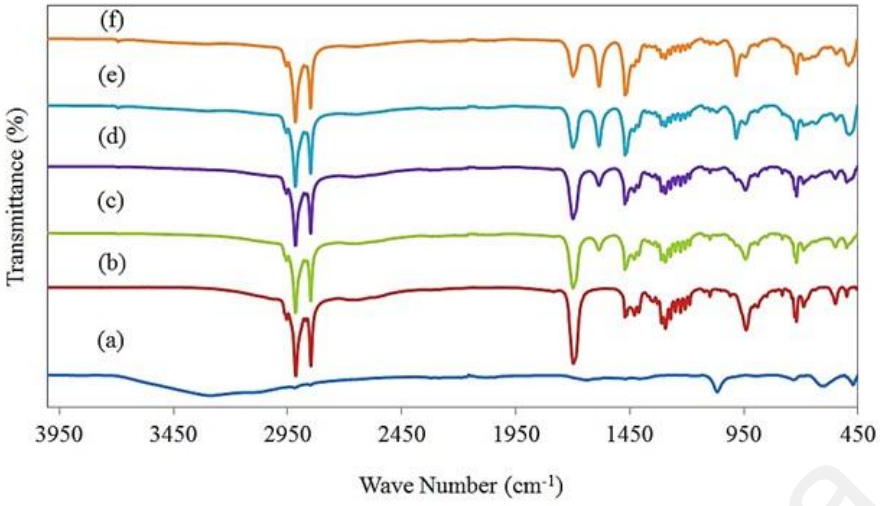

Figure 4-19: FTIR spectra of (a) Al_2O_3, (b) pure PA, (c) S4, (d) S3, (e) S2, and (f) S1

Figure 4-19(b) exhibits the spectrum of the pure PA. The peaks at 2912 cm^{-1} and 2846 cm^{-1} correspond to the symmetrical stretching vibration peaks of $–CH_3$ and $–CH_2$ in the PA. The absorption peak at 1691 cm^{-1} is associated with the C=O stretching vibration. The peak at 1293 cm^{-1} refers to the in-plane bending vibration of the –OH group of the PA, the peak at 937 cm^{-1} corresponds to the out-of-plane bending vibration of the –OH functional group and the peak at 720 cm^{-1} demonstrates the in-plane swinging vibration of the –OH functional group (Sari & Kaygusuz, 2002).

Figure 4-19(c)-(f) reveal that the absorption peaks in the PA at 2912, 2846, 1293, 937 and 720 cm^{-1} are essentially unchanged in the microcapsules. The effect of the absorption peaks of the Al_2O_3 shell at 480, 624, and 1080 cm^{-1} can also be found within the microcapsules spectra. The interaction between PA and Al_2O_3 crystals has been confirmed through the reduction of the intensity as well as the shifting of C=O stretching band of the PA initially at 1691 cm^{-1} to the lower frequency of 1595 cm^{-1} in the FTIR spectra of microcapsules. This shift proved that there were interface interactions between the COOH group of the PA and alkaline area in Al_2O_3, which can change the thermo-physical properties of encapsulated PA (Tang et al., 2014). The FTIR results confirmed that the Al_2O_3 shell was formed on the surface of the PA droplet

by considering that the Al_2O_3 can only be shaped around the interface of the PA in O/W emulsion.

4.4.2 Crystallography of the PA/Al_2O_3 MEPCMs

Figure 4-20 shows the XRD patterns of the Al_2O_3, pure PA and MEPCMs which reveal the crystalline structures. The broad peaks in Figure 4-20(a) at 28˚, 38˚, and 49˚could be assigned to the formation of boehmite phase while the weak and broad diffraction lines indicate the poor crystallinity.

Figure 4-20(b) shows that the peaks at 21.8° and 24.3° belong to the normal crystallization of the PA and Figure 4-20(c)-(f) show that the XRD peaks of the PA in microcapsules also contain the boehmite smooth peaks.

Figure 4-20(c)-(f) indicated that the strong and sharp diffraction peaks of the pure PA become weak and broad peaks due to the formation of microcapsules. The XRD analysis further proved that the PA in the core of Al_2O_3 microcapsules became a short-range order compared to the high-melting-point pure PA crystals, therefore some changes in the thermal properties of the MEPCMs might be expected.

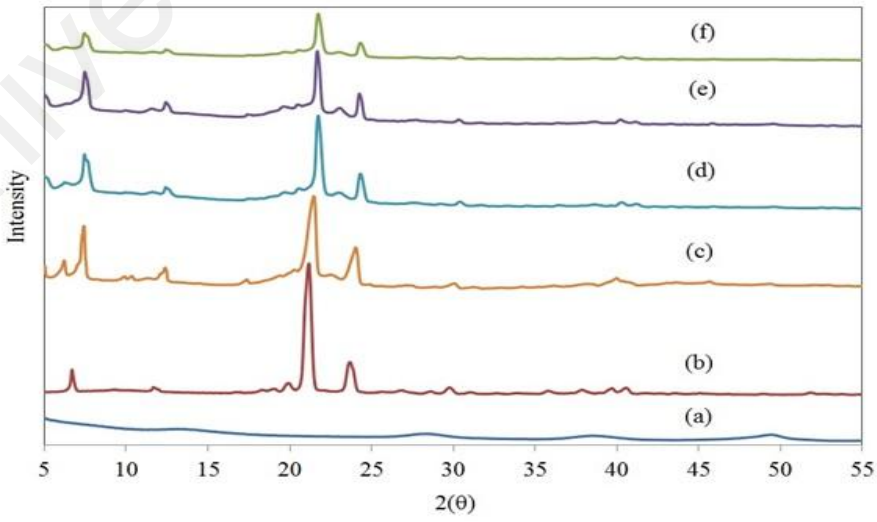

Figure 4-20: XRD patterns of (a) Al_2O_3, (b) pure PA, (c) S4, (d) S3, (e) S2, and (f) S1

4.4.3 Surface Morphology and Surface Element Analysis of PA/Al_2O_3 MEPCMs

Figure 4-21 and Figure 4-22 present the morphologies of the microcapsules synthesized with four different weight ratios of PA/AIP and it can be seen that the microcapsules were spherical. It can be seen in Figure 4-21a-d that the weight ratio of PA/AIP influences the diameter and surface morphology of the MEPCMs. The images indicated that S1and S2 have a smooth and compact surface without any porosity on the shell. Additionally, Figure 4-22a, b confirmed that the size distribution of the microcapsules in S4 was not homogeneous and uniform compared to the size distribution of the microcapsules in S1.

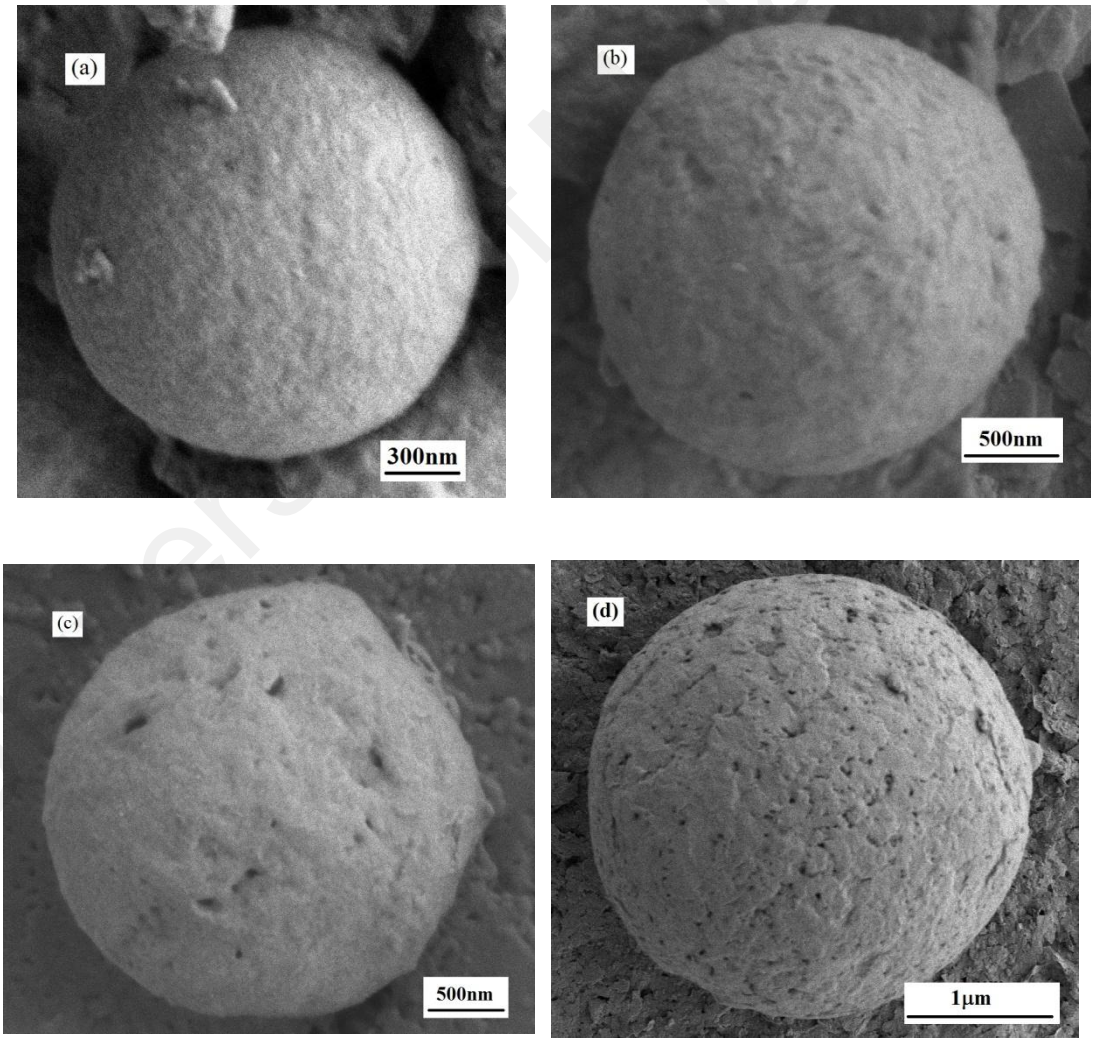

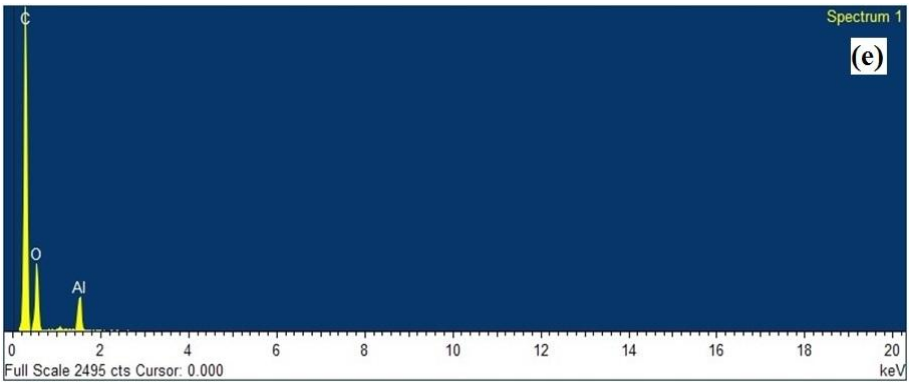

Figure 4-21: SEM micrographs of the microcapsules of samples (a) S1, (b) S2, (c) S3, (d) S4 (e) The EDS analysis of MEPCMs in sample S1

The surface elemental composition of the MEPCMs was characterized by Energy-dispersive X-ray spectroscopy (EDS) and typical results are shown in Figure 4-21e. Figure 4-21e indicates that aluminium and oxygen were the primary elements in Al_2O_3. In the case of encapsulation of the PA, peaks of carbon emerged clearly, which further confirmed that the PA was encapsulated successfully. Furthermore, the mole ratio of O/Al is calculated to be 4.56:1, indicating an oxygen-rich Al_2O_3 shell with a lot of hydroxyl groups. Figure 4-22c and d illustrate the particle size distribution (PSD) of the MEPCMs. The mean diameter of the microcapsules changed from 1.689 to 3.730 μm according to the S1 to S4, because of the large size of the PA droplets in O/W emulsion. The broad particle size distribution curve in S4 suggested that at higher weight ratios of PA/AIP the distribution of the MEPCMs are not uniform. The core/shell structure of the microcapsules in sample S2 is also illustrated in Figure 4-22e. the dark part shows the core PCM and the pale part illustrates the shell material.

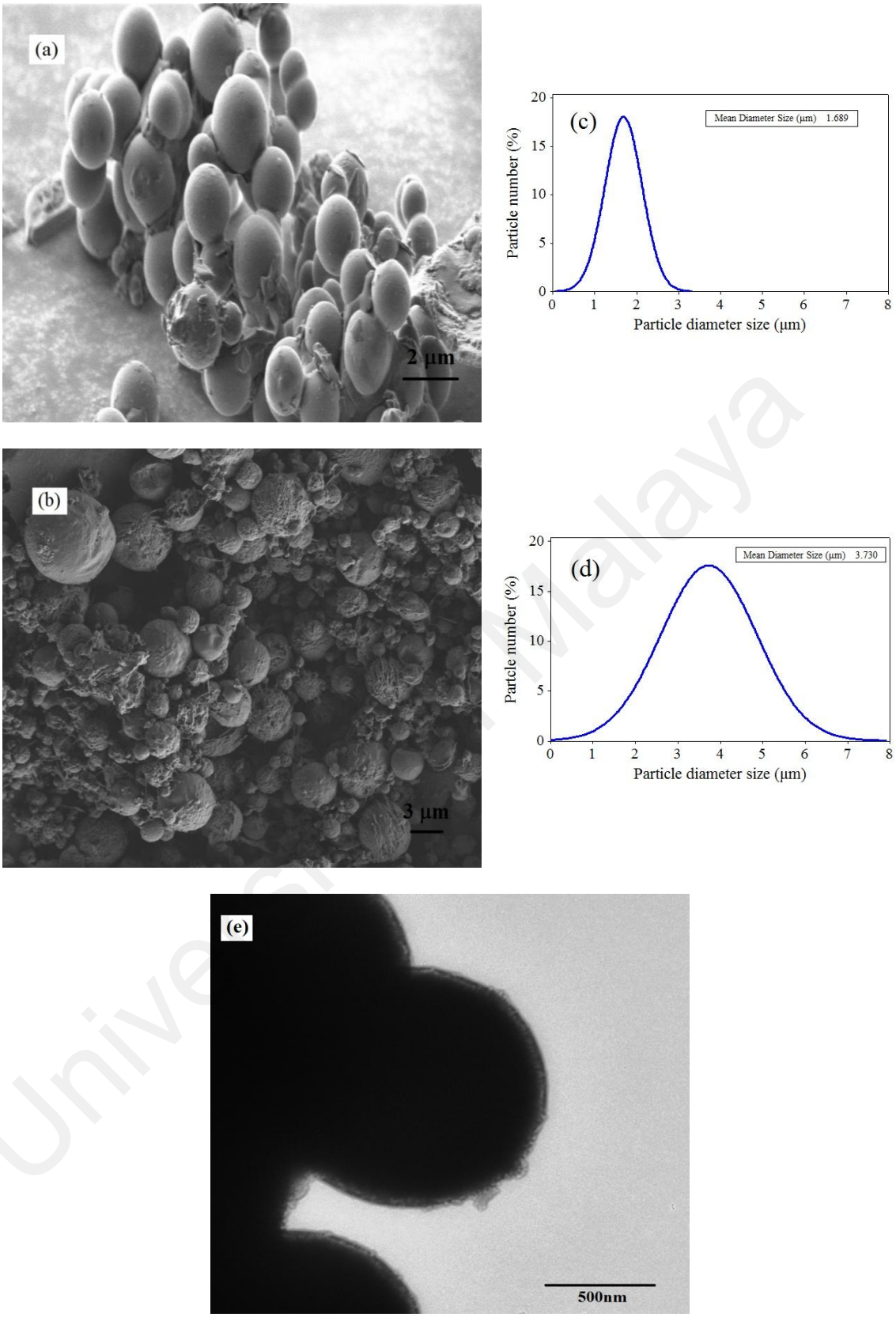

Figure 4-22: SEM images of sample numbers (a) S1, (b) S4, the size distribution graphs of microcapsules in sample (c) S1, (d) S4 and (e) the TEM image of sample S2

4.4.4 Thermal Energy Storage Properties of PA/Al_2O_3 MEPCMs

The heating and cooling DSC scans were carried out at the scanning rate of 5℃/min to investigate the effects of Al_2O_3 shell on the phase-change characteristics of the PA microcapsules with different weight ratios of PA/AIP. The DSC results are exhibited in Figure 4-23 and the phase change characterizations obtained via DSC analysis are listed in Table 4-6.

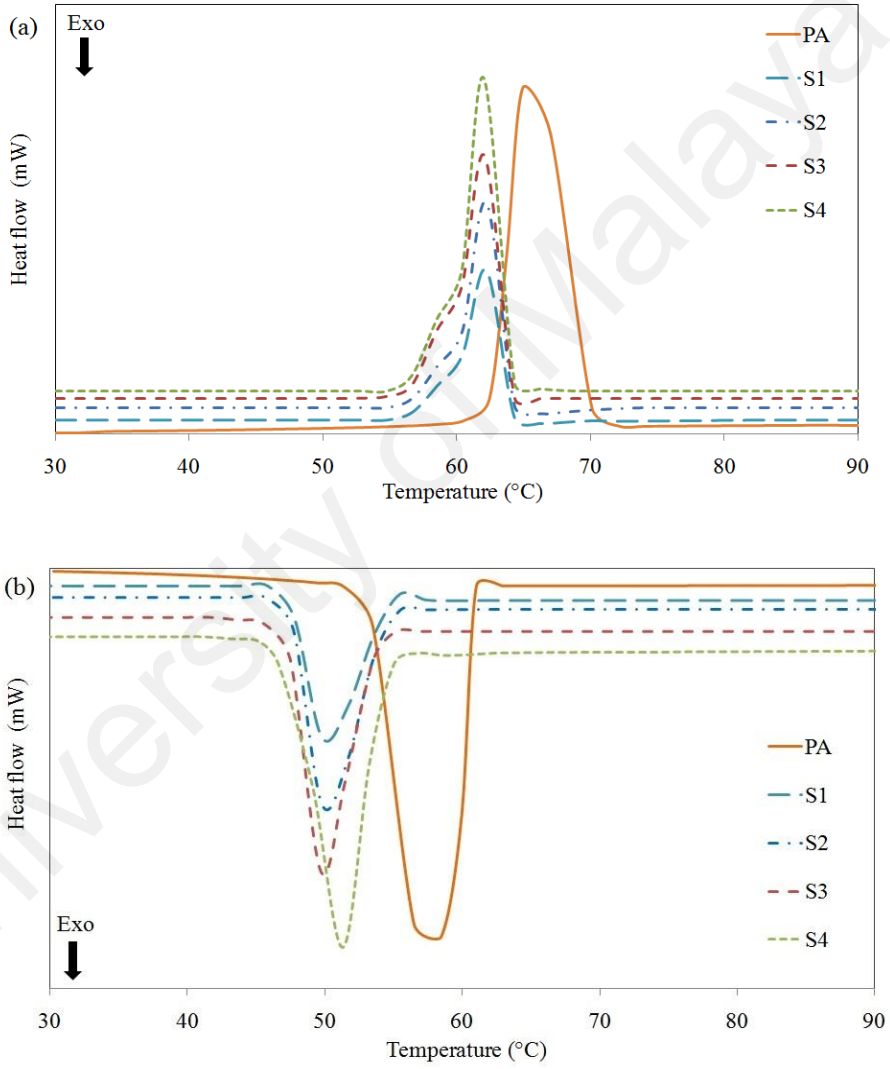

Figure 4-23: DSC thermograms of the (a) heating and (b) cooling of pure PA and MEPCMs

All DSC curves in Figure 4-23a exhibit one endothermic peak with T_{peak} located in the temperature range of 62–66℃, which is ascribed to the melting of the PA. The

melting points of the MEPCMs were lower than the melting temperature of the PA due to the confinement effect by shell–PA interactions. As is shown in Figure 4-23, the melting and solidification temperatures of the MEPCMs were close to each other so there is little supercooling. It is found that the theoretical core loadings for all of the MEPCMs were different because of the different PA/AIP weight ratio. Samples S1-S4 show lower actual core loading which are noted in Table 4-6 compared to their theoretical core loading of 50-80%. This indicates that not all of the reactants could be incorporated within the shell materials. Some of the Al_2O_3 was not assembled on the surfaces of PA micelles but directly precipitated as solid particles during the synthesis process and also not all of the PA particles can be encapsulated within the shell materials which were removed during the washing process, accordingly resulting in a decrease in actual core loading. However, the latent heat of the prepared microcapsules is still sufficient for being relevant in thermal energy storage.

Table 4-6: The phase-change properties of the PA and MEPCMs

sample	Melting			Solidifying							
	T_{onset} (℃)	T_{peak} (℃)	T_{end} (℃)	T_{onset} (℃)	T_{peak} (℃)	T_{end} (℃)	ΔH_m (kJ/kg)	ΔH_c (kJ/kg)	E_r (%)	E_e (%)	Φ (%)
S1	56.75	62.2	66.25	55.44	49.78	45.83	55.58	55.37	30.46	30.11	98.78
S2	55.7	62.2	65.25	55.4	49.76	45.73	77.09	77.13	42.26	41.86	99.06
S3	55.16	62.09	65.98	55.12	49.68	45.52	97.31	97.71	53.34	52.9	99.24
S4	55.37	62.03	66.25	55.05	51.33	45.22	121.97	123.93	66.86	66.75	99.83
PA	60.58	65.22	72.08	61.94	57.47	51.44	182.42	185.96	-	-	-

The encapsulation ratio and encapsulation efficiency illustrate the efficient encapsulation of the PA and the working effectiveness of the PCMs within microcapsules, respectively. Normally, the higher the actual core loading, the higher the encapsulation ratio, which was confirmed by the results. The small internal space of

some produced nano-sized microcapsules may lead to a confinement effect on the crystallization of the PA. In this case, a small amount of the encapsulated PA cannot change phase and does not contribute to heat storage. As shown in Table 4-6, the thermal storage capability of the MEPCMs synthesized at different concentrations of AIP exhibits the thermal storage capabilities higher than 98%, which indicates that the PA in suitable sizes was encapsulated by Al_2O_3 shell, and thus, most of the encapsulated PA could effectively store and release the latent heat through the phase change process.

The shell thickness of the prepared microcapsules was also calculated by using the outcomes of the DSC analysis. The density of the shell material was measured 3.1g/cm^3. The mean shell thickness of the MEPCMs is in the range of 0.07-0.12 μm for S4-S1. The lower shell thickness of microcapsules in sample S4 could be evidence to the porosity and non compact shell material in these capsules.

Latent heat is particularly attractive due to its ability to provide high-energy storage density in a quasi-isothermal process. But the energy storage density can be further increased using PCM having a large sensible heat within the temperature range of the storage while the total heat stored in a PCM can be calculated as follows:

$$Q_t = \int_{T_1}^{T_m} C_{p,s} \, . \, dT + \Delta H_L + \int_{T_m}^{T_2} C_{p,1} . \, dT \qquad (4\text{-}1)$$

Where Q_t is the total heat stored per mass, $C_{p,s}$ and $C_{p,l}$ are the specific heat of solid and liquid PCM, respectively. ΔH_L is the heat of fusion at the phase change temperature T_m. It can be seen that the specific heat also affects the total heat storage. The specific heat of the pure PA and encapsulated PA was measured by the multiple curves method for temperatures between 35℃ and 45℃ and the results are shown in Figure 4-24.

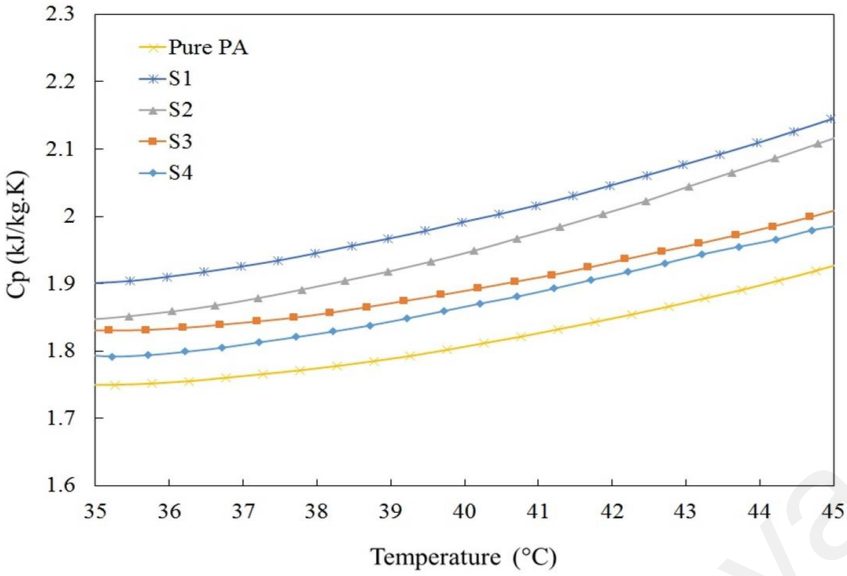

Figure 4-24: Specific heat curves of PA and encapsulated PA

The results show that the specific heat of the capsules was higher than that of the pure PA. It can be seen clearly that at higher weight amount of the shell material the specific heat values increases which partly makes up for the lower latent heat of these capsules.

4.4.5 Thermal Conductivity of PA/Al_2O_3 MEPCMs

It is well known that the low thermal conductivity of the PA increases its thermal response time for storage and release of latent heat. Thus, enhancing the thermal conductivity of PCMs is a major aim in designing a microencapsulated material. The thermal diffusivity was measured by the laser flash method and the thermal conductivity was calculated as described in CHAPTER 3. The calculated thermal conductivities of the microcapsules and the pure PA in solid state (35℃) are given in Table 4-7.

Table 4-7: Thermal conductivity of encapsulated PCMs and Pure PA

Sample	Thermal conductivity (W/mK)	Thermal conductivity enhancement (%)
Pure PA	0.282	-
S1	0.530	87.94
S2	0.449	59.21
S3	0.410	45.39
S4	0.352	24.82

The thermal conductivity of all encapsulated PCMs was higher than that of PA, due to the high thermal conductivity of Al_2O_3 as the shell material. Additionally, it is notable that the thermal conductivities of microencapsulated PA samples are considerably related to the encapsulation ratio. The lower thermal conductivity enhancements were achieved at higher encapsulation ratios. This suggests that the Al_2O_3 shell performs an important function in improving the heat transfer of microencapsulated PA.

In samples S1 and S2 the Al_2O_3 creates an entirely continuous and compact shell around the PA, this can be considered as a virtual heat transfer network. So, this can enhance the heat transfer rate over the entire microcapsules and so attain a significantly improved thermal conductivity.

4.4.6 Thermal Stability of PA/Al_2O_3 MEPCMs

Thermal stability is a significant factor in evaluating the microencapsulated PCMs for the applications of heat energy storage or thermal regulation. The thermal degradation behaviours of the microcapsule samples synthesized in different weight ratios were investigated by the TGA. The TGA thermograms in Figure 4-25 show the weight loss of the microcapsules (S1, S2, S3, and S4) and that of pure PA. Figure 4-25

demonstrates that pure PA loses weight at approximately 200-520℃ with only one step, which corresponds to the volatilization of PA.

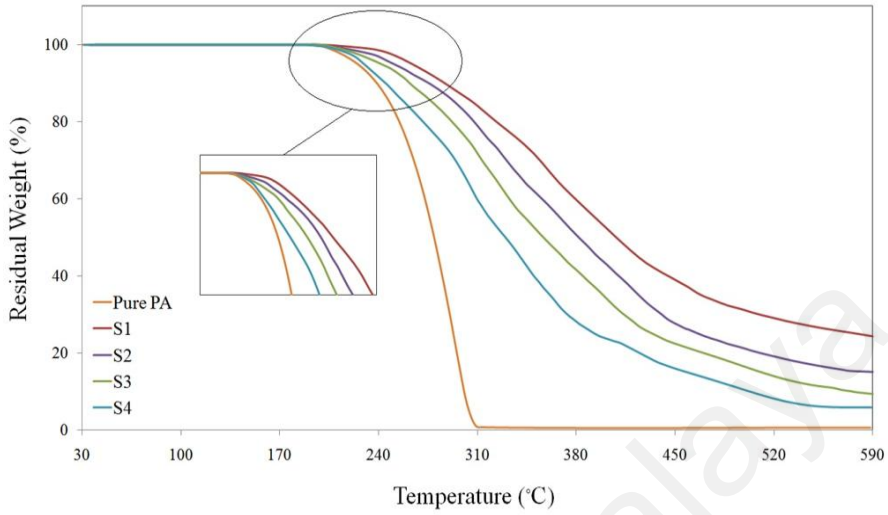

Figure 4-25: TGA thermograms of the pure PA and MEPCMs

According to Figure 4-25 microcapsules of the four samples (S1-S4) degrade in one step as well as the pure PA. It is believed that the increase of AIP proportion could lead to a thicker alumina shell for the microcapsules and thus generates a better barrier to prevent the encapsulated PA from decomposing. Moreover, the microencapsulated PA samples produced a considerable amount of residual char to be associated with the theoretical PA loading in the microcapsules.

Table 4-8: Decomposition temperatures of the PA and MEPCMs

Sample code	Onset decomposition temperature (℃)	Maximum weight loss temperature (℃)
Pure PA	183.25	277.33
S1	212.48	355.68
S2	206.69	323.48
S3	203.45	306.81
S4	194.80	286.16

Additionally, the onset temperatures of degradation for all are higher than that of pure PA (Table 4-8), which indicates that the thermal stability of phase change material increases after being encapsulated. Moreover the microcapsule samples show a maximum weight loss at higher temperatures compared to the pure PA which indicates that the Al_2O_3 wall can prevent the encapsulated PA from evaporating at the normal boiling point and improve the degradation temperature of the microcapsules. On the other hand the degradation temperature of sample S1 and S2 compared to the other two samples are higher, which proves that the thick and non-porous Al_2O_3 shell in the microcapsules of these two samples may favor the improvement in thermal stability of the microcapsules.

It is significant that the weight loss of the microcapsules strongly depends on the encapsulation ratios of PA to the microcapsules and on the PA/AIP weight ratio, therefore sample S4 which was synthesized with the weight ratio of 80/20 achieved the highest weight loss. The occurrence of a small weight loss before 130°C is mainly due to the incomplete removal of water.

4.4.7 Thermal Effusivity of PA/Al_2O_3 MEPCMs

The thermal effusivity is a measure of a material's ability to exchange thermal energy with its surroundings. The thermal effusivity is considered to be a critical physical quantity to depict the unsteady state heat transfer in a LHTES system. The effusivity of a material is the square root of the product of the thermal conductivity, density and heat capacity:

$$e = \sqrt{\rho K C_p} \tag{4-2}$$

Where e ($kJ/(K.m^2.s^{0.5})$) is thermal effusivity, k is thermal conductivity ($W/(m\cdot K)$), ρ is density (kg/m^3) and C_p is specific heat capacity ($kJ/(kg\cdot K)$). The thermal effusivity of the PA and MEPCMs are evaluated at 35℃ and listed in Table 4-9.

Table 4-9: Thermal effusivity of the PA and MEPCMs

Sample	Thermal effusivity ($kJ/(K.m^2.s^{0.5})$)
Pure PA	0.640
S1	0.877
S2	0.803
S3	0.770
S4	0.711

The thermal effusivity of all MEPCMs is larger than that of pure PA, which is beneficial for the LHTES systems.

4.4.8 Thermal Reliability and Durability of PA/Al_2O_3 MEPCMs

Thermal reliability of the MEPCMs is critical to evaluate the possibility of their long term use of TES systems. A PCM needs to maintain its TES attributes even when it is put through a prolonged thermal cycling process. For the prepared materials the thermal reliability of the composite PCMs was examined after the exposure to 1500 melting-freezing cycles. The changes of latent heat in composite PCMs after thermal cycling were evaluated to determine whether they are thermally reliable.

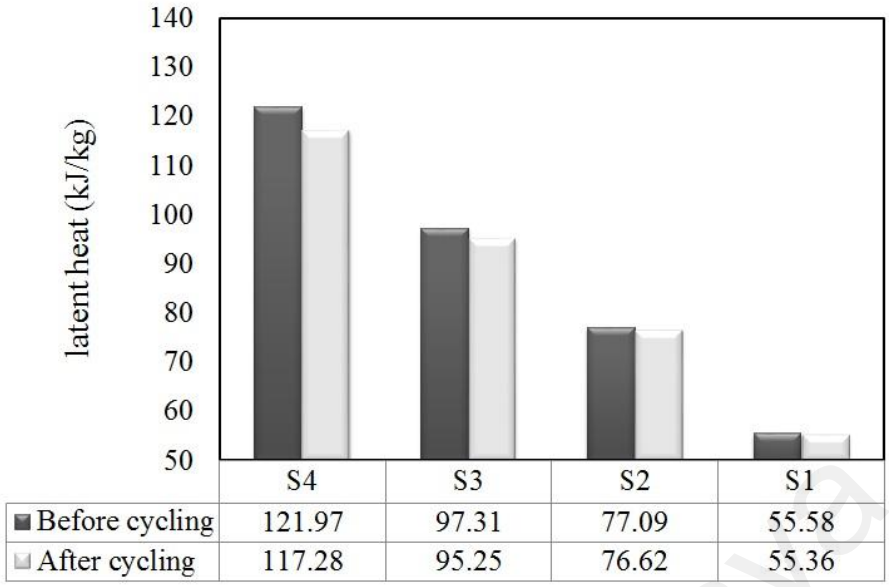

	S4	S3	S2	S1
Before cycling	121.97	97.31	77.09	55.58
After cycling	117.28	95.25	76.62	55.36

Figure 4-26: The latent heat values of the MEPCMs before and after thermal cycling

After 1500 cycles the MEPCMs still showed a single phase transition curve with onset temperature as before the cycling. In other words, there were no extra peaks related to chemical decomposition or phase segregation within the MEPCMs. Through comparing the latent heat values in Figure 4-26, the maximum change in latent heat capacity was determined as 3.84% for S4 and the minimum was 0.39% for S1. These results suggested that the changes in the latent heat capacity of the composites after thermal cycling were less than 1% for S1 and S2 demonstrating their good thermal reliability. The results indicate that S3 and S4 may have had some leakage during cycling that caused effects on the latent heat capacity of the MEPCMs.

4.5 Comparison of Properties of Prepared NE/MEPCMs

Choosing an ideal PCM is extremely important and crucial for thermal energy storage. The proper PCM should have sufficient properties according to the suggested application. The major specifications any PCM should have are including adequate melting temperature, desirable heat of fusion, thermal conductivity, thermal stability and reliability and negligible corrosion effects on the surrounding materials.

In addition; in some applications for encapsulated PCMs, especially in slurry systems, the size and the size distribution of the NE/MEPCMs are substantial parameters. In this study three different metal oxides were utilized to prepare different novel NE/MEPCMs for thermal energy storage applications. Due to the various properties of the shell materials, to compare the characteristics of the prepared materials, the extents of the enhancement of the major features are considered. For the comparison, the results are reported based on the 50/50 weight ratio of the core PCM material to the precursor of the shell material and are displayed in Figure 4-27, Figure 4-28 and Table 4-10.

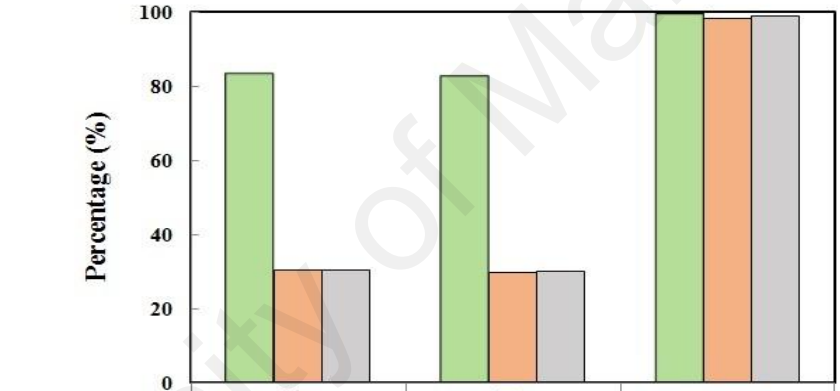

	Er	Ee	φ
PA/SiO2	83.25	82.53	99.13
SA/TiO2	30.36	29.84	98.32
PA/Al2O3	30.46	30.11	98.78

Figure 4-27: Encapsulation features of encapsulated PA/SiO_2, SA/TiO_2 and PA/Al_2O_3

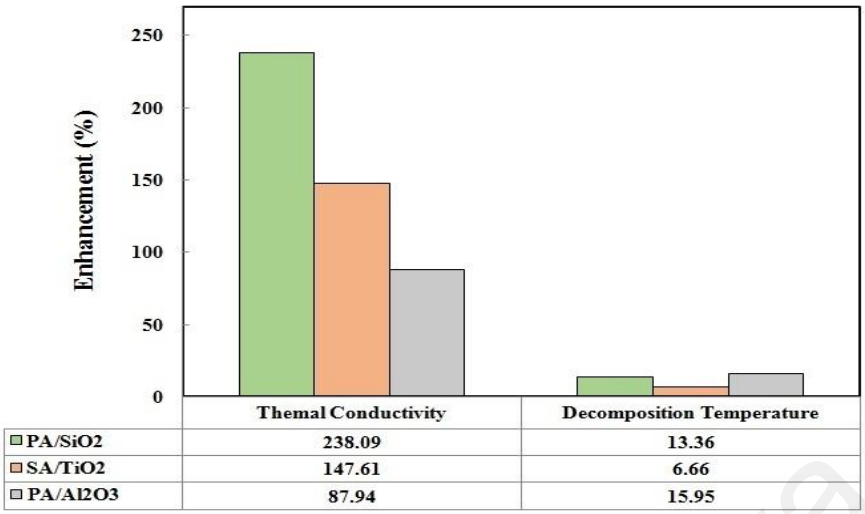

Figure 4-28: Thermal conductivity and decomposition temperature enhancement of encapsulated PA/SiO_2, SA/TiO_2 and PA/Al_2O_3

Figure 4-27 demonstrates that the encapsulation ratio and encapsulation efficiency of SiO_2 encapsulated PCMs is significantly superior to those of the TiO_2 and Al_2O_3. This arises due to the hydrolysis and condensation rates of the precursors throughout the preparation method. The lower hydrolysis rate of the TEOS in silica preparation compare to TTIP and AIP provides a more controllable synthesis process of NEPCMs, therefore; the most homogenous size distribution of produced capsules as compared to the other two materials. However; in all three types of prepared materials the high thermal storage capability that indicates the output efficiency of the PCMs which enclosed within shell materials in storage process, make the prepared capsules suitable for thermal storage applications. In some fields, specifically in latent functionally thermal fluids, because the large size of particles of the PCM microcapsules increase the fluid's viscosity, microencapsulated PCMs are not appropriate for repeated cycling, thus it is essential to develop encapsulated PCMs with smaller particle sizes as compared with microcapsules. It is noticeable that the prepared SA/TiO_2 and PA/SiO_2 nanocapsules have large latent heat and thermal conductivity despite of their small particle size. Therefore the prepared nanocapsules are adequate for

utilizing in thermal energy storage applications specifically in thermal fluids heat transfer.

Comparison of the thermal conductivity and thermal stability enhancements for the three types of samples in 50/50 weight ratio of PCM to the precursor of shell material are illustrated in Figure 4-28. As shown in Figure 4-28 the thermal conductivity of capsules are all improved remarkably compared to the pure PCMs. The results suggest that the highest thermal conductivity enhancement (238.09%) was achieved by using SiO_2 as a shell material with 50/50 weight ratio of the core PCM to the precursor of the shell material. The thermal conductivity of capsules with silica and titania as the shell supporting materials are enhanced more than the alumina due to the mean diameter size of those samples (Table 4-10). The smaller diameter sizes of silica and titania encapsulated PCMs increase the contact surface area of the capsules that affect the thermal conductivity substantially. Additionally; the onset decomposition temperatures of the capsules are all improved compared to the pure PCMs but the prepared capsules by alumina shell materials have higher enhancement than the other two ones which demonstrates that the ability of the alumina to improve the thermal stability is much more higher than that of the other materials.

Table 4-10: Mean diameter size of encapsulated PA/SiO_2, SA/TiO_2 and PA/Al_2O_3

Sample	Mean diameter size
PA/SiO_2 (SI1)	183.7 nm
SA/TiO_2 (ST1)	317.6 nm
PA/Al_2O_3 (S1)	1.68 µm

Totally for existing applications specially in slurry and nanofluid heat transfer systems the proposed metal oxides (SiO_2, TiO_2 and Al_2O_3) in this project will help to

conquer and reduce the obstacles of the PCMs. With encapsulation of the metal oxides mostly at low loading contents of the shell material (as evident from the small shell thickness of the prepared materials), thermal conductivity and thermal stability enhancement can be simultaneously accomplished while high latent heat is retained. In addition, thermal reliability of the all prepared materials makes them appropriate for utilizing in numerous melting-solidifying cycles in many thermal energy storage applications. The compatibility of these materials with most materials makes them convenient for using in applications of thermal storage specially heat transfer slurries, however choosing the beneficial NE/MEPCM to apply depends on the application parameters like the region of used temperature, the properties and demeanor of the surrounding materials and etc.

4.6 Summary

The fabrication and structural features of the novel NE/MEPCMs with inorganic shell materials and the relationships between the thermo-physical properties of PCMs coated by the three kinds of metal oxides have been examined systematically in this study. The effectiveness of the processing parameters like adjusted pH value and the weight ratio of core to precursor of coating material on the morphology, chemical characteristics, melting and solidifying temperatures, thermal stability, thermal conductivity, thermal reliability, etc have been examined. The NE/MEPCMs in all samples were spherically shaped with no or negligible interactions between the core and shell material. The SEM and TEM images of all materials display the spherical and core/shell structures of the prepared materials. All the coating surfaces are compact and smooth excluding the PA/Al_2O_3 samples prepared with weight ratios of 70/30 and 80/20 of PA/AIP which had some porosity in the shell surface of MEPCMs due to the higher diameter size of the capsules.

The melting/solidifying enthalpies have been found to reduce as a result of encapsulation of the fatty acids and some variations occurred with weight ratio and adjusted pH value. The melting/solidification temperatures were slightly changed because of the shell reduction of steric hindrance of the PCM core materials. The encapsulation ratio and efficiency of all samples are in a satisfactory range for employing in thermal storage applications. Additionally the high thermal storage capabilities of all samples are in the range of 97% to 99% that approve the high efficiency of the PCMs in the shell materials.

The thermal conductivity of the NE/MEPCMs improves using metal oxides as shell material while silica and titania show a greater thermal conductivity improvement than alumina due to the smaller mean particle diameter. From the results, we have found the maximum thermal conductivity enhancement of 238.09% for PA/SiO_2 NEPCMs with a mean diameter of 183.7nm at PA/TEOS weight ratio of 50/50 while the minimum enhancement was found for PA/Al_2O_3 MEPCMs (24.82%) with 80/20 weight ratio of PA/AIP. The thermal stability of all prepared materials was also improved compared to the pure PCMs core materials. The thermal reliability after 1500-2500 melting/solidifying cycles reveals the adequacy of the materials in thermal cycling systems. All outcomes inclusively suggested that the prepared materials can be considered as potential and favorable candidates for thermal storage applications specifically in thermal storage and heat transfer slurry systems.

CHAPTER 5
CONCLUSION AND RECOMMENDATION

This chapter elucidates the conclusions deduced from the experimental results and some suggestions for further procedure and experiments which could have been done if limitations in experimental instruments and time were not a factor to accomplish further investigations.

5.1 Conclusion

With respect to the identified research difficulties as presented in the CHAPTER 1, like, the low thermal conductivity, the leakage of PCMs throughout the utilization, the low thermal stability, and etc, the main objectives of this thesis were focused on the improving the PCMs by encapsulation of the PCMs within compact inorganic shell materials. Specifically, encapsulation of low cost PCMs such as palmitic acid and stearic acid with three different types of metal oxides (SiO_2, TiO_2, and Al_2O_3) for a storage system in a temperature range of 50-80℃ has been studied. NE/MEPCMs were successfully prepared using the sol-gel method. The effects of the weight ratio of PCMs/precursor of the shell materials (TEOS, TTIP and AIP for the SiO_2, TiO_2 and Al_2O_3, respectively) and the adjusted pH value throughout the synthesis process on the phase transition properties of the PCM capsules have been investigated. The understanding of the synthesis process, extent of accomplishment and the full experimental design that has been carried out to investigate physical, chemical and thermal properties of the prepared NE/MEPCMs were reported. To highlight our research results some characterization conclusions are summarized for the prepared materials as presented in sequence:

The SEM and TEM images confirmed that all of the presented samples were successfully shaped with relatively spherical profiles and core/shell structures with

different mean diameter sizes and size distributions. The mean diameter sizes are 183.7 nm for PA/SiO_2 (SI1), 317.6 nm for SA/TiO_2 (ST1) and 1.68 μm for PA/Al_2O_3 (S1). The results indicated that the mean diameter size of the capsules not only strongly related to the type of shell material, the preparation circumstances (such as pH value) and the demeanor of the precursor shell material but also, the amount of the PCM core to the amount of the precursor of the shell material weight ratio. In some fields, specifically in latent functionally thermal fluids, because the large size of particles of the PCM microcapsules increase the fluid's viscosity, microencapsulated PCMs are not appropriate for repeated cycling, thus it is essential to develop encapsulated PCMs with smaller particle sizes as compared with microcapsules. It is noticeable that the prepared SA/TiO_2 and PA/SiO_2 nanocapsules have large latent heat and thermal conductivity despite their small particle size. Therefore the prepared nanocapsules are adequate for utilizing in thermal energy storage applications specifically in thermal fluids heat transfer. The FTIR outcomes signified that no chemical reactions occurred between the core and shell materials of the prepared NE/MEPCMs. The XRD results indicated that the NE/MEPCMs retained good crystallinity. All characteristic peaks of PCMs and shell materials were also observed in the FTIR spectra.

The thermal characteristics of the prepared NE/MEPCMs as one of the main objectives of this research were also studied. The DSC results demonstrated that at higher pH value of synthesis process and also for samples prepared with higher weight ratio amount of core to the amount of the precursor of shell material, the encapsulation ratio and encapsulation efficiency were increased. Therefore, latent heats of the capsules were enhanced by increasing their diameter size. The melting/solidifying temperatures of the prepared capsules were slightly changed due to the shell reduction of steric hindrance of the PCM core materials. The thermal stability analysis (TGA) implied that the thermal stability and decomposition temperature of PCMs increased after being

encapsulated by the enhancement percentage range of 6.6% to 15.9%. The thermal conductivity as one of the most important parameters in thermal energy storage applications was also measured. The thermal conductivity of all the prepared NE/MEPCMs ascertained the improvement of 87.9% to 238% compared to the pure PCMs. Moreover, the prepared NE/MEPCMs exhibited good thermal reliability and chemical stability even after being subjected to 2500 melting/solidification cycles.

Conforming to all the discussed results; the improved thermal properties, thermal and chemical reliability, thermal conductivity and compatible morphology and enhanced heat storage characteristics of the NE/MEPCMs facilitate the prepared materials to be considered as potential candidates for thermal storage applications specifically in slurry systems.

5.2 Recommendations

A facile technology has been developed to encapsulate some low cost PCMs with metal oxides. Three high thermal conductive metal oxides were utilized according to this aim. The thermal performance and the cyclic stability of these metal oxide encapsulated PCMs were studied. However; the thermal features can be improved by optimizing the quality of the metal oxide coatings. Also there is a wide variety of different inorganic materials as well as the metal oxides which can have the sufficient properties to be applied as the coating materials for the PCMs.

Another potential concept which can be investigated in future is the application of the encapsulated PCMs exclusively in thermal storage slurries. Moreover in the NE/MEPCMs heat transfer employment, dispersion of NE/MEPCMs in polar solvents should be further studied. The preliminary issue to be addressed is the dispersion and stability of the NE/MEPCMs in the surrounding fluids in such functions. In order to understand the validity of the proposed approaches, numerical analyses that are based

on those approaches are useful. At present, numerical studies in the literature about this issue are not sufficient to reach a conclusion about the accuracy of the approaches. Detailed experimental investigation of the effects of most of the organic within inorganic NE/MEPCMs parameters on heat transfer has not been performed yet. Systematic studies about these aspects of NE/MEPCMs on heat transfer will provide profitable information for the optimization of heat transfer enhancement obtained with NE/MEPCMs. In the case of product engineering several improvements and suitable developments can be wished, first of all the test of the NE/MEPCMs by a test rig or by some field tests. Concisely; more attempts must be conducted to both fundamental and applied investigations of different types of NE/MEPCMs with the aid of advanced experimental and numerical techniques.

LIST OF PUBLICATIONS AND PAPERS PRESENTED

1. Tahan Latibari, S., Mehrali, M., Mehrali, M., Indra Mahlia, T. M., & Cornelis Metselaar, H. S. (2013). Synthesis, characterization and thermal properties of nanoencapsulated phase change materials via sol–gel method. Energy, 61(0), 664-672. **Impact factor 4.844 (Q1)**
2. Tahan Latibari, S., Mehrali, M., Mehrali, M., Afifi, A. B. M., Mahlia, T. M. I., Akhiani, A. R., & Metselaar, H. S. C. (2015). Facile synthesis and thermal performances of stearic acid/titania core/shell nanocapsules by sol–gel method. Energy, 85(0), 635-644. **Impact factor 4.844 (Q1)**
3. Tahan Latibari, S., Mehrali, M., Mehrali, M., Mahlia, T. M. I., & Metselaar, H. S. C. (2015). Fabrication and Performances of Microencapsulated Palmitic Acid with Enhanced Thermal Properties. Energy & Fuels, 29(2), 1010-1018. **Impact factor 2.790 (Q1)**

The conference proceeding:

1. 5th International Conference for Colloids and Interfaces 2015. 21 - 24 June 2015, Amsterdam, Netherlands. “Microencapsulation of Palmitic Acid phase change material with enhancement of thermal performance”

REFERENCES

Abhat, A. (1983). Low temperature latent heat thermal energy storage: Heat storage materials. *Solar Energy*, 30(4), 313-332.

Agyenim, F., Hewitt, N., Eames, P., & Smyth, M. (2010). A review of materials, heat transfer and phase change problem formulation for latent heat thermal energy storage systems (LHTESS). *Renewable and Sustainable Energy Reviews*, 14(2), 615-628.

Aho, A., Antonietti, M., Arndt, S., Behrens, M., Bill, E., Brandner, A., Centi, G., Claus, P., Cox, N., & DeBeer, S. (2012). *Chemical Energy Storage*: De Gruyter.

Alay, S., Göde, F., & Alkan, C. (2010). Preparation and characterization of poly(methylmethacrylate-coglycidyl methacrylate)/n-hexadecane nanocapsules as a fiber additive for thermal energy storage. *Fibers and Polymers*, 11(8), 1089-1093.

Alkan, C., Sarı, A., Karaipekli, A., & Uzun, O. (2009). Preparation, characterization, and thermal properties of microencapsulated phase change material for thermal energy storage. *Solar Energy Materials and Solar Cells*, 93(1), 143-147.

Anisur, M. R., Mahfuz, M. H., Kibria, M. A., Saidur, R., Metselaar, I. H. S. C., & Mahlia, T. M. I. (2013). Curbing global warming with phase change materials for energy storage. *Renewable and Sustainable Energy Reviews*, 18(0), 23-30.

Babich, M. W., Benrashid, R., & Mounts, R. D. (1994). DSC studies of new energy storage materials. Part 3. Thermal and flammability studies. *Thermochimica Acta*, 243(2), 193-200.

Baetens, R., Jelle, B. P., & Gustavsen, A. (2010). Phase change materials for building applications: A state-of-the-art review. *Energy and Buildings*, 42(9), 1361-1368.

Baker, J. N., & Collinson, A. (1999). Electrical energy storage at the turn of the Millennium. *Power Engineering Journal*, 13(3), 107-112.

Banaszek, J., Domañski, R., Rebow, M., & El-Sagier, F. (1999). Experimental study of solid–liquid phase change in a spiral thermal energy storage unit. *Applied Thermal Engineering*, 19(12), 1253-1277.

Baran, G., & Sari, A. (2003). Phase change and heat transfer characteristics of a eutectic mixture of palmitic and stearic acids as PCM in a latent heat storage system. *Energy Conversion and Management*, 44(20), 3227-3246.

Bayés-García, L., Ventolà, L., Cordobilla, R., Benages, R., Calvet, T., & Cuevas-Diarte, M. A. (2010). Phase Change Materials (PCM) microcapsules with different shell compositions: Preparation, characterization and thermal stability. *Solar Energy Materials and Solar Cells*, 94(7), 1235-1240.

Baylin, F., & Institute, S. E. R. (1979). *Low Temperature Thermal Energy Storage: A State-of-the-art Survey*: Department of Energy, [Office of Energy Technology], Solar Energy Research Institute.

Bershteĭn, V. A., & Egorov, V. M. (1994). *Differential Scanning Calorimetry of Polymers: Physics, Chemistry, Analysis, Technology*: Ellis Horwood.

Birchenall, C. E., & Riechman, A. (1980). Heat storage in eutectic alloys. *Metallurgical Transactions A*, 11(8), 1415-1420.

Black, J. K., Tracy, L. E., Roche, C. P., Henry, P. J., Pesavento, J. B., & Adalsteinsson, T. (2010). Phase transitions of hexadecane in poly(alkyl methacrylate) core - shell microcapsules. *Journal of Physical Chemistry B*, 114(12), 4130-4137.

Brinker, C. J., & Scherer, G. W. (2013). *Sol-Gel Science: The Physics and Chemistry of Sol-Gel Processing*: Elsevier Science.

Buddhi, D., & Sharma, S. D. (1999). Measurements of transmittance of solar radiation through stearic acid: a latent heat storage material. *Energy Conversion and Management*, 40(18), 1979-1984.

Bugaje, I. M. (1997). Enhancing the thermal response of latent heat storage systems. *International Journal of Energy Research*, 21(9), 759-766.

Cabeza, L. F., Castell, A., Barreneche, C., de Gracia, A., & Fernández, A. I. (2011). Materials used as PCM in thermal energy storage in buildings: A review. *Renewable and Sustainable Energy Reviews*, 15(3), 1675-1695.

Cai, Y., Wei, Q., Huang, F., Lin, S., Chen, F., & Gao, W. (2009). Thermal stability, latent heat and flame retardant properties of the thermal energy storage phase change materials based on paraffin/high density polyethylene composites. *Renewable Energy*, 34(10), 2117-2123.

Cao, F., & Yang, B. (2014). Supercooling suppression of microencapsulated phase change materials by optimizing shell composition and structure. *Applied Energy*, 113, 1512-1518.

Carslaw, H. S., & Jaeger, J. C. (1986). *Conduction of Heat in Solids*: Clarendon Press.

Chen, H., Cong, T. N., Yang, W., Tan, C., Li, Y., & Ding, Y. (2009). Progress in electrical energy storage system: A critical review. *Progress in Natural Science*, 19(3), 291-312.

Chen, L., Wang, T., Zhao, Y., & Zhang, X.-R. (2014). Characterization of thermal and hydrodynamic properties for microencapsulated phase change slurry (MPCS). *Energy Conversion and Management*, 79(0), 317-333.

Chen, S.-L., Chen, C.-L., Tin, C.-C., Lee, T.-S., & Ke, M.-C. (2000). An experimental investigation of cold storage in an encapsulated thermal storage tank. *Experimental Thermal and Fluid Science*, 23(3–4), 133-144.

Chen, S. L., Zuo, Y., Liang, H., & Chang, Y. A. (1997). A thermodynamic description for the ternary Al-Mg-Cu system. *Metallurgical and Materials Transactions A*, 28(2), 435-446.

Cho, K., & Choi, S. H. (2000). Thermal characteristics of paraffin in a spherical capsule during freezing and melting processes. *International Journal of Heat and Mass Transfer*, 43(17), 3183-3196.

Choi, S.-S., Lee, S., Im, S., Kim, S., & Joo, Y. (2003). Silica nanofibers from electrospinning/sol-gel process. *Journal of Materials Science Letters*, 22(12), 891-893.

Christensen, C. (1983). *Advanced phase-change storage: analysis of materials and configurations*.

Demirbas, M. F. (2006). Thermal Energy Storage and Phase Change Materials: An Overview. *Energy Sources, Part B: Economics, Planning, and Policy*, 1(1), 85-95.

Dincer, I., & Dost, S. (1996). A perspective on thermal energy storage systems for solar energy applications. *International Journal of Energy Research*, 20(6), 547-557.

Dincer, I., & Rosen, M. (2002). *Thermal Energy Storage: Systems and Applications*: John Wiley & Sons.

Ding, W.-X., & Yin, X.-M. (2004). Dissection of the multiple mechanisms of TNF-α-induced apoptosis in liver injury. *Journal of Cellular and Molecular Medicine*, 8(4), 445-454.

Ehsan Bitaraf, H., Zahid, A., Itziar, L., Seyed Aliakbar, M., Mohammadreza, B., Rahmatollah, K., & Björn, P. (2012). Screening Single Phase Laminar Convective Heat Transfer of Nanofluids in a Micro-tube. *Journal of Physics: Conference Series*, 395(1), 012036.

Esen, M., Durmuş, A., & Durmuş, A. (1998). Geometric design of solar-aided latent heat store depending on various parameters and phase change materials. *Solar Energy*, 62(1), 19-28.

Ettouney, H. M., Alatiqi, I., Al-Sahali, M., & Ahmad Al-Ali, S. (2004). Heat transfer enhancement by metal screens and metal spheres in phase change energy storage systems. *Renewable Energy*, 29(6), 841-860.

Fan, Y. F., Zhang, X. X., Wang, X. C., Li, J., & Zhu, Q. B. (2004). Super-cooling prevention of microencapsulated phase change material. *Thermochimica Acta*, 413(1–2), 1-6.

Fang, G., Chen, Z., & Li, H. (2010a). Synthesis and properties of microencapsulated paraffin composites with SiO2 shell as thermal energy storage materials. *Chemical Engineering Journal*, 163(1–2), 154-159.

Fang, G., Li, H., Chen, Z., & Liu, X. (2010b). Preparation and characterization of stearic acid/expanded graphite composites as thermal energy storage materials. *Energy*, 35(12), 4622-4626.

Fang, G., Li, H., Yang, F., Liu, X., & Wu, S. (2009). Preparation and characterization of nano-encapsulated n-tetradecane as phase change material for thermal energy storage. *Chemical Engineering Journal*, 153(1–3), 217-221.

Fang, G., Tang, F., & Cao, L. (2014). Preparation, thermal properties and applications of shape-stabilized thermal energy storage materials. *Renewable and Sustainable Energy Reviews*, 40, 237-259.

Fang, Y., Kuang, S., Gao, X., & Zhang, Z. (2008). Preparation and characterization of novel nanoencapsulated phase change materials. *Energy Conversion and Management*, 49(12), 3704-3707.

Farid, M. M., Khudhair, A. M., Razack, S. A. K., & Al-Hallaj, S. (2004). A review on phase change energy storage: materials and applications. *Energy Conversion and Management*, 45(9–10), 1597-1615.

Farid, M. M., Kim, Y., & Kansawa, A. (1990). Thermal Performance of a Heat Storage Module Using PCM's With Different Melting Temperature: Experimental. *Journal of Solar Energy Engineering*, 112(2), 125-131.

Feldman, D., Shapiro, M. M., Banu, D., & Fuks, C. J. (1989). Fatty acids and their mixtures as phase-change materials for thermal energy storage. *Solar Energy Materials*, 18(3–4), 201-216.

Finke, H. L., Gross, M. E., Waddington, G., & Huffman, H. M. (1954). Low-temperature Thermal Data for the Nine Normal Paraffin Hydrocarbons from Octane to Hexadecane. *Journal of the American Chemical Society*, 76(2), 333-341.

Frankl, P., & Nowak, S. (2010). *Technology roadmap: solar photovoltaic energy*: OECD/IEA.

Gao, H., & Yang, J. (2010). Nanoscale silicon dioxide prepared by sol-gel process. *Modern Applied Science*, 4(9), p152.

Ghahremanzadeh, F., Khoddami, A., & Carr, C. M. (2010). Improvement in fastness properties of phase-change material applied on surface modified wool fabrics. *Fibers and Polymers*, 11(8), 1170-1180.

Gharsallaoui, A., Roudaut, G., Chambin, O., Voilley, A., & Saurel, R. (2007). Applications of spray-drying in microencapsulation of food ingredients: An overview. *Food Research International*, 40(9), 1107-1121.

Gil, A., Medrano, M., Martorell, I., Lázaro, A., Dolado, P., Zalba, B., & Cabeza, L. F. (2010). State of the art on high temperature thermal energy storage for power generation. Part 1—Concepts, materials and modellization. *Renewable and Sustainable Energy Reviews*, 14(1), 31-55.

Glaser, P. M., & Pantano, C. G. (1984). Effect of the H2O/TEOS ratio upon the preparation and nitridation of silica sol/gel films. *Journal of Non-Crystalline Solids*, 63(1–2), 209-221.

Goldstein, J., Newbury, D. E., Echlin, P., Joy, D. C., Romig, A. D., Lyman, C. E., Fiori, C., & Lifshin, E. (2012). *Scanning Electron Microscopy and X-Ray Microanalysis: A Text for Biologists, Materials Scientists, and Geologists*: Springer US.

Goswami, D. Y., Kreith, F., & Kreider, J. F. (2000). *Principles of Solar Engineering, Second Edition*: Taylor & Francis.

Griffiths, P. W., & Eames, P. C. (2007). Performance of chilled ceiling panels using phase change material slurries as the heat transport medium. *Applied Thermal Engineering*, 27(10), 1756-1760.

Hasnain, S. M. (1998). Review on sustainable thermal energy storage technologies, Part I: heat storage materials and techniques. *Energy Conversion and Management*, 39(11), 1127-1138.

Hatakeyama, T., & Quinn, F. X. (1999). *Thermal analysis: fundamentals and applications to polymer science*: Wiley.

Hawes, D. W., Feldman, D., & Banu, D. (1993). Latent heat storage in building materials. *Energy and Buildings*, 20(1), 77-86.

Hawlader, M. N. A., Uddin, M. S., & Khin, M. M. (2003). Microencapsulated PCM thermal-energy storage system. *Applied Energy*, 74(1–2), 195-202.

Hawlader, M. N. A., Uddin, M. S., & Zhu, H. J. (2002). Encapsulated phase change materials for thermal energy storage: Experiments and simulation. *International Journal of Energy Research*, 26(2), 159-171.

Hayat, K., Gondal, M. A., Khaled, M. M., Ahmed, S., & Shemsi, A. M. (2011). Nano ZnO synthesis by modified sol gel method and its application in heterogeneous photocatalytic removal of phenol from water. *Applied Catalysis A: General*, 393(1–2), 122-129.

He, B., Martin, V., & Setterwall, F. (2004). Phase transition temperature ranges and storage density of paraffin wax phase change materials. *Energy*, 29(11), 1785-1804.

Huggins, R. (2010). Mechanical Energy Storage *Energy Storage* (pp. 55-68): Springer US.

Humphries, W. R., Griggs, E. I., United, S., National, A., Space, A., Scientific, & Technical Information, O. (1977). *A design handbook for phase change thermal control and energy storage devices*. Washington; Springfield, Va.: National Aeronautics and Space Administration, Scientific and Technical Information Office ; For sale by the National Technical Information Service.

Ibrahim, H., Ilinca, A., & Perron, J. (2008). Energy storage systems—Characteristics and comparisons. *Renewable and Sustainable Energy Reviews*, 12(5), 1221-1250.

Jamekhorshid, A., Sadrameli, S. M., & Farid, M. (2014). A review of microencapsulation methods of phase change materials (PCMs) as a thermal energy storage (TES) medium. *Renewable and Sustainable Energy Reviews*, 31, 531-542.

Jegadheeswaran, S., & Pohekar, S. D. (2009). Performance enhancement in latent heat thermal storage system: A review. *Renewable and Sustainable Energy Reviews*, 13(9), 2225-2244.

Jin, X., Medina, M. A., & Zhang, X. (2013). On the importance of the location of PCMs in building walls for enhanced thermal performance. *Applied Energy*, 106(0), 72-78.

Jin, Y., Lee, W., Musina, Z., & Ding, Y. (2010). A one-step method for producing microencapsulated phase change materials. *Particuology*, 8(6), 588-590.

Joo, S. H., Park, J. Y., Tsung, C.-K., Yamada, Y., Yang, P., & Somorjai, G. A. (2009). Thermally stable Pt/mesoporous silica core-shell nanocatalysts for high-temperature reactions. *Nat Mater*, 8(2), 126-131.

Kaneko, R., Suzuki, E., Jikei, M., & Kakimoto, M.-A. (2002). Preparation and properties of hyperbranched aromatic polyamide-silica composites by sol-gel method. *High Performance Polymers*, 14(2), 105-114.

Kenisarin, M., & Mahkamov, K. (2007). Solar energy storage using phase change materials. *Renewable and Sustainable Energy Reviews*, 11(9), 1913-1965.

Kenisarin, M. M., & Kenisarina, K. M. (2012). Form-stable phase change materials for thermal energy storage. *Renewable and Sustainable Energy Reviews*, 16(4), 1999-2040.

Khartchenko, N. V., & Kharchenko, V. M. (2013). *Advanced Energy Systems, Second Edition*: Taylor & Francis.

Khatib, H. (2012). IEA World Energy Outlook 2011—A comment. *Energy policy*, 48, 737-743.

Khodadadi, J. M., & Hosseinizadeh, S. F. (2007). Nanoparticle-enhanced phase change materials (NEPCM) with great potential for improved thermal energy storage. *International Communications in Heat and Mass Transfer*, 34(5), 534-543.

Khudhair, A. M., & Farid, M. M. (2004). A review on energy conservation in building applications with thermal storage by latent heat using phase change materials. *Energy Conversion and Management*, 45(2), 263-275.

Klein, L. C. (2013). *Sol-Gel Optics: Processing and Applications*: Springer US.

Konuklu, Y., Unal, M., & Paksoy, H. O. (2014). Microencapsulation of caprylic acid with different wall materials as phase change material for thermal energy storage. *Solar Energy Materials and Solar Cells*, 120, Part B, 536-542.

Kureti, S., & Weisweiler, W. (2002). A novel sol–gel method for the synthesis of γ-aluminium oxide: development of the sol–gel transformation and characterization of the xerogel. *Journal of Non-Crystalline Solids*, 303(2), 253-261.

Kuznik, F., David, D., Johannes, K., & Roux, J.-J. (2011). A review on phase change materials integrated in building walls. *Renewable and Sustainable Energy Reviews*, 15(1), 379-391.

Kwon, H., Cheong, I., & Kim, J. (2010). Preparation of n-octadecane nanocapsules by using interfacial redox initiation in miniemulsion polymerization. *Macromolecular Research*, 18(9), 923-926.

Lane, G. A. (1983). *Solar heat storage: Latent heat materials*.

Lee, S.-W., Ichinose, I., & Kunitake, T. (1998). Molecular Imprinting of Azobenzene Carboxylic Acid on a TiO2 Ultrathin Film by the Surface Sol-Gel Process. *Langmuir*, 14(10), 2857-2863.

Lekeufack, D. D., Brioude, A., Mouti, A., Alauzun, J. G., Stadelmann, P., Coleman, A. W., & Miele, P. (2010). Core-shell Au@(TiO2, SiO2) nanoparticles with tunable morphology. *Chemical Communications*, 46(25), 4544-4546.

Lepot, N., Van Bael, M. K., Van den Rul, H., D'Haen, J., Peeters, R., Franco, D., & Mullens, J. (2008). Synthesis of platelet-shaped boehmite and γ-alumina nanoparticles via an aqueous route. *Ceramics International*, 34(8), 1971-1974.

Li, B., Liu, T., Hu, L., Wang, Y., & Gao, L. (2013). Fabrication and Properties of Microencapsulated Paraffin@SiO2 Phase Change Composite for Thermal Energy Storage. *ACS Sustainable Chemistry & Engineering*, 1(3), 374-380.

Li, J., Pan, Y., Xiang, C., Ge, Q., & Guo, J. (2006). Low temperature synthesis of ultrafine α-Al2O3 powder by a simple aqueous sol–gel process. *Ceramics International*, 32(5), 587-591.

Li, W., Zhang, X.-X., Wang, X.-C., & Niu, J.-J. (2007). Preparation and characterization of microencapsulated phase change material with low remnant formaldehyde content. *Materials Chemistry and Physics*, 106(2–3), 437-442.

Li, W., Zhang, X.-x., Wang, X.-c., Tang, G.-y., & Shi, H.-f. (2012). Fabrication and morphological characterization of microencapsulated phase change materials (MicroPCMs) and macrocapsules containing MicroPCMs for thermal energy storage. *Energy*, 38(1), 249-254.

Libor, Z., & Zhang, Q. (2009). The synthesis of nickel nanoparticles with controlled morphology and SiO2/Ni core-shell structures. *Materials Chemistry and Physics*, 114(2–3), 902-907.

Ling, T.-C., & Poon, C.-S. (2013). Use of phase change materials for thermal energy storage in concrete: An overview. *Construction and Building Materials*, 46(0), 55-62.

Livage, J., Henry, M., & Sanchez, C. (1988). Sol-gel chemistry of transition metal oxides. *Progress in Solid State Chemistry*, 18(4), 259-341.

Macwan, D. P., Dave, P., & Chaturvedi, S. (2011). A review on nano-TiO2 sol–gel type syntheses and its applications. *Journal of Materials Science*, 46(11), 3669-3686.

Mehalick, E. M., & Tweedie, A. T. (1975). Two component thermal energy storage material. Final report (pp. Medium: X; Size: Pages: 45).

Mehling, H., & Cabeza, L. (2007). PHASE CHANGE MATERIALS AND THEIR BASIC PROPERTIES. In: H. Paksoy (Ed.), *Thermal Energy Storage for Sustainable Energy Consumption* (Vol. 234, pp. 257-277): Springer Netherlands.

Mehling, H., & Cabeza, L. F. (2008). *Heat and cold storage with PCM: An up to date introduction into basics and applications*: Springer Berlin Heidelberg.

Mehrali, M., Latibari, S. T., Mehrali, M., Indra Mahlia, T. M., & Cornelis Metselaar, H. S. (2013a). Preparation and properties of highly conductive palmitic acid/graphene oxide composites as thermal energy storage materials. *Energy*, 58, 628-634.

Mehrali, M., Latibari, S. T., Mehrali, M., Indra Mahlia, T. M., Cornelis Metselaar, H. S., Naghavi, M. S., Sadeghinezhad, E., & Akhiani, A. R. (2013b). Preparation and characterization of palmitic acid/graphene nanoplatelets composite with remarkable thermal conductivity as a novel shape-stabilized phase change material. *Applied Thermal Engineering*, 61(2), 633-640.

Memon, S. A. (2014). Phase change materials integrated in building walls: A state of the art review. *Renewable and Sustainable Energy Reviews*, 31, 870-906.

Mesalhy, O., Lafdi, K., & Elgafy, A. (2006). Carbon foam matrices saturated with PCM for thermal protection purposes. *Carbon*, 44(10), 2080-2088.

Mettawee, E.-B. S., & Assassa, G. M. R. (2007). Thermal conductivity enhancement in a latent heat storage system. *Solar Energy*, 81(7), 839-845.

Mirmohammadi, S. A., & Behi, M. (2012). Investigation on Thermal Conductivity, Viscosity and Stability of Nanofluids.

Nagano, K., Mochida, T., Takeda, S., Domański, R., & Rebow, M. (2003). Thermal characteristics of manganese (II) nitrate hexahydrate as a phase change material for cooling systems. *Applied Thermal Engineering*, 23(2), 229-241.

Nakamura, H., & Matsui, Y. (1995). Silica Gel Nanotubes Obtained by the Sol-Gel Method. *Journal of the American Chemical Society*, 117(9), 2651-2652.

Nema, P., Nema, S., & Roy, P. (2012). An overview of global climate changing in current scenario and mitigation action. *Renewable and Sustainable Energy Reviews*, 16(4), 2329-2336.

Onder, E., Sarier, N., & Cimen, E. (2008). Encapsulation of phase change materials by complex coacervation to improve thermal performances of woven fabrics. *Thermochimica Acta*, 467(1–2), 63-72.

Oró, E., de Gracia, A., Castell, A., Farid, M. M., & Cabeza, L. F. (2012). Review on phase change materials (PCMs) for cold thermal energy storage applications. *Applied Energy*, 99(0), 513-533.

Pan, W., Ye, J., Ning, G., Lin, Y., & Wang, J. (2009). A novel synthesis of micrometer silica hollow sphere. *Materials Research Bulletin*, 44(2), 280-283.

Paris, J., Falardeau, M., & Villeneuve, C. (1993). Thermal Storage by Latent Heat: A Viable Option for Energy Conservation in Buildings. *Energy Sources*, 15(1), 85-93.

Parks, G. S., West, T. J., Naylor, B. F., Fujii, P. S., & McClaine, L. A. (1946). Thermal Data on Organic Compounds. XXIII. Modern Combustion Data for Fourteen Hydrocarbons and Five Polyhydroxy Alcohols. *Journal of the American Chemical Society*, 68(12), 2524-2527.

Pasquini, C. (2003). Near Infrared Spectroscopy: fundamentals, practical aspects and analytical applications. *Journal of the Brazilian Chemical Society*, 14, 198-219.

Pasupathy, A., Velraj, R., & Seeniraj, R. V. (2008). Phase change material-based building architecture for thermal management in residential and commercial establishments. *Renewable and Sustainable Energy Reviews*, 12(1), 39-64.

Pielichowska, K., & Pielichowski, K. (2014). Phase change materials for thermal energy storage. *Progress in Materials Science*, 65, 67-123.

Qiu, X., Li, W., Song, G., Chu, X., & Tang, G. (2012). Microencapsulated n-octadecane with different methylmethacrylate-based copolymer shells as phase change materials for thermal energy storage. *Energy*, 46(1), 188-199.

Rady, M. (2009). Study of phase changing characteristics of granular composites using differential scanning calorimetry. *Energy Conversion and Management*, 50(5), 1210-1217.

Regin, A. F., Solanki, S. C., & Saini, J. S. (2008). Heat transfer characteristics of thermal energy storage system using PCM capsules: A review. *Renewable and Sustainable Energy Reviews*, 12(9), 2438-2458.

Roy, S. K., & Sengupta, S. (1991). An evaluation of phase change microcapsules for use in enhanced heat transfer fluids. *International Communications in Heat and Mass Transfer*, 18(4), 495-507.

Rozanna, D., Chuah, T. G., Salmiah, A., Choong, T. S. Y., & Sa'ari, M. (2005). Fatty Acids as Phase Change Materials (PCMs) for Thermal Energy Storage: A Review. *International Journal of Green Energy*, 1(4), 495-513.

Rudd, A. F. (1993). Phase-change material wallboard for distributed thermal storage in buildings. Proceedings of ASHRAE Transactions (pp. 339-346).

Salunkhe, P. B., & Shembekar, P. S. (2012). A review on effect of phase change material encapsulation on the thermal performance of a system. *Renewable and Sustainable Energy Reviews*, 16(8), 5603-5616.

Samiey, B., Cheng, C.-H., & Wu, J. (2014). Organic-Inorganic Hybrid Polymers as Adsorbents for Removal of Heavy Metal Ions from Solutions: A Review. *Materials*, 7(2), 673.

Sánchez, L., Sánchez, P., Carmona, M., de Lucas, A., & Rodríguez, J. (2008). Influence of operation conditions on the microencapsulation of PCMs by means of suspension-like polymerization. *Colloid and Polymer Science*, 286(8-9), 1019-1027.

Sarı, A., Alkan, C., Karaipekli, A., & Uzun, O. (2009a). Microencapsulated n-octacosane as phase change material for thermal energy storage. *Solar Energy*, 83(10), 1757-1763.

Sarı, A., Biçer, A., & Karaipekli, A. (2009b). Synthesis, characterization, thermal properties of a series of stearic acid esters as novel solid–liquid phase change materials. *Materials Letters*, 63(13–14), 1213-1216.

Sari, A., & Kaygusuz, K. (2002). Thermal performance of palmitic acid as a phase change energy storage material. *Energy Conversion and Management*, 43(6), 863-876.

Sarier, N., & Onder, E. (2007). The manufacture of microencapsulated phase change materials suitable for the design of thermally enhanced fabrics. *Thermochimica Acta*, 452(2), 149-160.

Sharma, A., Tyagi, V. V., Chen, C. R., & Buddhi, D. (2009). Review on thermal energy storage with phase change materials and applications. *Renewable and Sustainable Energy Reviews*, 13(2), 318-345.

Sharma, S. D., & Sagara, K. (2005). Latent Heat Storage Materials and Systems: A Review. *International Journal of Green Energy*, 2(1), 1-56.

Shin, Y., Yoo, D.-I., & Son, K. (2005). Development of thermoregulating textile materials with microencapsulated phase change materials (PCM). IV. Performance properties and hand of fabrics treated with PCM microcapsules. *Journal of Applied Polymer Science*, 97(3), 910-915.

Siahpush, A., O'Brien, J., & Crepeau, J. (2008). Phase Change Heat Transfer Enhancement Using Copper Porous Foam. *Journal of Heat Transfer*, 130(8), 082301-082301.

Solomon, G. R., Karthikeyan, S., & Velraj, R. (2013). Sub cooling of PCM due to various effects during solidification in a vertical concentric tube thermal storage unit. *Applied Thermal Engineering*, 52(2), 505-511.

Song, X., Jiang, N., Li, Y., Xu, D., & Qiu, G. (2008). Synthesis of CeO2-coated SiO2 nanoparticle and dispersion stability of its suspension. *Materials Chemistry and Physics*, 110(1), 128-135.

Sorensen, B. (2015). *Solar Energy Storage*: Elsevier Science.

Stritih, U., & Butala, V. (2010). Experimental investigation of energy saving in buildings with PCM cold storage. *International Journal of Refrigeration*, 33(8), 1676-1683.

Su, J.-F., Wang, L.-X., & Ren, L. (2005). Preparation and characterization of double-MF shell microPCMs used in building materials. *Journal of Applied Polymer Science*, 97(5), 1755-1762.

Su, W., Darkwa, J., & Kokogiannakis, G. (2015). Review of solid–liquid phase change materials and their encapsulation technologies. *Renewable and Sustainable Energy Reviews*, 48(0), 373-391.

Sun, G., & Zhang, Z. (2002). Mechanical strength of microcapsules made of different wall materials. *International Journal of Pharmaceutics*, 242(1–2), 307-311.

Tang, B., Wu, C., Qiu, M., Zhang, X., & Zhang, S. (2014). PEG/SiO2–Al2O3 hybrid form-stable phase change materials with enhanced thermal conductivity. *Materials Chemistry and Physics*, 144(1–2), 162-167.

Tatsidjodoung, P., Le Pierrès, N., & Luo, L. (2013). A review of potential materials for thermal energy storage in building applications. *Renewable and Sustainable Energy Reviews*, 18, 327-349.

Tredwin, C. J., Georgiou, G., Kim, H.-W., & Knowles, J. C. (2013). Hydroxyapatite, fluor-hydroxyapatite and fluorapatite produced via the sol–gel method: Bonding to titanium and scanning electron microscopy. *Dental Materials*, 29(5), 521-529.

Tseng, Y. H., Fang, M. H., Tsai, P. S., & Yang, Y. M. (2005). Preparation of microencapsulated phase-change materials (MCPCMs) by means of interfacial polycondensation. *J Microencapsul*, 22(1), 37-46.

Tumirah, K., Hussein, M. Z., Zulkarnain, Z., & Rafeadah, R. (2014). Nano-encapsulated organic phase change material based on copolymer nanocomposites for thermal energy storage. *Energy*, 66, 881-890.

Tyagi, V. V., Buddhi, D., Kothari, R., & Tyagi, S. K. (2012). Phase change material (PCM) based thermal management system for cool energy storage application in building: An experimental study. *Energy and Buildings*, 51(0), 248-254.

Verdonck, E., Schaap, K., & Thomas, L. C. (1999). A discussion of the principles and applications of Modulated Temperature DSC (MTDSC). *Int J Pharm*, 192(1), 3-20.

Vinogradov, V., Vinogradov, A., Kraev, A., Agafonov, A., & Kessler, V. (2013). Sol–gel synthesis, characterization and catalytic activity of γ-alumina with bimodal mesopore distribution. *Journal of Sol-Gel Science and Technology*, 68(2), 155-161.

Vinogradov, V. V., Agafonov, A. V., Vinogradov, A. V., Gulyaeva, T. I., Drozdov, V. A., & Likholobov, V. A. (2010). Sol–gel synthesis, characterization and catalytic activity of mesoporous γ-alumina prepared from boehmite sol by different methods. *Journal of Sol-Gel Science and Technology*, 56(3), 333-339.

Wang, X., Niu, J., Li, Y., Wang, X., Chen, B., Zeng, R., Song, Q., & Zhang, Y. (2007). Flow and heat transfer behaviors of phase change material slurries in a horizontal circular tube. *International Journal of Heat and Mass Transfer*, 50(13–14), 2480-2491.

Waqas, A., & Kumar, S. (2012). Phase Change Material (Pcm)-Based Solar Air Heating System For Residential Space Heating In Winter. *International Journal of Green Energy*, 10(4), 402-426.

Wefers, K., & Misra, C. (1987). *Oxides and Hydroxides of Aluminum*: Alcoa Research Laboratories.

Wen, D., & Ding, Y. (2004). Experimental investigation into convective heat transfer of nanofluids at the entrance region under laminar flow conditions. *International Journal of Heat and Mass Transfer*, 47(24), 5181-5188.

Will, G. (2006). *Powder Diffraction: The Rietveld Method and the Two Stage Method to Determine and Refine Crystal Structures from Powder Diffraction Data*: Springer.

Yamagishi, Y., Takeuchi, H., Pyatenko, A. T., & Kayukawa, N. (1999). Characteristics of microencapsulated PCM slurry as a heat-transfer fluid. *American Institute of Chemical Engineers. AIChE Journal*, 45(4), 696.

Yinping, Z., & Yi, J. (1999). A simple method, the-history method, of determining the heat of fusion, specific heat and thermal conductivity of phase-change materials. *Measurement Science and Technology*, 10(3), 201.

Yoldas, B. (1975). Alumina sol preparation from alkoxides. *Am Ceram Soc Bull*, 54, 289-290.

Zalba, B., Marín, J. M., Cabeza, L. F., & Mehling, H. (2003). Review on thermal energy storage with phase change: materials, heat transfer analysis and applications. *Applied Thermal Engineering*, 23(3), 251-283.

Zhang, H., & Wang, X. (2009). Synthesis and properties of microencapsulated n-octadecane with polyurea shells containing different soft segments for heat energy storage and thermal regulation. *Solar Energy Materials and Solar Cells*, 93(8), 1366-1376.

Zhang, L., Zhu, J., Zhou, W., Wang, J., & Wang, Y. (2012). Thermal and electrical conductivity enhancement of graphite nanoplatelets on form-stable polyethylene glycol/polymethyl methacrylate composite phase change materials. *Energy*, 39(1), 294-302.

Zhang, M.-L., Ding, L.-G., Jing, X.-Y., & Hou, X.-Q. (2004a). Preparation, modification and application of nanoscale SiO_2 [J]. *Applied Science and Technology*, 6, 023.

Zhang, P., Ma, Z. W., & Wang, R. Z. (2010). An overview of phase change material slurries: MPCS and CHS. *Renewable and Sustainable Energy Reviews*, 14(2), 598-614.

Zhang, S., & Lee, W. E. (2003). Improving the water-wettability and oxidation resistance of graphite using Al2O3/SiO2 sol-gel coatings. *Journal of the European Ceramic Society*, 23(8), 1215-1221.

Zhang, X. X., Fan, Y. F., Tao, X. M., & Yick, K. L. (2004b). Fabrication and properties of microcapsules and nanocapsules containing n-octadecane. *Materials Chemistry and Physics*, 88(2–3), 300-307.

Zhang, Y., Wang, S., Rao, Z., & Xie, J. (2011). Experiment on heat storage characteristic of microencapsulated phase change material slurry. *Solar Energy Materials and Solar Cells*, 95(10), 2726-2733.

Zhao, C. Y., & Zhang, G. H. (2011). Review on microencapsulated phase change materials (MEPCMs): Fabrication, characterization and applications. *Renewable and Sustainable Energy Reviews*, 15(8), 3813-3832.

Zheng, Y., Zhao, W., Sabol, J. C., Tuzla, K., Neti, S., Oztekin, A., & Chen, J. C. (2013). Encapsulated phase change materials for energy storage – Characterization by calorimetry. *Solar Energy*, 87(0), 117-126.

Zhou, D., & Zhao, C. Y. (2011). Experimental investigations on heat transfer in phase change materials (PCMs) embedded in porous materials. *Applied Thermal Engineering*, 31(5), 970-977.

Zhou, D., Zhao, C. Y., & Tian, Y. (2012). Review on thermal energy storage with phase change materials (PCMs) in building applications. *Applied Energy*, 92(0), 593-605.

Zhou, W., Apkarian, R., Wang, Z., & Joy, D. (2007). Fundamentals of Scanning Electron Microscopy (SEM). In: W. Zhou & Z. Wang (Eds.), *Scanning Microscopy for Nanotechnology* (pp. 1-40): Springer New York.